THERMAL ENERGY STORAGE AGGREGATE USING LOW-COST ORGANIC PHASE CHANGE MATERIALS

A DISSERTATION IN
Civil Engineering
and
Geosciences

Presented to the Faculty of the University
of Missouri-Kansas City in partial fulfillment of
the requirements for the degree

DOCTOR OF PHILOSOPHY

by

ROSICKY METHODE KALOMBE

B.Tech., Cape Peninsula University of Technology, 2016

M.Eng., Cape Peninsula University of Technology, 2018

Kansas City, Missouri

2022

THERMAL ENERGY STORAGE AGGREGATE USING LOW-COST ORGANIC PHASE CHANGE MATERIALS

Rosicky Methode Kalombe, Candidate for the Doctor of Philosophy Degree

University of Missouri-Kansas City, 2022

ABSTRACT

The extent of energy economization of the structure depends on the thermal envelope performance. Thus, creating building materials capable of enhancing energy efficiency in the buildings is crucial. On the other hand, the icing of pavements during cold temperatures represents significant pedestrian and vehicle safety concerns. De-icing salts and other routine winter maintenance activities are intended to improve safety but have considerable cost and environmental runoff concerns and cause decreased infrastructure lifespan. As a remedy, the literature has recently investigated using different phase change material (PCM) types and their incorporation techniques into cement-based materials (CBMs). The outcome of such analysis has demonstrated similar negative and positive impacts on the overall performance of CBMs. So, it is challenging for the researchers to select one PCM type or incorporate a technique over the other. But, if appropriate PCMs and means of integration are employed, they can minimize these undesirable properties of PCMs on the CBMs.

This study has developed thermal energy storage aggregates (TESA) to cope with the aforementioned problems. TESA is made through vacuum impregnation of expanded clay lightweight aggregate (LWA) with low-cost and widely available organic PCMs such as individual or blends of coconut oil (CO), soybean oil (SO), and paraffin wax (PW). TESA is coated with anti-

bleeding materials to prevent leakage. TESA is made to produce concrete with good thermal, durability, and mechanical properties.

This study's findings showed that the differential scanning calorimetry (DSC) analysis of the as-received PW or prepared PWSO and COSO or after multiple thermal cycles showed high latent heat of fusions necessary to store a large quantity of heat. A wide range of melting points could be suitable for different degrees of phase transitions. Vacuum impregnated TESA showed PCMs absorption capacity of 30.20% for PW, 28.00% for PWSO, and 27.42% for COSO. Moreover, to prevent leakage, the TESA was coated with latex. The application of low-cost/widely available PCMs/TESA, developed in this study, can be beneficial for improving the thermal infrastructure performance in different weather conditions such as summer and winter.

In summer, TESA concrete developed better thermal performance due to the sensible and latent heat behaviour of PCMs impregnated in TESA. TESA enhanced the thermal conductivities but slightly decreased the compressive strength of concrete compared to the control. However, at the top surface layer of concrete, about 25 mm thick, TESA concrete stored a large quantity of heat due to sensible and latent heat mechanisms occurring during the absorption of sunlight; thus, TESA concrete provided higher thermal insulation than the control sample. Therefore, TESA may control and minimize the temperature fluctuation in concrete and could utilize it to enhance the thermal inertia of buildings during hot seasons or tropical climates.

In winter, TESA concrete showed the relative contribution of both sensible and latent heat storage behaviours. A methodology considering system energy input and discharge using a battery storage analogy is presented, allowing heat movement quantification under actual winter conditions. TESA concrete demonstrated the most significant increase in heat storage and delayed freezing. While many studies have shown PW to provide good high-temperature behaviour, the

relatively high melting point means that only PW can realize sensible heat improvement alone. Thus, blending SO with PW or CO enhanced the thermal performance of concrete in the winter season by leveraging the lower melting points and latent heat capacity. TESA concrete is one potential approach requiring little operational management to reduce the amount of de-icing salts or other winter maintenance while minimizing environmental impacts and safety concerns. Hence, TESA could provide a sustainable and feasible option for cold regions.

This study demonstrated the positive impacts of low-cost PCMs in producing new building materials capable of providing excellent thermal insulation in summer, and great resisting freezing and thawing cycles in winter, thus improving the thermal infrastructure performance in developed/developing countries in different weather conditions.

APPROVAL PAGE

The faculty listed below, appointed by the Dean of the School of Graduate Studies, have examined a dissertation titled "Thermal Energy Storage Aggregate using Low-Cost Organic Phase Change Materials," presented by Rosicky Methode Kalombe, candidate for the Doctor of Philosophy degree, and certify that in their opinion it is worthy of acceptance.

Supervisory Committee

John T. Kevern, Ph.D., P.E., FACI, LEED AP, Committee Chair

Department of Civil and Mechanical Engineering

Ceki Halmen, Ph.D., P.E.

Department of Civil and Mechanical Engineering

Sarvenaz Sobhansarbandi, Ph.D.

Department of Civil and Mechanical Engineering

Jejung Lee, Ph.D.

Department of Earth and Environmental Sciences

Caroline Davies, Ph.D.

Department of Earth and Environmental Sciences

Table of Contents

LIST OF ILLUSTRATIONS

LIST OF TABLES

ACKNOWLEDGMENTS

I would like to thank my supervisor, Prof John Kevern, for his constant guidance and encouragement throughout this project. It was an honor to be a student of such a prominent professor. He has assisted as my supervisor for this project and given me adequate opportunities to communicate the research outcomes in many ways. I would also like to thank the rest of my dissertation committee: Dr. Ceki Halmen, Dr. Sarvenaz Sobhansarbandi, Dr. Caroline Davies, and Dr. Jejung Lee, for their input and advise. Lastly, I would like to thank my mom and dad for their love and my brothers and sisters for their prayer, support, and motivation.

CHAPTER 1: INTRODUCTION

1.1. Statement of the research problem

In the latent heat thermal energy storage (LHTES) system, energy is stored during melting and recovered during freezing of a phase change material (PCM). Currently, the utilization of PCMs covers several fields, including applications requiring a wide temperature range from -20 °C to 200 °C for heating, cooling, and hybrid mixing of heating and cooling (Faraj, Khaled et al. 2020). PCMs use the latent heat during the change of phase process to control temperatures within a specific range (Faraj, Khaled et al. 2020). Organic PCMs cover paraffin and non-paraffin materials (i.e., fatty acids, sugar alcohols, and glycols as subdivisions). Organic PCMs are mainly utilized for continuous melting and freezing cycles without phase isolation or degradation. Organic PCMs are chemically stable, do not experience supercooling, are non-corrosive, and are recyclable (Zeinelabdein, Omer et al. 2018). But it is challenging for researchers to select one type of PCM or integrate techniques over others due to the lack of international standards for selection, characterization techniques, or applications. Numerous studies have suggested impregnating PCM into a highly absorptive lightweight aggregate (LWA) as an efficient technique to incorporate PCM into cement-based materials (Mohseni, Tang et al. 2019, Sukontasukkul, Sangpet et al. 2020). However, almost every research group has developed a particular operating procedure to impregnate and characterize PCMs into concrete, which is sometimes difficult to replicate due to the lack of standard methods.

Organic paraffin seems to be one of the most suitable latent heat storage materials used in concrete (Qu, Chen et al. 2020). Meanwhile, there are thousands of PCMs with considerable melting and solidification processes that could significantly improve the thermal performance of

concrete. For instance, biobased PCMs or food-grade materials such as palm kernel oil, palm oil, coconut oil, and soybean oil have been used mainly in heat ventilation and air-conditioning (HVAC) (Dhamodharan and Bakthavatsalam 2020, Safira, Putra et al. 2020, Okogeri and Stathopoulos 2021). Biobased PCMs could also produce PCM-LWA.

The surface of the impregnated LWA or PCM-LWA is usually coated with different anti-bleeding materials to prevent leakage and enhance thermal conductivity (Liu, Wang et al. 2017, Kakar, Refaa et al. 2019, Sukontasukkul, Sangpet et al. 2020). However, coating materials and conductive powder increase the overall cost and sometimes weakens the PCM performance (Mohseni, Tang et al. 2019, Nizovtsev, Borodulin et al. 2019, Hasanabadi, Sadrameli et al. 2021). When LWA-PCM is improperly coated, it creates micro-cracks in cement-based materials. The micro-cracks could occur due to the extra water absorbed by LWA-PCM, which could wet the cement particles and lead to additional hydration products, thus causing internal stress (Šavija 2018, Drissi, Ling et al. 2019). Therefore, there is still a need to explore other anti-bleeding materials to prevent PCM leakage and provide it with sufficiently high thermal conductivity and good intrinsic strength.

PCMs can offset temperature changes and reduce gradients in concrete structures through their ability to capture heat. But they can also influence concrete properties (Šavija 2018). Thus, PCM-LWA concretes decreased by 40% in compressive strength (Hasanabadi, Sadrameli et al. 2021). Therefore, if appropriate PCMs and means of integration are employed, they can minimize these undesirable properties. The thermal conductivity and specific heat depend strongly on the state of PCM (Sukontasukkul, Sangpet et al. 2020). Thus, reducing the peak values of the heat flux passing through the concrete material and limiting the material temperature range during heating

for a long time, reducing the energy consumption by lowering the indoor temperature (Nizovtsev, Borodulin et al. 2019, She, Wei et al. 2019).

Since PCM can store or release heat that means when PCM has a large latent heat storage capacity and a low melting point can release heat necessary to melt snow and ice on the surface of concrete pavements (Sharifi 2016, Jung Heum Yeon 2018, Faraj, Khaled et al. 2020, Sharma, Jang et al. 2022). However, previous studies about freeze and thaw cycles of concrete containing PCMs were carried out in the thermally controlled environmental chamber. The authors utilized artificial snow or ice and modeling programs to simulate conditions similar to actual road pavement conditions during winter (Bentz and Turpin 2007, Sakulich and Bentz 2012). Thus, the suggestions and predictions made in the literature could be diverse if the tests were performed outside in actual winter weather conditions. Hence, the necessity of performing actual field winter climate tests on concrete containing PCMs.

About the gaps highlighted above, this research presents a straightforward impregnating method of low-cost organic PCMs into expanded clay LWA to form thermal energy storage aggregates (TESA) coated with low-cost anti-bleeding materials. TESA is characterized and applied as a substitute for LWA in concrete production. The produced TESA concretes are analyzed, then exposed to different actual field weather seasons to identify the potential use of TESA in the building and construction industry.

1.2. Research objectives

This study aims to create different types of low-cost organic PCMs and TESA to improve the thermal performance of building materials, particularly concretes during different climates. The main objectives of this study include to:

1) Characterize thermodynamic performances of different materials, which could be low-cost PCMs.
2) Develop a process to create low-cost TESA, including low-cost carriers such as LWA and anti-bleeding materials.
3) Determine the thermal and mechanical properties of TESA concretes.
4) Quantify heat storage of the selected TESA under current summer and winter field conditions.
5) Estimate potential energy savings and potential applications of TESA.

1.3. Research questions

This research will provide answers to the following questions:

1) Can cooking oil be used as a phase change material?
2) What are the most reliable low-cost PCM and anti-bleeding materials to create TESA?
3) What are the thermal, and mechanical properties of TESA concretes?
4) What is the heat storage of the selected TESA under actual field summer and winter weather conditions?
5) What are the potential energy savings and potential applications of TESA?

1.4. Outline of the following chapters

The chapters remaining in this study will be set out as presented below:

Chapter 2: This chapter includes the literature review on thermal energy storage, PCMs, incorporation technique of PCMs and analytical techniques, coating materials, leakage test, and LWA description.

Chapter 3: This chapter gives the detailed methodology and characterization used to achieve this study's objectives.

Note: This study reported chapters 4 to 6 in the format of journal papers.

Chapter 4: This Chapter discusses the preparation and characterization of PCMs and TESA.

Chapter 5: This chapter presents for the first time the actual field performance data of TESA concrete collected in summer weather.

Chapter 6: This Chapter present for the first time the actual field performance data of TESA concrete collected in winter weather.

Chapter 7: This chapter gives the general conclusions about the significant findings obtained from this study and recommendations for further research important to this study.

1.5. References

Bentz, D. P. and R. Turpin (2007). "Potential applications of phase change materials in concrete technology." Cement and Concrete Composites. **29:** 527-532.

Dhamodharan, P. and A. K. Bakthavatsalam (2020). "Experimental investigation on thermophysical properties of coconut oil and lauryl alcohol for energy recovery from cold condensate." Journal of Energy Storage, Elsevier Ltd. **31**.

Drissi, S., T. C. Ling, K. H. Mo and A. Eddhahak (2019). "A review of microencapsulated and composite phase change materials: Alteration of strength and thermal properties of cement-based materials." Renewable and Sustainable Energy Reviews, Elsevier Ltd. **110:** 467-484.

Faraj, K., M. Khaled, J. Faraj, F. Hachem and C. Castelain (2020). "Phase change material thermal energy storage systems for cooling applications in buildings: A review." Renewable and Sustainable Energy Reviews, Elsevier Ltd. **119**.

Hasanabadi, S., S. M. Sadrameli and S. Sami (2021). "Preparation, characterization and thermal properties of surface-modified expanded perlite/paraffin as a form-stable phase change composite in concrete." Journal of Thermal Analysis and Calorimetry, Springer Science and Business Media B.V. **144:** 61-69.

Jung Heum Yeon, a. K.-K. K. b. (2018). "Potential applications of phase change materials to mitigate freeze-thaw deteriorations in concrete pavement." Construction and Building Materials **177**: 202-209.

Kakar, M. R., Z. Refaa, J. Worlitschek, A. Stamatiou, M. N. Partl and M. Bueno (2019). "Impregnation of lightweight aggregate particles with phase change material for its use in asphalt mixtures." International Symposium on Asphalt Pavement & Environment, Springer.

Liu, F., J. Wang and X. Qian (2017). "Integrating phase change materials into concrete through microencapsulation using cenospheres." Cement and Concrete Composites, Elsevier Ltd. **80:** 317-325.

Mohseni, E., W. Tang and S. Wang (2019). "Development of thermal energy storage lightweight structural cementitious composites by means of macro-encapsulated PCM." Construction and Building Materials, Elsevier Ltd. **225:** 182-195.

Nizovtsev, M. I., V. Y. Borodulin, V. N. Letushko, V. I. Terekhov, V. A. Poluboyarov and L. K. Berdnikova (2019). "Heat transfer in a phase change material under constant heat flux."

Thermophysics and Aeromechanics, Kutateladze Institute of Thermophysics SB RAS. **26:** 313-324.

Okogeri, O. and V. N. Stathopoulos (2021). "What about greener phase change materials? A review on biobased phase change materials for thermal energy storage applications." International Journal of Thermofluids, Elsevier B.V. **10**.

Qu, Y., J. Chen, L. Liu, T. Xu, H. Wu and X. Zhou (2020). "Study on properties of phase change foam concrete block mixed with paraffin / fumed silica composite phase change material." Renewable Energy, Elsevier Ltd. **150:** 1127-1135.

Safira, L., N. Putra, T. Trisnadewi, E. Kusrini and T. M. I. Mahlia (2020). "Thermal properties of sonicated graphene in coconut oil as a phase change material for energy storage in building applications." International Journal of Low-Carbon Technologies, Oxford University Press. **15:** 629-636.

Sakulich, A. R. and D. P. Bentz (2012). "Incorporation of Phase Change Materials in Cementitious Systems via fine lightweight aggregate." Construction and Building Materials. Elsevier Ltd. **35:** 483-490.

Šavija, B. (2018). "Smart crack control in concrete through use of phase change materials (PCMs): A review." Materials, MDPI AG. **11**.

Sharifi, N. P. (2016). "Application of phase change materials to improve the thermal performance of buildings and pavements. Dissertation for the degree of doctoral of philosophy in structural engineering. Worcester polytechnic institute. Massachussetts.

Sharma, R., J. G. Jang and J. W. Hu (2022). "Phase-change materials in concrete: opportunities and challenges for sustainable onstruction and Building Materials." Materials (Basel) **15**(1).

She, Z., Z. Wei, B. A. Young, G. Falzone, N. Neithalath, G. Sant and L. Pilon (2019). "Examining the effects of microencapsulated phase change materials on early-age temperature evolutions in realistic pavement geometries." Cement and Concrete Composites, Elsevier Ltd. **103:** 149-159.

Sukontasukkul, P., T. Sangpet, M. Newlands, D. Y. Yoo, W. Tangchirapat, S. Limkatanyu and P. Chindaprasirt (2020). "Thermal storage properties of lightweight concrete incorporating phase change materials with different fusion points in hybrid form for high temperature applications." Heliyon, Elsevier Ltd. **6**.

Zeinelabdein, R., S. Omer, E. Mohamed and G. Gan (2018). "Free cooling using phase change material for buildings in hot-arid climate." International Journal of Low-Carbon Technologies, Oxford University Press. **13:** 327-337.

CHAPTER 2: LITERATURE REVIEW

2.1. Introduction

As the global population increases, so does the need for power (Kalombe, Ojumu et al. 2020). Higher consumption of fossil fuels has led to higher emissions of CO_2, which contributes to ecological pollution (Frigione, Lettieri et al. 2019). Thus, the limitations of energy resources have encouraged scientists to search for new energy harvesting and conservation approaches in various sectors. For instance, the building sector consumes the most significant energy globally than the transportation and industry sectors (Marani and Nehdi 2019). The energy-saving level of a building depends on the pros and cons of enveloping thermal performance (Cui, Xie et al. 2017). Therefore, creating novel building materials capable of improving energy efficiency in buildings has been an area of research explored by different scientists worldwide. Thermal energy storage is a valuable tool for improving energy efficiency and increasing energy savings in buildings (Frigione, Lettieri et al. 2019).

2.2. Thermal energy storage

Thermal energy storage (TES) stores the existing thermal energy to reuse it during its shortage. The most significant value of TES is that it can solve the mismatch between the supply and demand of energy (Al-Absi, Isa et al. 2020). As an illustration, solar energy can be stored for heating the cold at night during the day. This cycle continues with the coolness during the night, and this coolness can use for cooling the warm of the day (Iten, Liu et al. 2016). Similar processes are possible for seasonal thermal energy storage when the heat can be stored during warm summer months for heating in winter and the coolness of the winter months for cooling the summer. This

cycle helps meet the energy needs caused by seasonal temperature fluctuations. Water and ice are frequently viewed as the preferred storage mediums for heating and cooling.

Barzin et al. (2015) and Al-Absi et al. (2020) highlighted that the TES could improve the heat exchange and energy efficiency of buildings and can help in reducing fuel consumption through the effective use of equipment and systems utilize thermal energy (Barzin, Chen et al. 2015, Al-Absi, Isa et al. 2020). In addition, the wasted low-cost energy, where its time of generation differs from the thermal demand period, such as passive and active solar heating and the internal heat produced by occupants, lighting, cooking, and appliances, can be used through TES (Kenisarin, Mahkamov et al. 2020). Also, low-cost energy can be purchased during off-peak periods and stored for high-rate periods. Thus, TES reduces the peaks in energy demand, which, in turn, reduces its associated cost (Kenisarin, Mahkamov et al. 2020). TES captures, stores, and reuses thermal energy (Al-Absi, Isa et al. 2020). As shown in Figure 2.1, there are three ways to store thermal energy (Akeiber, Wahid et al. 2014):

- Chemical heat by breaking and forming molecular bonds.
- Sensible heat by heating and cooling material.
- Latent heat thermal energy storage by melting and solidifying a material.

Kenisarin and Mahkamov (2016) indicated that latent heat thermal energy storage (LHTES) is the most attractive approach due to its high storage capacity and minor temperature variations from storage to retrieval (Kenisarin, Mahkamov et al. 2020). In such a system, energy is stored during melting and recovered during freezing of a phase change material (PCM) (Frigione, Lettieri et al. 2019, Al-Absi, Isa et al. 2020). Phase change materials used in LHTES approaches can fill the gap between energy supply and demand by absorbing excess energy in buildings, making it a promising technology. Currently, the utilization of PCMs covers several fields, including

applications requiring a wide temperature range from -20 °C to 200 °C for heating, cooling, and hybrid mixing of heating and cooling (Faraj, Khaled et al. 2020).

2.3. Phase change material in buildings

Phase change materials use the latent heat during the change of phase process to control temperatures within a specific range (Faraj, Khaled et al. 2020). They have been introduced to improve the thermal properties of building materials, such as thermal mass, thermal inertia, and specific heat capacity. Also, PCMs can store and release thermal energy when they undergo phase transitions (Marani and Nehdi 2019).

PCM technology in buildings will lower the heating and cooling loads by reducing the heat transferred through the building envelope. PCM technology will maintain the indoor temperature within the thermal comfort range of occupants by lowering temperature swings. Consequently, the total energy consumption of the building will be reduced significantly by load reduction or shifting (Frigione, Lettieri et al. 2019). The thermal performance of PCMs integrated into structures depends entirely upon the following (Sivanathan, Dou et al. 2020):

- Melting temperature.
- Thermal conductivity.
- Thermal energy storage density.

PCMs with rapid melting and crystallization or solidification points are considered suitable candidates for TES applications (Kasaeian, bahrami et al. 2017). Designing a heat storage system is a complex task since it is not restricted to the system's thermal performance only but also involves taking into consideration the cost, safety, and sustainability of materials used and processes employed (Gandhi, Kumar et al. 2020, Sivanathan, Dou et al. 2020).

2.4. Classification of PCMs

Figure 2.1 shows that PCMs used for LHTES systems are classified into four states according to the phase change mechanism they are subjected to and the phase transition temperature:

- Solid – solid.
- Solid-liquid.
- Solid – gas.
- Liquid – gas.

One of the advantages that solid-solid PCMs have over solid-liquid PCMs is that they require no encapsulation since no fluid (i.e., gas or liquid) gets generated during the phase transition process. So, the solid-solid PCM will reduce the overall cost because microencapsulation technology will not be required. Therefore, solid-solid PCMs can be directly incorporated into building materials. The solid-solid PCMs have good compatibility with building materials; however, no study has investigated the compatibility between the synthesized solid-solid PCMs and building materials (Gandhi, Kumar et al. 2020, Sivanathan, Dou et al. 2020).

Solid-liquid PCMs are generally preferred and used in buildings because other PCMs (i.e., solid-gas and liquid–gas) are not compatible with building materials (Faraj, Khaled et al. 2020, Sivanathan, Dou et al. 2020). Due to some technical limitations (Akeiber, Wahid et al. 2014), including the significant volume changes during the phase transition process and the high pressure of the gas phase in the system.

Endothermic (charging) and exothermic (discharging) are the two main processes occurring in solid-liquid PCMs. And they can be described as follows: (i) when the temperature surrounding the PCM rises such that the PCM reaches its melting point, the chemical bonds initiate its breakage with an endothermic process allowing the PCM to absorb energy. At the same time, the material

melts, changing its state from solid to liquid; this is the charging process of PCM. (ii) When the temperature decreases to reach the freezing point of the PCM, bonds will regenerate. PCM will release heat exothermally while the PCM is regaining its solid state. Thus, PCM is described as a thermal reservoir (Wang, Ren et al. 2018). A small volume change accompanies the whole process of charging and discharging, less than 10% of its initial volume (Amaral, Vicente et al. 2017). PCMs, experience sensible and latent heat processes based on the instantaneous PCM temperature compared to the melting and freezing range (Faraj, Khaled et al. 2020).

PCMs that have their charging/discharging process within the solid-liquid transition category are classified into three main classes: Organic, inorganic, and eutectic PCM, as reported in Figure 2.1 (Baetens, Jelle et al. 2010, Amaral, Vicente et al. 2017). These classes are subdivided further into sub-categories. Organic PCMs cover paraffin and non-paraffin materials, by which the latter contains fatty acids, sugar alcohols, and glycols as subdivisions. Inorganic PCMs are classified as salt-hydrates, molten salts, or metals. In addition, eutectic PCMs are obtained by mixing two or more organics, inorganics, or organic with inorganic PCMs (Zeinelabdein, Omer et al. 2018). Thus, Figure 2.1 recapitulates the TES classification in connection with the classifications of PCMs.

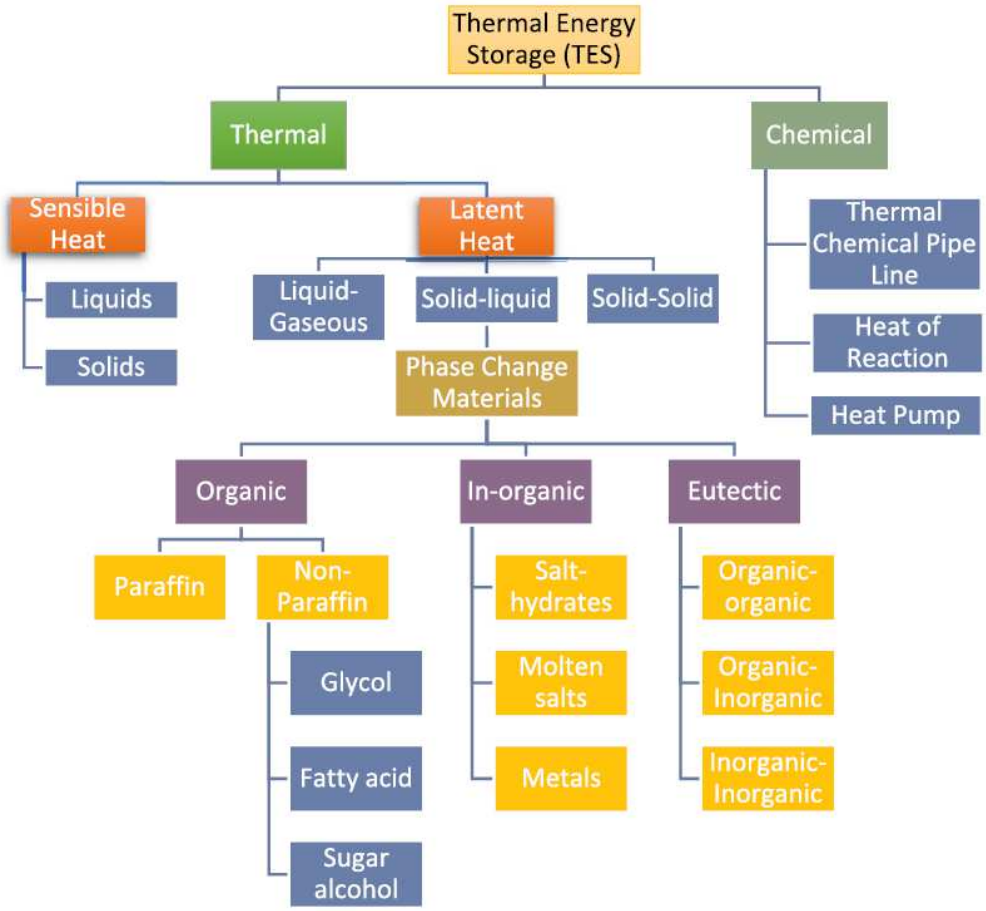

Figure 2.1: TES and PCM classifications (Faraj, Khaled et al. 2020)

The process of latent heat storage begins when PCM melts as it nears its phase change temperature; it absorbs heat and stores it until the material transitions back to a solid-state when the stored energy is then released into the environment. As depicted in Figure 2.2. the latent heat is symbolized by the horizontal line under isothermal conditions. Still, sensible heat storage is represented by the sloped lines before and after the charge phase (Sharma, Neithalath et al. 2013, Yang, Yim et al. 2019).

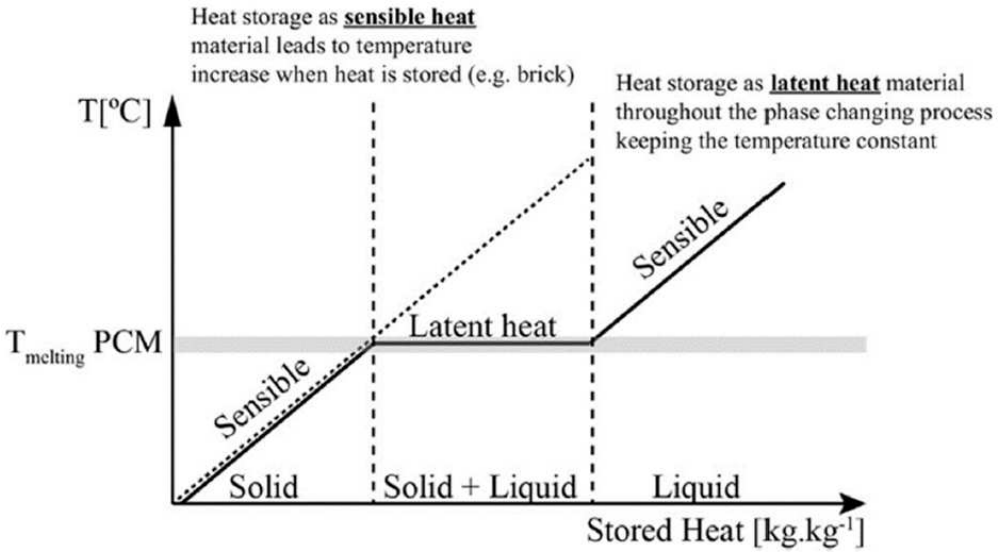

Figure 2.2: The thermal process of latent heat and sensible heat (Yang, Yim et al. 2019)

2.5. Advantages and disadvantages of PCMs

Latent heat solid-liquid PCMs consist of different PCMs, and each of them has advantages and disadvantages when utilized in building materials. For instance, (i) organic PCMs are hydrocarbon materials or materials found in nature that mainly consist of carbon-hydrogen chains. The advantages of organic PCMs are several, with certain disadvantages that limit their effectiveness. Organic PCMs can have continuous melting and freezing without phase isolation or degradation. Organic PCMs are chemically stable, do not have supercooling, are non-corrosive, and are recyclable. However, Organic PCMs have low thermal conductivity and are flammable (Tyagi, Kaushik et al. 2011, Faraj, Khaled et al. 2020). (ii) Inorganic PCMs are materials that offer the advantages of very high latent heat storage capacity, non-inflammability, and sharper phase transitions. However, inorganic PCMs main disadvantages are being naturally corrosive, featured with phase segregation, and supercooling (Chandel and Agarwal 2017). (iii) Eutectics are available as alloys of organics and inorganics, and mostly (inorganic salt-hydrates) that feature congruent melting and freezing with no phase segregation (Zhou, Zhou et al. 2019, Faraj, Khaled et al. 2020).

2.6. Selection of PCMs

Phase change materials have a wide melting temperature range with different classes and categories. Each has a specified latent heat storage capacity of melting, as depicted in Table 2.1. Therefore, the melting process is the primary variable to consider while choosing a suitable PCM for a specified application (Faraj, Khaled et al. 2020).

Table 2.1: PCMs for building applications: composition, category, melting temperature, and melting heat (Frigione et al., 2019).

Type	PCM	Melting point (°C)	Melting Heat (J/kg K)
Organic	Glycerin	18	198.7
	Hexadecane	18.1	236
	Butyl stearate	19	140
	Propyl palmitate	19	186
	Paraffin C_{16}–C_{18}	20-22	152
	Heptadecane	20.8-21.7	171-172
	Dimethyl sebacate	21	120-135
	Octadecyl 3-mencaptopropylate	21	143
	Lithium chloride ethanolate	21	188
	Paraffin C_{17}	21.7	213
	Erythritol palmitate	21.9	201
	Polyglycol E600	22	127.2
	Isopropyl stearate	22.1	113
	Paraffin C_{13}–C_{24}	22-24	189
	Octadecyl thioglycolate	26	90
	Lactic acid	26	184
	1-Dodecanol	26	200
	Vinyl stearate	27-29	122

	Paraffin C_{18}	28	244
	Octadecane	28-28.1	244-250.7
	Methyl palmitate	29	205
	Capric acid	30.1	158
	Tridecanol	31.6	223
	Tetradecanol	37.8	225
	Camphenilone	39	205
	Docasyl bromide	40	201
	Caprylone	40	259
Inorganic	$KF.4H_2O$	18.5	231
	$FeBr_3.6H_2O$	21	105
	$Mn(NO_3)_2.6H_2O$	25.8	125.9
	$CaCl_2.12H_2O$	29.8	174
	$CaCl_2.6H_2O$	29-30	171-192
	$LiNO_3.3H_2O$	30	296
	Ga	30	80.9
	$Na_2SO_4.10H_2O$	31-32.4	251.1-254
	$Na_2SO_4.3H_2O$	32	251
	$Na_2CO_3.10H_2O$	32-36	246.5-247
	$CaBr_2.6H_2O$	34	115.5
	$LiBr_2.2H_2O$	34	124
	$Zn(NO_3)_2.6H_2O$	35-36	265-281
	$Na_2HPO_4.12H_2O$	36-36.4	146.9-147
	$FeCl_3.6H_2O$	37	223
Eutectic mixtures	34% $C_{14}H_{28}O_2$ + 66% $C_{10}H_{20}O_2$	24	147.7
	50% $CaCl_2$ + 50% $MgCl_2.6H_2O$	25	95
	Octadecane + docosane	25.5-27	203.8
	Octadecane + heneicosane	25.8-26	173.93
	50% CH_3CONH_2 + 50% NH_2CONH_2	27	163

	47% $Ca(NO_3)_2.4H_2O$ + 53% $Mg(NO_3).6H_2O$	30	136
	60% $Na(CH_3COO).H_2O$ + 40%$CO(NH_2)_2$	30-31.5	200.5-226

Usually, a PCM undergoes phase change as a result of getting activated by a stimulus such as heat, light, or pressure within their specific boundary conditions, such as changes in temperature, light, the concentration of solvents, and pH (Sivanathan, Dou et al. 2020). Essentially, some properties are required to ensure the maximum thermal performance of PCMs (Hawes, Banu et al. 1992, Hawes and Feldman 1992, Pielichowska and Pielichowski 2014, Farnam, Krafcik et al. 2016). These properties consist of:

- Thermo-physical: the PCM must have a suitable melting temperature (T_m), high heat of fusion (L_H), high specific heat (C_p), high thermal conductivity (K), small transition volume change, high density, cycling stability, the low vapor pressure at T_m, and congruent melting.
- Kinetic: the PCM must have high nucleation and crystal growth rates.
- Chemical: the PCM must be chemically stable, have no corrosiveness, complete reversible cycle, anti-flammable, non-toxic, and non-explosive.
- Economical: the PCM must be effective cost and commercially available.
- Environmental: the PCM must be a low ecological impact, non-polluting, and recyclable.

The PCM should be readily available in large quantities at a low cost (Khudhair and Farid 2004, Sharma, Tyagi et al. 2009, Tyagi, Kaushik et al. 2011). In practice, the mentioned properties are not fully met by most PCMs. But recent progress in the design and characterization of novel

materials for energy storage, including nanomaterials, has opened new possibilities for enhanced performance with extended lifetimes (Pielichowska and Pielichowski 2014).

2.7. Characterization of PCMs

The thermophysical properties measurements must be representative and repeatable to successfully design and size PCM processes. But it isn't easy to directly compare the thermophysical properties of PCMs available in the literature since most research groups employ their approaches for characterizing thermal energy storage materials. Due to a critical lack of international standards for testing PCMs. However, there are many well-developed measurement methods for PCM characteristics, such as the water bath, differential scanning calorimetry (DSC), and T-history form, as shown in Figure 2.3 (Xie, Li et al. 2013, Hu, Guo et al. 2020).

Xie et al. (2013) reported that the DSC method provides the best precision with small samples having the uniform granularity and simple structure and composition. In contrast, the T-history method is used with relatively unconsolidated materials. This is due to its simplicity, high reproducibility, and low cost of implementation. Meanwhile, the water bath method is fast and straightforward and is easily performed in the lab (Xie, Li et al. 2013, Martínez, Carmona et al. 2020). These methods characterized the melting or freezing temperatures, enthalpies, and specific heats. However, each technique has its limitations (Hu, Guo et al. 2020). For instance, the sample is so tiny for the DSC, and there are supercooling and precipitation problems. For the water bath method, there are problems related to uneven heating. And the T-history technique is not commercially developed with standard guidance, making the comparison among measurements difficult (Badenhorst and Cabeza 2017, Bayon and Rojas 2019, Nazir, Batool et al. 2019). Among all the characterization techniques, DSC is the most widely used method for determining the thermophysical properties of PCMs (Martínez, Carmona et al. 2020).

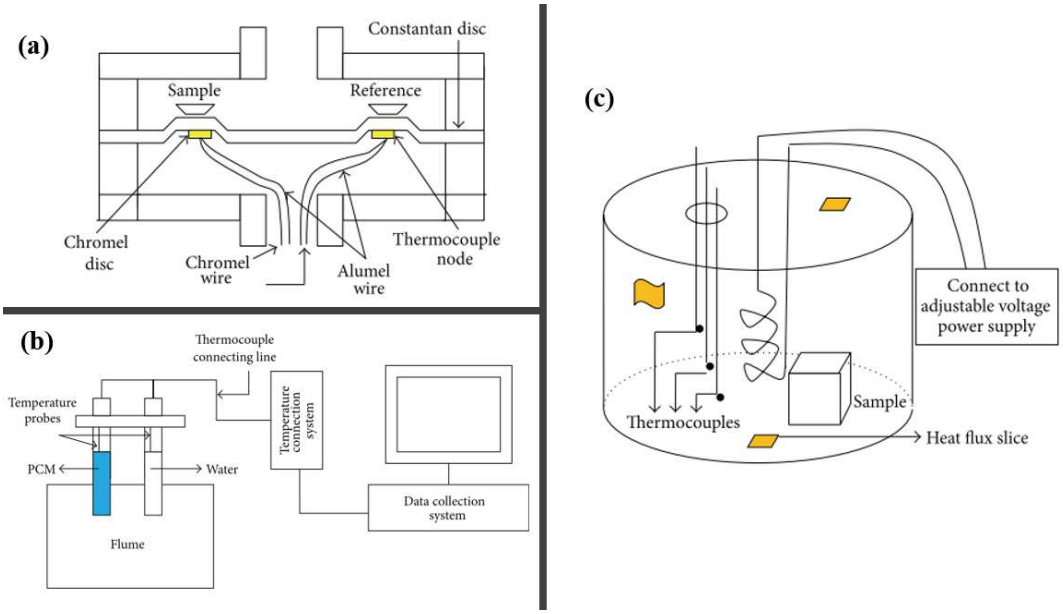

Figure 2.3: Thermal techniques for PCMs analysis, (a) DSC, (b) T-history method, and (c) water bath method (Xie, Li et al. 2013)

2.7.1. Differential scanning calorimetry

DSC is performed according to ASTM E793-06 (Jayalath, San Nicolas et al. 2016). This technique describes the determination of the temperature, the heat of melting (fusion), and crystallization (freezing). The operating temperature varies from -120 to 600 °C. The technician can extend the temperature range depending upon the instrumentation used. This test method is generally applicable to thermally stable materials with well-defined endothermic or exothermic behavior. The heat of melting and crystallization portion of ISO 11357-3 is equivalent to this standard (Jayalath, San Nicolas et al. 2016, Omaraa, Saman et al. 2017, Bayon and Rojas 2019, Muller, Rubio-Perez et al. 2020).

Several authors had previously carried out the DSC analysis of PCMs differently. Li et al. (2013) characterized Paraffin (PA) and a composite of paraffin with expanded graphite (EG/PA) using the DSC at the heating rate of 5 °C/min in a nitrogen atmosphere from 0 °C to 100 °C. The

melting temperature and latent heat of fusion were 28.8 °C and 209.3 J/g for PA and 28.55 °C and 183.0 J/g for EG/PA, respectively (Li, Wu et al. 2013).

Farnam et al. (2016) used LT-DSC to analyze 11±2 mg of paraffin oil and methyl laurate from−80 °C to 40 °C at a heating rate of 5 °C/min. The melting process showed 3.6 °C and 160.4 J/g for methyl laurate and 6.1°C and 129.4 J/g for paraffin oil. The authors indicated that paraffin oil and methyl laurate show good thermal properties for snow melting and deicing applications since they can produce sufficient heat (∼130–160 J/g) during their phase transition at ∼2–3 °C (Farnam, Krafcik et al. 2016).

Bao et al. 2017 prepared and ran a DSC analysis for PA, EG/PA, and graphite nanoparticle (GNP)/PA from 0 °C to 60 °C at a cooling and heating rate of 2 °C/min. Then, the melting point for PA, EG/PA, and GNP/PA was 23.77 °C, 22.82 °C, and 22.68 °C, respectively. The results show that, with the incorporation of EG and GNP, the melting point of the PCM decreased. The decrease in the melting temperature is believed to be due to higher thermal conductivities of EG and GNP, which in turn increased heat transfer. The latent heat of fusion for PA, EG/PA, and GNP/PA was 163.6 J/g, 152.8 J/g, and 47.22 J/g, respectively (Bao, Memon et al. 2017).

Figure 2.4 illustrates the DSC curve of paraffin and composite PCM (Paraffin + fumed silica). The DSC curve shows that paraffin had a solidification process at 44 °C and 260 J/g and a melting process at 46 °C and 259 J/g of latent heat. The solidification process of composite PCM was 46 °C and 112 J/g, and the melting process was 41 °C and 113.3 J/g. Thus, paraffin had a higher latent heat and phase change temperatures than the composite PCM (Qu, Chen et al. 2020).

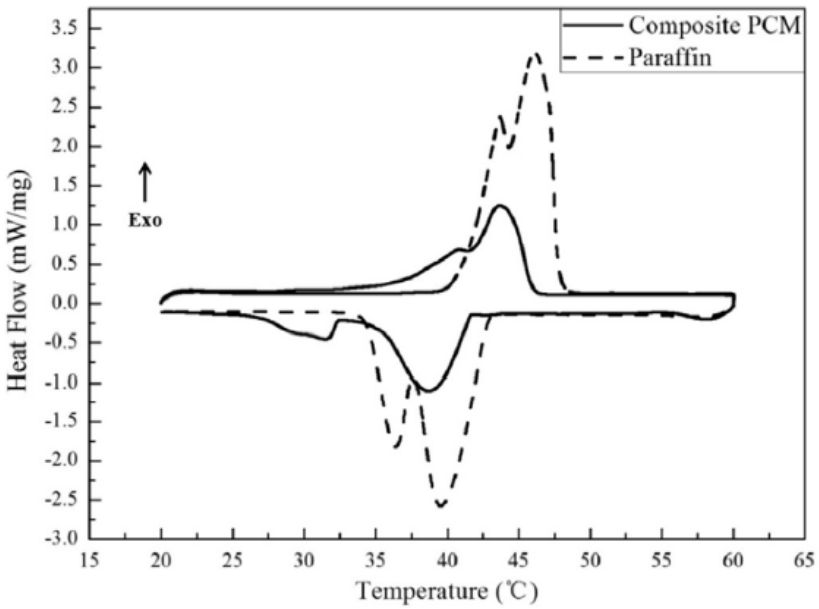

Figure 2.4: DSC curve of composite and Paraffin (Qu, Chen et al. 2020)

2.8. Incorporation techniques of PCM in building materials

PCMs can be integrated into building materials using different techniques, including direct incorporation, immersion through materials' pores, micro-encapsulation, and macro-encapsulation, as depicted in Figure 2.5. Thus, Figure 2.5a shows filling tubes with PCM to raise the latent heat of the concrete-tube system, thereby preventing freezing of ice or snow accumulation on the concrete pavement or micro-encapsulation method. Figure 2.5b demonstrates the integration of PCM through direct incorporation and impregnation using LWA or micro-encapsulation. Figure 2.5c indicates the inclusion of PCM within the concrete pores and voids on the surface of the pavement or the integration of PCM through the immersion method (Farnam, Krafcik et al. 2016). Researchers previously investigated the three techniques and methods of incorporating PCM into building materials as summarized in Table 2.3.

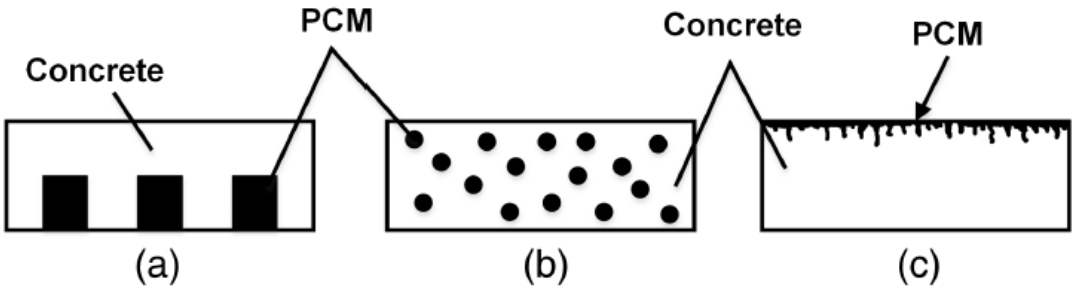

Figure 2.5: Three integration techniques of PCM in building materials, (a) using pipes of PCM (macro-encapsulation), using particles containing PCM (microencapsulation, impregnation, or direct), and (b) filling surface voids via PCM absorption (immersion) (Farnam, Krafcik et al. 2016)

Table 2.2: Previous studies on PCM incorporating techniques, experimental procedures, and outcomes in building materials

Incorporation methods	PCMs and Tests performed	References
Direct incorporation	Direct incorporation of butyl stearate (melting Point of 17-22 °C) as PCM into concrete. Tests performed: DSC, 1000 melting-freezing cycles, compressive strength, and PCM leakage from the porous structure of concrete.	(Cellat, Beyhan et al. 2017)
Immersion method	Paraffin wax and polyethylene glycol were impregnated into (porous) lightweight fine aggregates (expanded shale) nominally 3 mm in diameter. Tests performed: DSC and semi-adiabatic calorimetry.	(Bentz and Turpin 2007)
Immersion and impregnation method	Paraffin oil and methyl laurate was integrated into LWA using the ambient and vacuum conditions. The authors selected two approaches to incorporate PCM into the	(Farnam, Krafcik et al. 2016)

	mortar specimens: using lightweight aggregate (LWA) and using an embedded tube. Tests performed: DSC for PCM and mortar constituents, physical properties of the mortar (using ultrasonic pulse velocity and compressive strength), and PCM mass loss over time.	
Impregnation method	Paraffin oil ambient absorption was determined by saturating 500 g oven-dry expanded lightweight shale aggregate (LWA) with PCM for 72 h. Tests performed: LT-DSC, the properties of porous LWA (Particle Size Distribution and Absorption Capacity), thermal cycling of large-scale concrete slabs, and snow melting evaluation of large-scale concrete slabs with and without PCM. Note: The temperature of LT-DSC varied between -90 C and 50 C. However, -90C and -70 C trigger nucleation to ensure everything transforms into solid.	(Farnam, Esmaeeli et al. 2017)
Impregnation method	Paraffin (N-Nonacosane C29H60) (PA) as PCM was impregnated into the expanded perlite (EP) particles by the vacuum impregnation method, and a layer of polystyrene coated the prepared EP/PA composite. Tests: DSC, TGA, thermal conductivity, leakage, and compressive strength.	(Nizovtsev, Borodulin et al. 2019)

Impregnation and micro-encapsulation method	PCMs were prepared as follows: (i) Paraffin/fumed silica mass ratios of 4.5:5.5, 5:5, and 5.5:4.5 were used to form composite PCMs, then added to water, cement, and thickener (thickener and distilled water ratio of 1.5:1000) to create PCMs mortar. Tests were performed: DSC, XRD, SEM, thermal conductivity, and leakage test.	(Qu, Chen et al. 2020)
Impregnation method	Paraffin (PRF) (melting point of 57-59.9 °C) and polyethylene glycol type 1450 (PEG) (melting point 42–46 °C) were impregnated into aggregates using high temperatures. Tests performed: density test, water absorption test, abrasion resistance, compressive strength, flexural strength, steady-state thermal transmission properties through heat flow meter apparatus, and thermal storage properties of phase change materials and products.	(Sukontasukkul, Sangpet et al. 2020)
Micro-encapsulation method	The PCM utilized a mixture of paraffin waxes in powder form. The PCM was encapsulated in polymethyl methacrylate micro-capsules. Tests performed: DSC, SEM, particle size distribution, semi-adiabatic, thermal conductivity, specific heat capacity/thermal efficiency measurement, and Compressive strength.	(Hunger, Entrop et al. 2009)

Micro-encapsulation method	The PCM consisted of an aqueous dispersion of a mixture of formaldehyde-free microencapsulated paraffin. Tests performed: compressive strength, slump flow test, encapsulation breakage, and measurement of densities.	(Fenollera, Míguez et al. 2013)
Micro-encapsulation method	Soft inclusions in the form of a paraffin (powder) based microencapsulated PCM (melting point of 23 ± 3 °C, and latent heat of 110 kJ/kg), Micronal DS 5008X manufactured by BASF Corporation. Tests performed: heat absorption and release, the development of unrestrained/restrained thermal stresses and strains and the mechanical properties, including compressive strength, elastic modulus, and fracture behavior.	(Fernandes, Manari et al. 2014)
Macro-encapsulation method	Technical grade Paraffin was used and expanded clay (LWA) was used as a container for PCM. Tests performed: mercury intrusion porosimetry, the influence of viscosity on the absorption capacity of LWA, SEM, DSC, compressive strength, shrinkage, thermal performance of thermal energy storage LWAC – indoor testing, evaluation of the thermal performance of thermal energy storage LWAC – outdoor testing, and environmental.	(Memon, Cui et al. 2015)

Micro-encapsulation method	A paraffin core with a Poly (methyl methacrylate) highly cross-linked shell was used as the microencapsulated PCM (Micronal DS 5040X) with a transition temperature of 23 °C. Tests: Isothermal calorimetry, DSC, TGA, SEM, compressive strength, and thermal conductivity.	(Jayalath, San Nicolas et al. 2016)
Micro-encapsulation method	MPCM contained paraffin wax as PCM with acrylic shell (Micronal DS 5008 manufactured by BASF, Berlin, Germany). Tests performed: SEM, DSC, nano-indentation technique, elastic modulus, and emission of a volatile organic compound.	(Giro-Paloma, Al-Shannaq et al. 2016)
Micro-encapsulation method	The microencapsulated PCM consisted of a paraffin-based core material encased in a melamine-formaldehyde (MF) shell. The tests performed were: Isothermal calorimeter, thermocouple placement, and thermal cracking resistance.	(She, Wei et al. 2019)
Micro-encapsulation method	Paraffin (N-Tetradecane) as PCM (melting point of 4.5 °C) was encapsulated with a melamine-formaldehyde resin via an emulsification process before being added in concrete mixtures. Tests performed: thermal response of field concrete slabs, service life prediction, compressive and flexural strength.	(Urgessa, Yun et al. 2019)

Micro-encapsulation method	Paraffin wax was used as the core of both microcapsules. Tests performed were SEM, compressive strength, Freeze-thaw cycles, and Setting times.	(Pilehvar, Szczotok et al. 2019)
Micro-encapsulation method	The microencapsulated PCM consisted of vegetal wax in a powder format (melting range 23–27 °C, solicitation range 18–23 °C, and latent heat 160 J/g). Tests performed: SEM, thermal conductivity, DSC, compressive strength, and water porosity.	(Dakhli, Chaffar et al. 2019)
Impregnation and micro-encapsulation method	Diatomite was impregnated with paraffin. The chosen PCM is an aqueous dispersion of a mixture of formaldehyde-free microencapsulated paraffin. Tests performed: SEM, heat flux power, phase transition temperature range, and the characteristics of the phase change material were varied.	(Nizovtsev, Borodulin et al. 2019)

Based on Table 2.3, the authors could say that organic PCM, particularly paraffin, seems to be one of the most suitable latent heat storage materials used in concrete. The main reasons could be the chemical stability, inactivity in the alkaline environment of concrete, an appropriate transition temperature of about 26 °C (human thermal comfort), and low degree of supercooling; they could also be relatively inexpensive and have desirable thermal stability (Ling and Poon 2013).

As described in Table 2.3, most authors had focused on a specific technique to incorporate PCM into building materials for a series of objectives. It was found relevant to show some of the

setup used by these authors. For instance, some authors' vacuum impregnation of PCM in Table 2.3 is shown in Figure 2.6. During this process, porous LWA was placed inside a flask connected to a vacuum pump, a vacuum meter, and a container of liquid PCM. The authors sealed the connecting joints of the system with grease. The authors utilized the vacuum pump to evacuate air from the porous LWA and the vacuum meter to monitor the system's vacuum pressure. The evacuation process continued for about 30 min at a vacuum pressure of 88.1 kPa. The valve between the flask and the container of liquid PCM was turned open, and liquid PCM was allowed to flow into the flask to the level covering all LWA as depicted in Figure 2.6. Finally, the authors stopped the operation of the vacuum pump, and the air was allowed to enter the flask again to drive liquid PCM to penetrate the pore space of LWA. After about 30 min, the LWA was taken out of the flask and cleaned with a cotton towel (Zhang, Li et al. 2004, Šavija 2018, Nizovtsev, Borodulin et al. 2019).

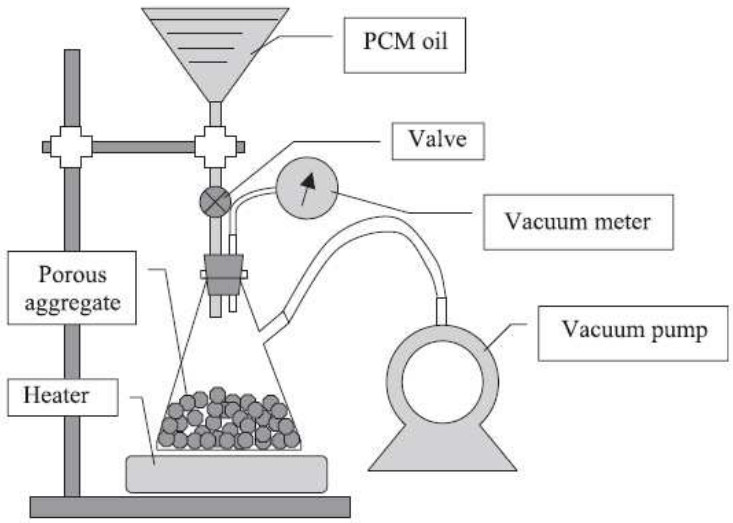

Figure 2.6: Schematic drawing vacuum impregnation setup (Zhang, Li et al. 2004, Šavija 2018, Nizovtsev, Borodulin et al. 2019)

An illustration of the microencapsulation method is depicted in Figure 2.7, and it was reported by Urgessa (2019) and Yeon and Kim (2018). An inert PCM was microencapsulated with

melamine-formaldehyde polymer shells via an emulsification process to prevent direct contact of raw PCM from cementing and possible leakage upon melting and improve the thermal efficiency of PCM by increasing specific surface area and dispersion in the matrix. The mPCM slurry used in this study consisted of 27.5 wt% raw PCM core, 10 wt% polymer shells enclosing the core material, and 62.5 wt% liquid; the liquid phase is not pure water but contains some chemical constituents such as anionic emulsifying agent, glutardialdehyde, and hydrogen chloride added during the microencapsulation process (Jung Heum Yeon 2018, Urgessa, Yun et al. 2019).

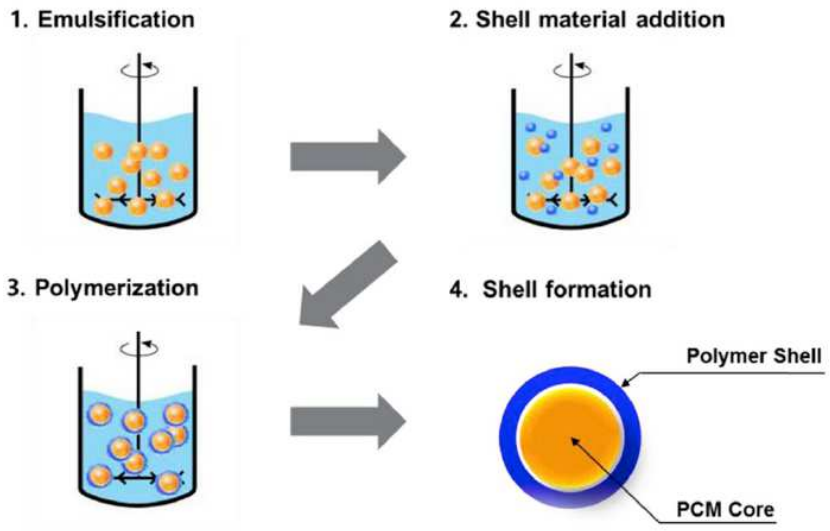

Figure 2.7: Microencapsulation of raw PCM using emulsification process (Jung Heum Yeon 2018, Urgessa, Yun et al. 2019)

To cast concrete or mortar sample for thermal tests, different models of molds were previously used by some of the authors mentioned in Table 2.3. Thus, Figure 2.8 shows two different molds with thermal insulation and mold with embedded pipes developed by Farnam et al. (2017).

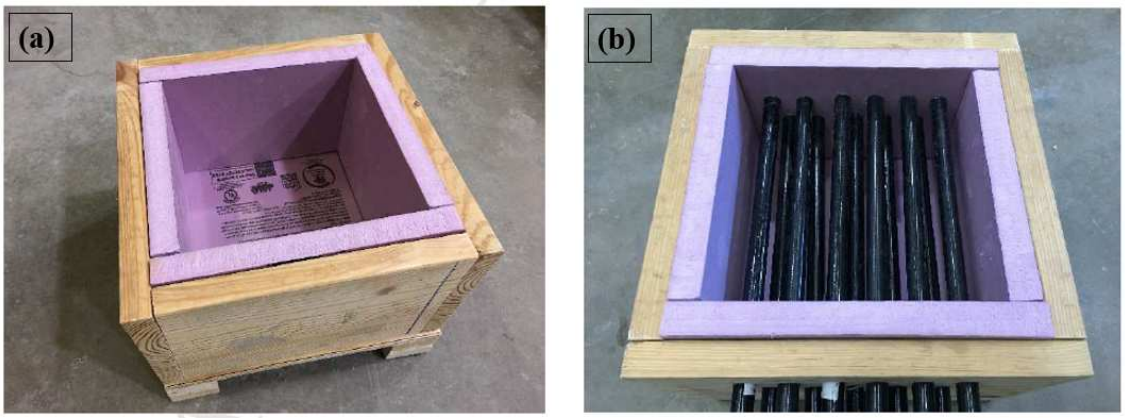

Figure 2.8: Design details for the large-scale concrete slab: (a) mold with thermal insulation, (b) mold with embedded pipes (Farnam, Esmaeeli et al. 2017).

After that, an experimental setup of the snow melting test was carried out by Farnam et al. (2017) using the scenario depicted in Figure 2.9. Thus, two slabs were tested concurrently in the chamber, and the authors used a time-lapse camera with 1 min capturing intervals on top of slabs to record snow melting behavior. Each slab was tilted slightly (2-5°) to allow molten snow (water) to easily flow on the surface of the concrete slab and into a plastic tube that was connected to a beaker on a scale used to collect molten snow (water). The mass change of the cup with molten snow (water) was recorded every 15 min. The temperature in the slab was also recorded every 1 min at eight different locations within the sample (Farnam, Esmaeeli et al. 2017).

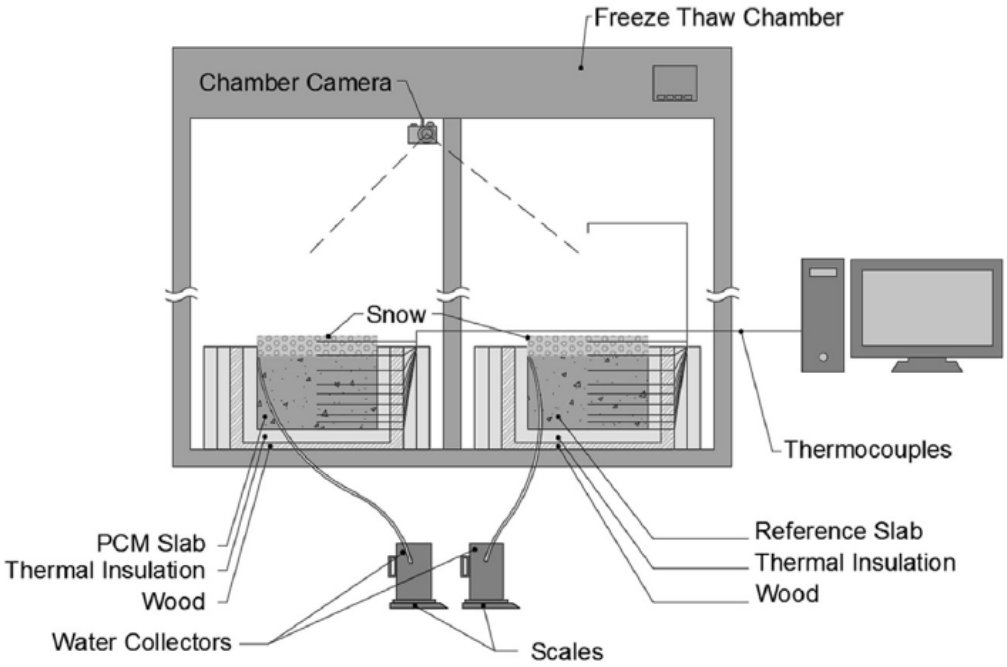

Figure 2.9: Experimental setup of snow melting experiment (the camera sees the surface of the slabs; and to prevent heat transfer through metal pipes, the authors installed additional outer thermal insulations on both sides of the framework where pipes were out of the wood framework) (Farnam, Esmaeeli et al. 2017).

Mohseni et al. (2019) carried out the thermal performance test of concrete containing PCM-LWA using a self-designed environmental chamber, as described in Figure 2.10. The section used to store small test room samples consisted of a wooden box (1 x 1 x1m^3) insulated with polystyrene foam and connected with a split air conditioner unit (a heating/cooling source). The test room samples consisted of six panels, out of which five were made up of wood, while the top panel with PCM-LWA concrete. The dimensions of the top panel were 200 x 200 x 40 mm^3. Thermocouples (Type K resolution ± 0.3 °C) were placed in the center of the test room and at the center, inner and outer surfaces of the concrete panel. The data-logger collected all readings at a recording time interval of 10 min, as shown in Figure 2.10 (Mohseni, Tang et al. 2019).

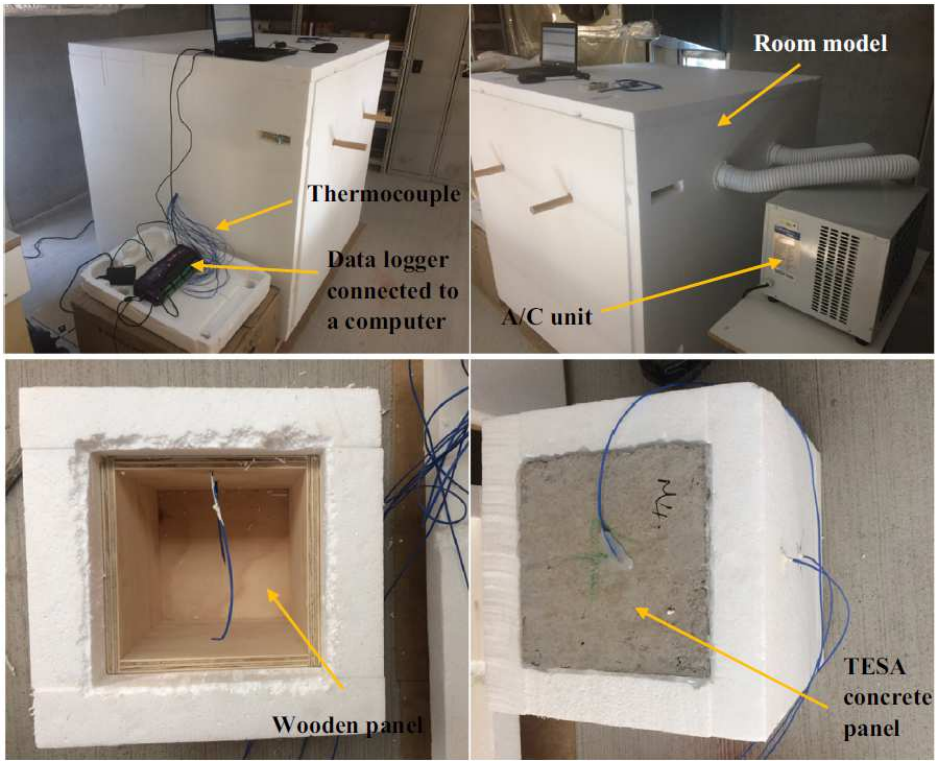

Figure 2.10: Thermal performance test setup (Mohseni, Tang et al. 2019)

2.9. Advantages and disadvantages of incorporation methods of PCMs in building materials

Table 2.3 shows the advantages and disadvantages of different types of incorporation techniques of PCM into building materials. PCMs can be integrated into building materials using many procedures, including (i) direct incorporation, (ii) immersion through materials' pores, (iii) micro-encapsulation, and (iv) macro-encapsulation.

Table 2.3: Methods of incorporating PCMs into building materials with advantages and disadvantages (Zhou, Zhao et al. 2012, Pielichowska and Pielichowski 2014, Farnam, Esmaeeli et al. 2017, Frigione, Lettieri et al. 2019)

Incorporation techniques	Advantages	Disadvantages
Direct incorporation	Simple and cheap. No extra equipment is needed.	Possible leakage of PCM in the melting state. Flammability of the impregnated; elements are potential. Incompatible with construction materials.
Immersion and impregnation method	Simple, practical, and cheap	Leakage and incompatibility can occur, affecting the mechanical properties and the durability of the construction elements.
Micro-encapsulation method	Reduced leakage of PCM during phase transition. Higher heat transfer rate. Improved chemical stability and thermal reliability.	The capsules are expensive; their rigidity may prevent natural convection and reduce the heat transfer rate. The mechanical properties of the construction materials may be affected.
Macro-encapsulation method	A significant quantity of PCM is packed in the container, easiness, and suitability for any specific application.	Poor thermal conductivity and tendency to solidify at the edges. Introduction to the structure must be carried out in situ.

As depicted in Table 2.3, each incorporation technique has advantages and disadvantages before selecting the PCM incorporation method for the building materials. Thus, the significant problems with PCM incorporation are leakage and evaporation of PCM and contact with the outer environment, which can deteriorate the matrix material properties (Jayalath, Mendis et al. 2011). Figure 2.11 illustrates the leakage of butyl stearate as PCM on the surface of the panels after they set (Niall, West et al. 2016).

Figure 2.11: Leakage of PCM from lightweight aggregates (Niall, West et al. 2016)

Concrete is a highly alkaline material, and the pore solution of concrete maintains a significantly high pH environment (Hawes, Banu et al. 1992, Sharma, Neithalath et al. 2013). In previous studies, various PCMs are unstable in an alkaline medium and when exposed to a high pH environment. Also, some polar PCMs experience hydrogen bonding with silica hydrates in concrete and the hydroxyl ions from $Ca(OH)_2$, affecting their incorporation into the system (Hawes and Feldman 1992). There are also known issues with PCMs in concrete associated with the relation between PCM addition and the overall mechanical performance of the concrete (Sharma, Neithalath et al. 2013). The cause of this decrease in mechanical performance has been attributed to chemical and physical interactions between the PCM and the cement hydration products. They may result in the formation of alternative hydration products or decrease the calcium silicate

hydrated (C-S-H) formation and the microstructural influences or inclusion of a weaker phase into the binder of cementitious systems (Hawes, Banu et al. 1992, Hawes and Feldman 1992).

As the nature of PCM is to absorb heat, it may result in a reduced curing temperature for the concrete as it absorbs heat that is being generated by the exothermic hydration reaction, possibly resulting in a lower degree of hydration as compared to OPC mixes without PCM (Hunger and Brouwers 2008, Sharma, Neithalath et al. 2013). The remediation of these issues consists of using pozzolans (i.e., fly ash, silica fume, etc.), which have a beneficial effect on concrete's workability, strength, and durability. The $Ca(OH)_2$ becomes less soluble C-S-H when pozzolanic materials are added. The strength and durability of the concrete are improved considerably. Moreover, the detrimental effects of $Ca(OH)_2$ are reduced by rendering the PCMs more stable in such concrete. The use of modified concrete was found to increase the stability of PCMs, particularly in the more alkaline concretes (Hawes, Banu et al. 1992).

Due to the disadvantages of PCM incorporation techniques mentioned in Table 2.3, PCMs are not used directly in many cases. Instead, some defensive approach is adopted, such as encapsulating or stabilizing them (Pons, Aguado et al. 2014). Therefore, the encapsulation of the PCM with a chemically and physically stable shell is required before PCM can be directly mixed into concrete. The shell can reinforce the PCM microcapsules' surface (cover) hardness by using Zeolite or Zeocarbon (Ling and Poon 2013). About immersion incorporation technique, the main factors affecting the absorption and retention of PCM in concrete are the concrete structure itself, the temperature of the materials, the viscosity of the PCM, duration of immersion in the liquid PCM, area through which absorption occurs, fluid pressure, effect of moisture removal, the polarity of the PCM and age of the concrete (Hawes and Feldman 1992).

2.10. Coating materials for PCM-LWA

To prevent PCM leakage from impregnated LWA, the authors developed different anti-bleeding materials and procedures to cover the surface of PCM-LWA. Memon et al. (2015) indicated that PCM–LWA was immersed in an epoxy mixture with 15% graphite powder for 5 min. The purpose of adding the graphite powder to epoxy was to enhance its thermal conductivity to improve the working efficiency of thermal energy storage LWAC. After that, the coated PCM–LWAs were taken out and put in the tray filled with silica fume. The authors did this to separate the coated PCM-LWA (Memon, Cui et al. 2015).

Meanwhile, Kastiukas et al. (2016) took the PCM-LWA, then either immersed them for 5 min or sprayed them with the Sikalatex (commercial synthetic rubber emulsion) and Weber dry-lastic (commercial liquid waterproof membrane) coating materials. Then Kastiukas et al. subjected the PCM-LWA to curing drying regimes in a revolving mechanical drum laid flat on a metal net in ambient air or the climatic chamber (Kastiukas, Zhou et al. 2016). In the case of the Palatal (polyester resin adhesive) coating, it was poured over the PCM-LWA and mixed with a plastic spatula for 3 min. The Palatal powder coating was further modified with carbon-based nanomaterials. One type of modification was incorporating milled carbon fibers (CF) (length of 80 microns) into the layer during resin mixing. The authors mixed the CF at 10 wt% of resin. Before the authors effectively used the filler material, its surface had to be treated with silane to improve the dispersion and bonding to the resin. The silane was used as hexamethyldisilazane and was used as 3 wt% of CF. the authors did the second type of modification by spraying the resin coatings with graphite spray (GS) (Kastiukas, Zhou et al. 2016). In 2017, Liu et al. soaked PCM-LWA into 25% silica sol for about 20 min at room temperature. The volume ratio between PCM-LWA and silica sol was about 1:3, and while soaking, the magnetic stirring with a speed of 60 rpm

was occasionally applied for a more homogenous effect. Then the PCM-LWA was filtered and dried over the air (Liu, Wang et al. 2017).

As illustrated in Figure 2.12, Mohseni et al. (2019) demonstrated the impregnation and coating scenario on LWA. According to the experimental procedure, the PCM-LWA was immersed in an epoxy mixture for 10 minutes. Then, the coated PCM-LWA were poured into a silica fume for a second coating layer. After that, the PCM-LWA was stored for seven days to allow the epoxy to cure before using it as thermal energy storage aggregates (TESA) in making concrete (Mohseni, Tang et al. 2019).

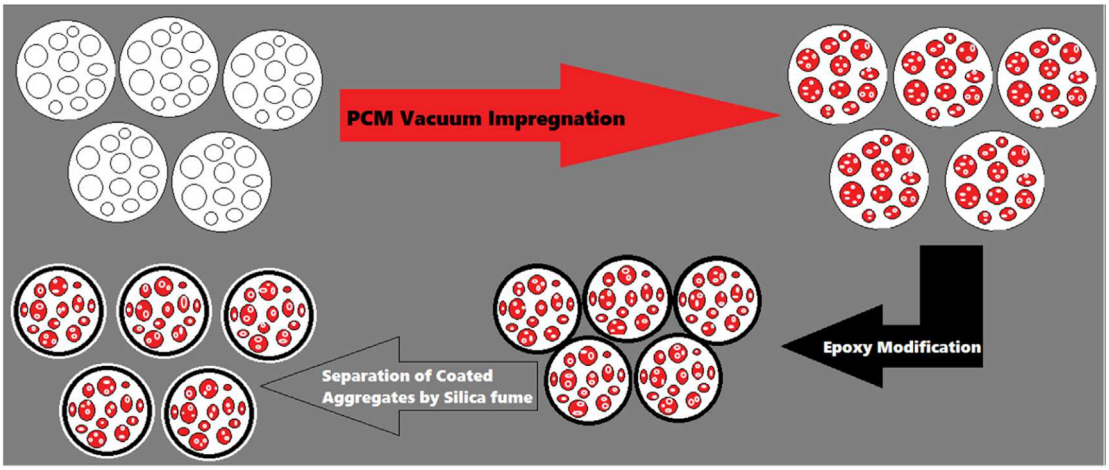

Figure 2.12: Coating process (Mohseni, Tang et al. 2019)

Kakar et al. (2020) utilized epoxy glue to coat PCM-LWA. The gluing material was prepared in a separate container, and the PCM-LWA particles were introduced while gently revolving the container horizontally by hand. Afterward, ordinary Portland cement (OPC) was used to cover the glue on the surface of the particles. After visually assuring the complete coating of particles, these coated particles were left for 10 h in the air to dry at room temperature. Then, the authors applied a final second layer of epoxy coating, and the particles were left at room

temperature for another 10 h. For control particles, the same coating procedure was carried out for particles without impregnation of PCM (Kakar, Refaa et al. 2019).

2.11. Lightweight aggregate

Stephen J. Hayde is the father of the Lightweight Concrete Industry From the remnants in a brick cull pile, the lightweight aggregate was developed By T.W. Bremner and John Ries (ACI Committee 213-14). Builders have long recognized the importance of reducing concrete density while maintaining its durability and strength. The Romans used natural deposits of vesicular aggregates such as pumice and scoria as the aggregates of choice for their structures even when normal density sand and river gravel were readily available (ACI Committee 213-14). Hayde was so sure of the virtues of his new material that he engaged a patent attorney on January 29, 1914. U.S. Patent No. 1,255,878 was subsequently issued in Hayde's name on February 18, 1918. The patent covered argillaceous material and specifically mentioned "special clay, slate, and shale rock," implying that not all argillaceous material is suitable and that the product must be heated to a temperature of 1220 °C (2228 °F) for about 2 hours. Lightweight aggregates (LWAs) are produced in several ways. Some are made in manufacturing plants from raw materials, including suitable shales, clays, slates, fly ashes, or blast-furnace slags. Naturally occurring LWAs are mined from volcanic deposits that include pumice and scoria. Pyro-processing methods include the rotary kiln and sintering processes. Solid and durable LWAs contain a uniformly distributed system of pores with a size range of approximately 5 to 300 μm, developed in a continuous, relatively crack-free, high-strength vitreous phase (ACI Committee 213-14), as shown in Figure 2.13 (Weiss and Burkan Isgor , Bentz and Turpin 2007, Weiss, Snyder et al. 2013, Mohseni, Tang et al. 2019).

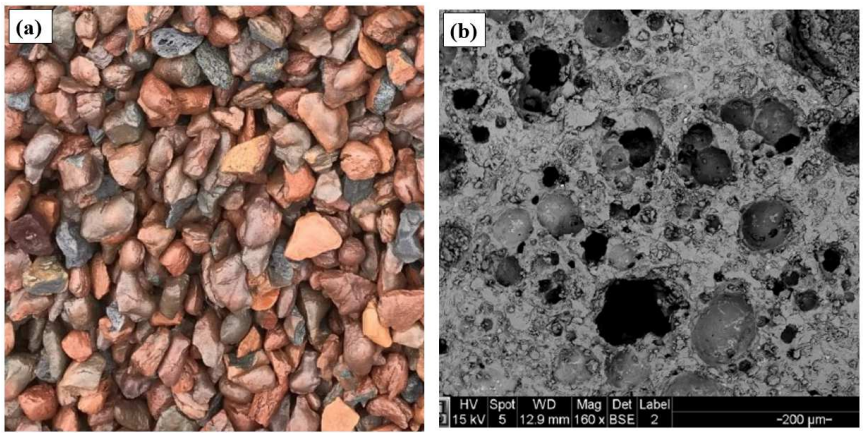

Figure 2.13: Lightweight aggregate: (a) LWA and (b) SEM of LWA (Mohseni, Tang et al. 2019)

In general, aggregates affect the quality of concrete through soundness (ASTM E90 sound transmission loss) and gradation (ASTM C33/C33M concrete aggregates). Aggregates do not take part in hydration reactions, but they are inert filler materials. Thus, they are necessary for certain exposure conditions (severe abrasion or sustained high temperature) that may require selected aggregates. Well-graded aggregates require less paste for coating and are more economical (Thienel, Haller et al. 2020).

Expanded clay is a lightweight porous aggregate with a water absorption capacity of 17.9%. Therefore, expanded clay could be helpful for internal water curing for concrete to store water and supply it to the cement paste during the cementitious reactions (Bentz 2008). Internal curing is a more efficient and enhanced method of curing concrete because of the process that the concrete undergoes, and it does not potentially require maintenance due to the presence of pre-saturated fine lightweight aggregate within the cement matrix (Dale P. Bentz 2010). The porous nature of the aggregate is advantageous for reducing the shrinkage of concrete (Choi, Ryu et al. 2019), this is due to its internal curing effect through the slow release of moisture from the saturated porous particles (Henkensiefken, Bentz et al. 2009). Concrete is also known for being

soundproof because it acts and absorbs sound waves; concrete is an effective barrier for noise (Stott 2019). Concrete mixed with paraffin (PCM) impregnated aggregate can store heat inside the concrete and prevent heat from transmitting further inside the concrete. In the case of sound transmission loss, the effect of paraffin filling up the voids of aggregates seems to lower the sound property of the concrete due to decreasing porosity (Sukontasukkul, Intawong et al. 2016).

2.12. Summary of the Chapter

Studies have been undertaken about the types, incorporation techniques, effects, and benefits of PCMs in building materials. However, a few aspects of PCMs still need more investigation to make PCMs more reliable in cement-based materials (CBM).

Regardless of the different classes and categories of PCMs, the most important criteria are that PCMs should be commercially available, low-cost, environmentally friendly, and recyclable. Organic PCM, particularly paraffin, met most of these criteria due to its effectiveness in cement-based materials. DSC analysis has been used to determine the thermal properties of PCMs by many authors.

Various authors have investigated the incorporation of PCMs through encapsulation methods (macro or microencapsulation) because these techniques packed a significant quantity of PCM and reduced leakage. However, the capsules or shells need to be very rigid for microencapsulation. The container for macro encapsulation should have a high thermal conductivity to increase the heat transfer rate and thus prevent partial melting. Although many studies have not been conducted, the impregnation method is simple, low cost, and reliable when well coated with appropriate anti-bleeding materials.

CBM containing PCMs has been tested for thermal performance in a hot and cold environment. However, most of these tests were carried out in thermally controlled environmental

chambers where artificial conditions were programed and simulated to predict the thermal performance of CBM containing PCM in actual summer or winter climate conditions.

This research proposes the utilization of laboratory-made low-cost organic PCMs and anti-bleeding materials. Then it develops a well-described impregnation method of PCMs into lightweight aggregates (LWA). The PCM-LWA produced are tested for leakage, water absorption, and specific gravity. Then, the concrete specimen blocks are studied for compressive strength, thermal conductivity, temperature fluctuation, and energy stored and discharged. In this study, the thermal performance of the concrete blocks is investigated in the field and exposed to actual winter and summer weather conditions.

2.13. Reference

ACI Committee 213-14. Available: http://web.nationalbuildingarts.org/collections/cementitious/expanded-shale-haydite/stephen-j-hayde-article/ Stephen J. Hayde: Father of the Lightweight Concrete Industry 2014.

Akeiber, H. J., M. A. Wahid, H. M. Hussen and A. T. Mohammad (2014). "Review of development survey of phase change material models in building applications." Scientific World Journal, Hindawi Publishing Corporation. **2014**.

Al-Absi, Z. A., M. H. M. Isa and M. Ismail (2020). "Phase change materials (PCMs) and their optimum position in building walls." Sustainability (Switzerland), MDPI. **12**.

Amaral, C., R. Vicente, P. A. A. P. Marques and A. Barros-Timmons (2017). "Phase change materials and carbon nanostructures for thermal energy storage: A literature review." Renewable and Sustainable Energy Reviews **79**: 1212-1228.

Badenhorst, H. and L. F. Cabeza (2017). "Critical analysis of the T -history method: A fundamental approach." Thermochimica Acta **650**: 95-105.

Baetens, R., B. P. Jelle and A. Gustavsen (2010). "Phase change materials for building applications: A state-of-the-art review." Energy and Buildings, Elsevier Ltd. **42:** 1361-1368.

Bao, X., S. A. Memon, H. Yang, Z. Dong and H. Cui (2017). "Thermal properties of cement-based composites for geothermal energy applications." Materials, MDPI AG. **10**.

Barzin, R., J. J. J. Chen, B. R. Young and M. M. Farid (2015). "Application of PCM underfloor heating in combination with PCM wallboards for space heating using price based control system." Applied Energy **148**: 39-48.

Bayon, R. and E. Rojas (2019). "Development of a new methodology for validating thermal storage media: Application to phase change materials." Int J Energy Res **43**(12): 6521-6541.

Bentz, D. P. (2008). "A review of early-age properties of cement-based materials." Cement and Concrete Research **38**(2): 196-204.

Bentz, D. P. and R. Turpin (2007). "Potential applications of phase change materials in concrete technology." Cement and Concrete Composites. **29:** 527-532.

Cellat, K., B. Beyhan, B. Kazanci, Y. Konuklu and H. Paksoy (2017). "Direct incorporation of butyl stearate as phase change material into concrete for energy saving in buildings." Journal of Clean Energy Technologies. **5:** 64-68.

Chandel, S. S. and T. Agarwal (2017). "Review of current state of research on energy storage, toxicity, health hazards and commercialization of phase changing materials." Renewable and Sustainable Energy Reviews **67**: 581-596.

Choi, S., G. S. Ryu, K. T. Koh, G. H. An and H. Y. Kim (2019). "Experimental study on the shrinkage behavior and mechanical properties of AAM mortar mixed with CSA expansive additive." Materials (Basel) **12**(20).

Cui, Y., J. Xie, J. Liu, J. Wang and S. Chen (2017). "A review on phase change material application in building." Advances in Mechanical Engineering, SAGE Publications Inc. **9**.

Dakhli, Z., K. Chaffar and Z. Lafhaj (2019). "The Effect of phase change materials on the physical, thermal and mechanical properties of cement." Sci, MDPI AG. **1:** 27.

Dale P. Bentz, W. J. W. (2010). "Internal curing: A 2010 state of the art review." National Institute of Standards and Technology.

Faraj, K., M. Khaled, J. Faraj, F. Hachem and C. Castelain (2020). "Phase change material thermal energy storage systems for cooling applications in buildings: A review." Renewable and Sustainable Energy Reviews, Elsevier Ltd. **119**.

Farnam, Y., H. S. Esmaeeli, P. D. Zavattieri, J. Haddock and J. Weiss (2017). "Incorporating phase change materials in concrete pavement to melt snow and ice." Cement and Concrete Composites, Elsevier Ltd. **84:** 134-145.

Farnam, Y., M. Krafcik, L. Liston, T. Washington, K. Erk, B. Tao and J. Weiss (2016). "Evaluating the use of phase change materials in concrete pavement to melt ice and snow." Journal of Materials in Civil Engineering, American Society of Civil Engineers (ASCE). **28:** 04015161.

Fenollera, M., J. L. Míguez, I. Goicoechea, J. Lorenzo and M. Á. Álvarez (2013). "The influence of phase change materials on the properties of self-compacting concrete." Materials. **6:** 3530-3546.

Fernandes, F., S. Manari, M. Aguayo, K. Santos, T. Oey, Z. Wei, G. Falzone, N. Neithalath and G. Sant (2014). "On the feasibility of using phase change materials (PCMs) to mitigate thermal cracking in cementitious materials." Cement and Concrete Composites, Elsevier Ltd. **51:** 14-26.

Frigione, M., M. Lettieri and A. Sarcinella (2019). "Phase change materials for energy efficiency in buildings and their use in mortars." Materials, MDPI AG. **12**.

Gandhi, M., A. Kumar, R. Elangovan, C. S. Meena, K. S. Kulkarni, A. Kumar, G. Bhanot and N. R. Kapoor (2020). "A review on shape-stabilized phase change materials for latent energy storage in buildings." Sustainability (Switzerland), MDPI. **12:** 1-17.

Giro-Paloma, J., R. Al-Shannaq, A. I. Fernández and M. M. Farid (2016). "Preparation and characterization of microencapsulated phase change materials for use in building applications." Materials, MDPI AG. **9**.

Hawes, D. W., D. Banu and D. Feldman (1992). "The stability of phase change materials in concrete." Solar Energy Materials and Solar Cells **27:** 103-118.

Hawes, D. W. and D. Feldman (1992). "Absorption of phase change materials in concrete." Solar Energy Materials and Solar Cells **27:** 91-101.

Henkensiefken, R., D. Bentz, T. Nantung and J. Weiss (2009). "Volume change and cracking in internally cured mixtures made with saturated lightweight aggregate under sealed and unsealed conditions." Cement and Concrete Composites **31**(7): 427-437.

Hu, Y., R. Guo, P. K. Heiselberg and H. Johra (2020). "Modeling PCM phase change temperature and hysteresis in ventilation cooling and heating applications." Energies **13**(23).

Hunger, M. and H. J. H. Brouwers (2008). "Natural stone waste powders applied to SCC mix design." Restoration of Buildings and Monuments **14:** 131-140.

Hunger, M., A. G. Entrop, I. Mandilaras, H. J. H. Brouwers and M. Founti (2009). "The behavior of self-compacting concrete containing micro-encapsulated Phase Change Materials." Cement and Concrete Composites **31:** 731-743.

Iten, M., S. Liu and A. Shukla (2016). "A review on the air-PCM-TES application for free cooling and heating in the buildings." Renewable and Sustainable Energy Reviews **61**: 175-186.

Jayalath, A., P. Mendis, R. Gammampila and L. Aye (2011). "Applications of phase change materials in concrete for sustainable built environment: a review." Proceedings of the International Conference on Structural Engineering, Construction and Management **1** (1): 1-13.

Jayalath, A., R. San Nicolas, M. Sofi, R. Shanks, T. Ngo, L. Aye and P. Mendis (2016). "Properties of cementitious mortar and concrete containing micro-encapsulated phase change materials." Construction and Building Materials, Elsevier Ltd. **120:** 408-417.

Jung Heum Yeon, a. K.-K. K. b. (2018). "Potential applications of phase change materials to mitigate freeze-thaw deteriorations in concrete pavement." Construction and Building Materials **177**: 202-209.

Kakar, M. R., Z. Refaa, J. Worlitschek, A. Stamatiou, M. N. Partl and M. Bueno (2019). "Impregnation of lightweight aggregate particles with phase change material for its use in asphalt mixtures." International Symposium on Asphalt Pavement & Environment, Springer.337-345

Kalombe, R. M., V. T. Ojumu, C. P. Eze, S. M. Nyale, J. Kevern and L. F. Petrik (2020). "Fly Ash-Based Geopolymer Building Materials for Green and Sustainable Development." Materials (Basel) **13**(24).

Kasaeian, A., L. bahrami, F. Pourfayaz, E. Khodabandeh and W. M. Yan (2017). "Experimental studies on the applications of PCMs and nano-PCMs in buildings: A critical review." Energy and Buildings, Elsevier Ltd. **154:** 96-112.

Kastiukas, G., X. Zhou and J. Castro-Gomes (2016). "Development and optimisation of phase change material-impregnated lightweight aggregates for geopolymer composites made from aluminosilicate rich mud and milled glass powder." Construction and Building Materials, Elsevier Ltd. **110:** 201-210.

Kenisarin, M. M., K. Mahkamov, S. C. Costa and I. Makhkamova (2020). "Melting and solidification of PCMs inside a spherical capsule: A critical review." Journal of Energy Storage **27**.

Khudhair, A. M. and M. M. Farid (2004). "A review on energy conservation in building applications with thermal storage by latent heat using phase change materials." Energy Conversion and Management, Elsevier Ltd. **45:** 263-275.

Li, M., Z. Wu and J. Tan (2013). "Heat storage properties of the cement mortar incorporated with composite phase change material." Applied Energy, Elsevier Ltd. **103:** 393-399.

Ling, T. C. and C. S. Poon (2013). "Use of phase change materials for thermal energy storage in concrete: An overview." Construction and Building Materials. **46:** 55-62.

Liu, F., J. Wang and X. Qian (2017). "Integrating phase change materials into concrete through microencapsulation using cenospheres." Cement and Concrete Composites, Elsevier Ltd. **80:** 317-325.

Marani, A. and M. L. Nehdi (2019). "Integrating phase change materials in construction materials: Critical review." Construction and Building Materials, Elsevier Ltd. **217:** 36-49.

Martínez, A., M. Carmona, C. Cortés and I. Arauzo (2020). "Characterization of thermophysical properties of phase change materials using unconventional experimental technologies." Energies **13**(18).

Memon, S. A., H. Z. Cui, H. Zhang and F. Xing (2015). "Utilization of macro encapsulated phase change materials for the development of thermal energy storage and structural lightweight aggregate concrete." Applied Energy, Elsevier Ltd. **139:** 43-55.

Mohseni, E., W. Tang and S. Wang (2019). "Development of thermal energy storage lightweight structural cementitious composites by means of macro-encapsulated PCM." Construction and Building Materials, Elsevier Ltd. **225:** 182-195.

Muller, L., G. Rubio-Perez, A. Bach, N. Munoz-Rujas, F. Aguilar and J. Worlitschek (2020). "Consistent DSC and TGA methodology as basis for the measurement and comparison of thermo-physical properties of phase change materials." Materials (Basel) **13**(20).

Nazir, H., M. Batool, F. J. Bolivar Osorio, M. Isaza-Ruiz, X. Xu, K. Vignarooban, P. Phelan, Inamuddin and A. M. Kannan (2019). "Recent developments in phase change materials for energy storage applications: A review." International Journal of Heat and Mass Transfer **129:** 491-523.

Niall, D., R. P. West and S. McCormack (2016). "Assessment of two methods of enhancing thermal mass performance of concrete through the incorporation of phase-change materials." SDAR* Journal of Sustainable Design & Applied Research Research. **4:** 2016-2027.

Nizovtsev, M. I., V. Y. Borodulin, V. N. Letushko, V. I. Terekhov, V. A. Poluboyarov and L. K. Berdnikova (2019). "Heat transfer in a phase change material under constant heat flux." Thermophysics and Aeromechanics, Kutateladze Institute of Thermophysics SB RAS. **26:** 313-324.

Omaraa, E., W. Saman, F. Bruno and M. Liu (2017). "Modified T-history method for measuring thermophysical properties of phase change materials at high temperature." AIP Conference Proceedings. **1850**(1).

Pielichowska, K. and K. Pielichowski (2014). "Phase change materials for thermal energy storage." Progress in Materials Science, Elsevier Ltd. **65:** 67-123.

Pilehvar, S., A. M. Szczotok, J. F. Rodríguez, L. Valentini, M. Lanzón, R. Pamies and A. L. Kjøniksen (2019). "Effect of freeze-thaw cycles on the mechanical behavior of geopolymer concrete and Portland cement concrete containing micro-encapsulated phase change materials." Construction and Building Materials, Elsevier Ltd. **200:** 94-103.

Pons, O., A. Aguado, A. I. Fernández, L. F. Cabeza and J. M. Chimenos (2014). "Review of the use of phase change materials (PCMs) in buildings with reinforced concrete structures." Materiales de Construccion, Inst. de Ciencias de la Construccion Eduardo Torroja. **64**.

Qu, Y., J. Chen, L. Liu, T. Xu, H. Wu and X. Zhou (2020). "Study on properties of phase change foam concrete block mixed with paraffin / fumed silica composite phase change material." Renewable Energy, Elsevier Ltd. **150:** 1127-1135.

Šavija, B. (2018). "Smart crack control in concrete through use of phase change materials (PCMs): A review." Materials, MDPI AG. **11**.

Stott, G. February 25th 2019. "Can Sound Travel Through Concrete Wall. Concrete fencing experts. Advance forming technology." Available at: https://aftec.com/concrete-construction/can-sound-travel-through-concrete-walls/ hhh Accessed on June 4th, 2021.

Sharma, A., V. V. Tyagi, C. R. Chen and D. Buddhi (2009). "Review on thermal energy storage with phase change materials and applications." Renewable and Sustainable Energy Reviews. **13:** 318-345.

Sharma, B., N. Neithalath, S. Rajan and B. Mobasher (2013). "Incorporation of phase change materials into cementitious systems." Master's Thesis. Arizona State University, Phoenix, USA.

She, Z., Z. Wei, B. A. Young, G. Falzone, N. Neithalath, G. Sant and L. Pilon (2019). "Examining the effects of microencapsulated phase change materials on early-age temperature evolutions in realistic pavement geometries." Cement and Concrete Composites, Elsevier Ltd. **103:** 149-159.

Sivanathan, A., Q. Dou, Y. Wang, Y. Li, J. Corker, Y. Zhou and M. Fan (2020). "Phase change materials for building construction: An overview of nano-/micro-encapsulation." Nanotechnology Reviews, De Gruyter Open Ltd. **9:** 896-921.

Sukontasukkul, P., E. Intawong, P. Preemanoch and P. Chindaprasirt (2016). "Use of paraffin impregnated lightweight aggregates to improve thermal properties of concrete panels." Materials and Structures/Materiaux et Constructions, Kluwer Academic Publishers. **49:** 1793-1803.

Sukontasukkul, P., T. Sangpet, M. Newlands, D. Y. Yoo, W. Tangchirapat, S. Limkatanyu and P. Chindaprasirt (2020). "Thermal storage properties of lightweight concrete incorporating phase change materials with different fusion points in hybrid form for high temperature applications." Heliyon, Elsevier Ltd. **6**.

Thienel, K. C., T. Haller and N. Beuntner (2020). "Lightweight concrete-from basics to innovations." Materials (Basel) **13**(5).

Tyagi, V. V., S. C. Kaushik, S. K. Tyagi and T. Akiyama (2011). "Development of phase change materials based microencapsulated technology for buildings: A review." Renewable and Sustainable Energy Reviews. **15:** 1373-1391.

Urgessa, G., K. K. Yun, J. Yeon and J. H. Yeon (2019). "Thermal responses of concrete slabs containing microencapsulated low-transition temperature phase change materials exposed to realistic climate conditions." Cement and Concrete Composites, Elsevier Ltd. **104**.

Wang, R., M. Ren, X. Gao and L. Qin (2018). "Preparation and properties of fatty acids based thermal energy storage aggregate concrete." Construction and Building Materials, Elsevier Ltd. **165:** 1-10.

Weiss, J., K. Snyder, J. Bullard and D. Bentz (2013). "Using a saturation function to interpret the electrical properties of partially saturated concrete." Journal of Materials in Civil Engineering, American Society of Civil Engineers (ASCE). **25:** 1097-1106.

Weiss, W. J. and O. Burkan Isgor (2018). "Examining how saturation and pore solution chemistry impact durability test methods, specifications and service life models (Keynote)." Reactive-Transport Modeling in Porous MediaResistivity. Formation Factor and Transport.

Xie, J., Y. Li, W. Wang, S. Pan, N. Cui and J. Liu (2013). "Comments on thermal physical properties testing methods of phase change materials." Advances in Mechanical Engineering **5**.

Yang, G., Y. J. Yim, J. W. Lee, Y. J. Heo and S. J. Park (2019). "Carbon-filled organic phase-change materials for thermal energy storage: A review." Molecules, MDPI AG. **24**.

Zeinelabdein, R., S. Omer, E. Mohamed and G. Gan (2018). "Free cooling using phase change material for buildings in hot-arid climate." International Journal of Low-Carbon Technologies, Oxford University Press. **13:** 327-337.

Zhang, D., Z. Li, J. Zhou and K. Wu (2004). "Development of thermal energy storage concrete." Cement and Concrete Research. **34:** 927-934.

Zhou, D., C. Y. Zhao and Y. Tian (2012). "Review on thermal energy storage with phase change materials (PCMs) in building applications." Applied Energy, Elsevier Ltd. **92:** 593-605.

Zhou, D., Y. Zhou, Y. Liu, X. Luo and J. Yuan (2019). "Preparation and performance of capric-myristic acid binary eutectic mixtures for latent heat thermal energy storages." Journal of Nanomaterials, Hindawi Limited. **2019**.

CHAPTER 3: METHODOLOGY

3.1. Experimental outline

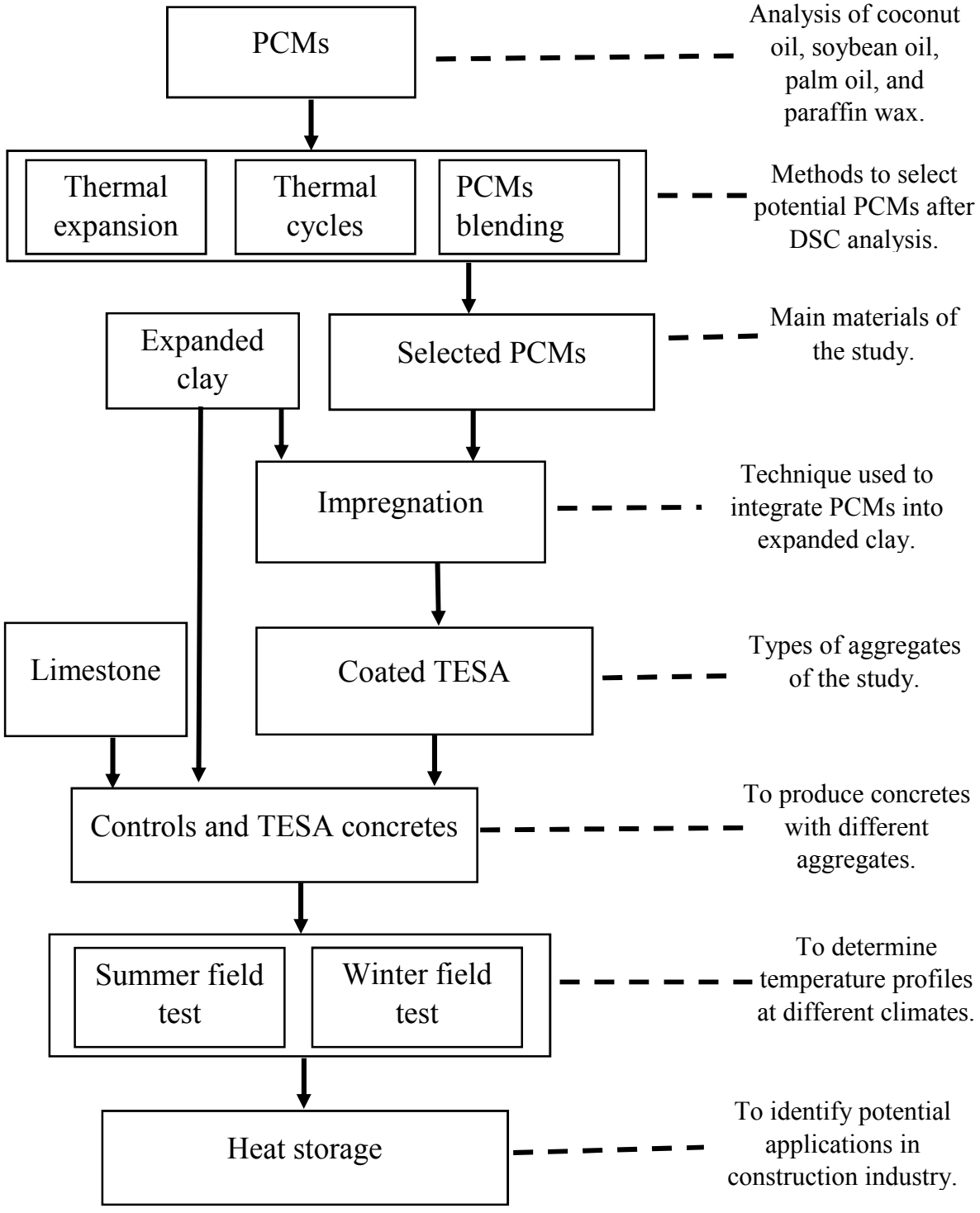

Figure 3.1: Experimental outline

3.2. Materials and chemicals

3.2.1. Sampling and storage of materials

This study utilized low-cost and readily available organic PCMs, including paraffin wax (PW), soybean oil (SO), red palm oil (PO), and coconut oil (CO). The porous LWA used was expanded clay supplied by Arcosa (Baton Rouge, LA). The present project used the coating materials consisting of latex (concrete bonding adhesive/acrylic fortifier), acrylic (generic coating in xylene type 1), epoxy, and paste (water/cement ratio of 0.75).

3.2.2. Chemicals and equipment

The chemicals and equipment used in this study are depicted in Table 3.1 and Table 3.2, respectively.

Table 3.1: Chemicals and suppliers

Chemical	Location
Blended Paraffin waxes	
Generic coating resin in xylene type 1 (Acrylic)	
Non-GMO Gourmet Soybean oil	
Nutiva Organic, Refined Coconut Oil	USA
Pure unrefined red Palm oil	
Sikadur -22 Lo-Mod Epoxy	
SikaLatex R (Latex)	
WD 40	

Table 3.2: Equipment and supplier

Equipment	Location
20 qt Planetary Mixer - Bench Model	
Automatic roaster oven	
Belt driver fan and blower motor	
CR1000, multiplexers, lithium battery	
Filter paper	
Hot Plate Extra Burner	USA
Molds (iron)	
Nylon rod	
Paper towel	
Type t-wire thermocouples	
Vacuum pump	
Wire connectors	
Volumetric flask	

3.3. Experimental procedures

3.3.1. Thermal analysis

The differential scanning calorimetry (DSC) was carried out to determine the melting and crystallization processes of PCMs after preparing sample through thermal expansion, thermal cycles, and blended test. Each of these techniques was performed as described below:

3.3.2. Differential scanning calorimetry (DSC) analysis

DSC (2500 TA instruments) DSC measures temperatures and heat flow associated with thermal transitions in a material (TA Instruments 2022). DSC techniques measure properties such as glass transitions, cold (crystallization), phase changes, melting, crystallization, product stability, cure/cure kinetics, and oxidative stability. DSC technology significantly improves baseline flatness, transition resolution, and sensitivity. It allows direct heat capacity measurement and makes the analytical experiments faster and more accurate (TA Instruments 2022).

As shown in Figure 3.2 and Table 3.3, the DSC 2500 (manufactured by TA instruments) was used to determine crystallization and melting temperatures, and latent heat of fusion. During the test, PCMs were poured into used Tzero Aluminum Hermetic pans with airtight lids to contain the PCMs. DSC operated between -90 °C to 80 °C, heating/cooling rate of 3 °C/min with 2 min isothermal holds at both minimum and maximum temperatures. This test was performed under an inert nitrogen atmosphere at a 20 mL/min flow rate. The mass of PCMs was 13 ± 2 mg.

Table 3.3: PCMs and temperature range used for DSC analysis

PCMs	Temperature (°C)
PW	-30 – 80
CO	-30 – 80
SO	-90 – 80
PO	-30 – 80

Note: PW, CO, SO, PO, and wt% stands for paraffin wax, coconut oil, soybean oil, and palm oil.

Figure 3.2: DSC equipment used for thermal analysis of PCMs

3.3.3. Blending of PCMs

After obtaining the thermal properties results of the as-received PCMs, different combinations of PCMs illustrated in Table 3.4 were prepared and investigated to improve melting and crystallization processes across a wider temperature range. Thus, two or three different types of PCMs (in liquid state) were mixed in a beaker using a stirring bar while heating up on a hot plate at about 80 °C for 10 mins. The blended PCMs were allowed to cool and analyzed using DSC.

Table 3.4: PCMs blending proportions

ID name	PCMs (wt.%)
PWCO	PW (50)+ CO (50)
PWSO	PW (50) + SO (50)
COSO	CO (50) + SO (50)
PWCOSO	SO (30) + CO (30) + PW (40)

Note: wt.% stands for weight percent, blended paraffin wax with coconut oil (PWCO), paraffin wax with soybean (PWSO), coconut oil with soybean oil (COSO), paraffin wax, coconut oil with soybean oil (PWCOSO).

3.3.4. Thermal cycles of PCMs

The thermal cycle test was performed by placing a specific amount of PCM into a container and placing it in the oven, then heating it at 80 °C for 6 hours, then removing it to cool at room temperature for 6 hours in one cycle as depicted in Figure 3.3. The experiment was repeatedly run (heating and cooling) 11 times, equivalent to 11 cycles. After that, the PCMs were analyzed using DSC to identify the new melting and solidification processes.

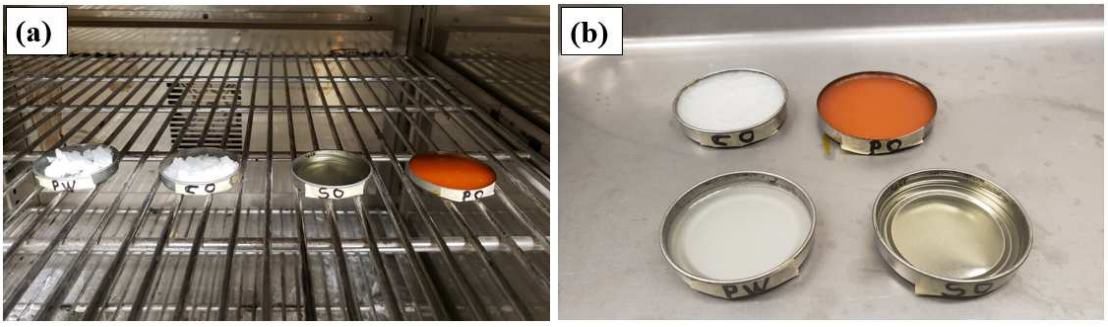

Figure 3.3: Thermal cycles analysis of PCMs, (a) in the oven and (b) at room temperature

3.3.5. Thermal expansion of PCMs

The thermal expansion test determined the volume change of PCMs after one full cycle. PCMs were heated on a hot plate at about 80 °C for 10 mins, then the melted solution of PCMs was poured into a graduated cylinder, where its initial volume and mass were recorded. Then, the graduated cylinder was put in the freezer set at -23 °C for 120 mins. After that, the thermal expansion was determined using equation (3.1).

$$\beta = \frac{1}{V_o}\frac{\Delta V}{\Delta T} \qquad (3.1)$$

where: β: thermal expansion (1/°C) (or volumetric thermal expansion coefficient), V_o: particular volume measurement (mL), ΔV: change in volume (mL), and ΔT: change in temperature (°C).

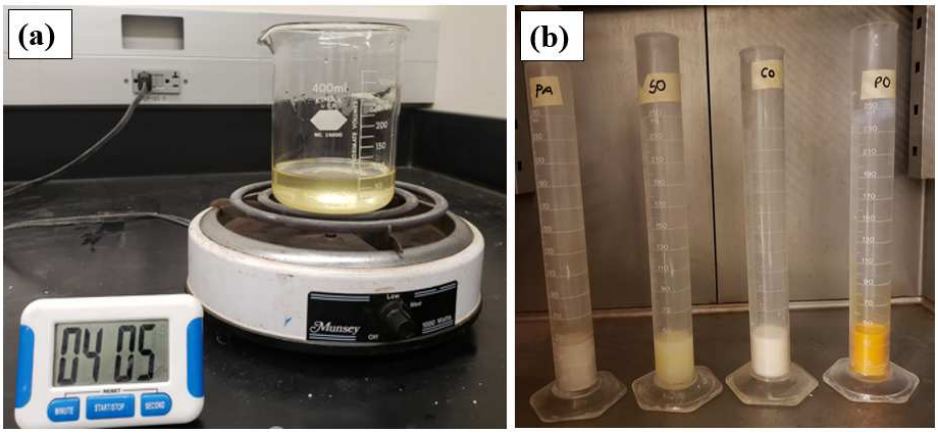

Figure 3.4: Thermal expansion steps, (a) melting PCM and (b) PCMs in the freezer

3.4. Production of thermal energy storage aggregates (TESA)

After characterizing different PCMs, TESA was produced using expanded clay as lightweight aggregate (LWA). LWA was impregnated with the selected PCMs, then coated with anti-bleeding materials such as cement paste, latex, acrylic, and epoxy. The production of TESA concrete was carried out as described below.

3.4.1. Impregnation of PCMs into the expanded shale and use of anti-bleeding

The as-received expanded clay LWA was first dried in an oven at 110 °C for 72 hrs. Then, the oven dried LWA was graded 4.75 mm minimum. The graded LWA was blown dry with compressed air to remove surface and pores dust. Then, a specific quantity of LWA was weighed, poured in the volumetric flask, and vacuumed for 20 mins to further remove the air in the pores, as shown in Figure 3.5a-d.

Figure 3.5: (a) As received expanded shale, (b) sieving process, (c) dusting with a compressed air, and (d) pump vacuuming of LWA

The impregnation technique consisted of filling the pores of expanded clay LWA with PCMs (in liquid state) using a vacuum pump, as shown in Figure 3.6. After air was entrapped within the LWA's pores were removed, under vacuum pressure at about -860 mbar, for as much as the pump could release (visual judgment). Liquid PCM was then allowed to enter the vacuum chamber, and LWA was submerged in the PCM. Vacuum was applied until no visible air bubbles were seen emanating from the LWA for approximately 30 mins. The air was then allowed to enter the volumetric flask to help force the PCM into the pores of LWA for about 20 mins. Afterwards, the PCM-LWA was vacuum impregnated for an additional 10 mins at a pressure of -860 mbar. The temperature during the entire impregnation process was kept above the melting point of PCM as shown in Figure 3.6a. Afterwards, particles were removed and excess PCM were allowed to drain from the surface of the particles for about 45 seconds (Figure 3.6b). PCM-LWA particles were dried using paper towels to reach saturated surface-dry (SSD) condition (Figure 3.6c) to form TESA (Figure 3.6d). The TESA was stored in the environmental chamber at 23.03±2 °C and 50% relative humidity for seven days before any coating.

Figure 3.6: Steps for impregnating PCM into expanded clay (a) impregnation of PCM into LWA's pores, (b) drainage of PCM, (c) SSD process, and (d) TESA as final products.

3.4.2. Coating TESA with anti-bleeding materials

In this study, to prevent leakage of PCMs from TESA, a coating material was applied on the surface of TESA, as depicted in Figure 3.7. The anti-bleeding materials consisted of cement paste (water to cement ratio of 0.75), latex, acrylic, and epoxy. The quantity of coating material used was equivalent to 10 wt% of the mass of TESA to be coated. Therefore, TESA was coated by pouring a specific amount of TESA in a 5 gallons bucket; this bucket was placed on a belt drive and blower motor. Then the liquid solution of the coating material was poured into the bucket. This heterogeneous mixture was stirred using a belt drive and blower motor for about 10 min. During this period, a spoon was gently used by hand to ensure a complete coating of all TESA particles (visual judgment). The coated TESA particles were spread out on a table covered with plastic sheets and left in the air to dry at room temperature for 24 h. After that, the coated TESA was stored at 23.02 ± 2 °C and 50% RH in the environmental chamber for seven days to allow the coating material to cure. Then, the mass gained by TESA after coating was estimated.

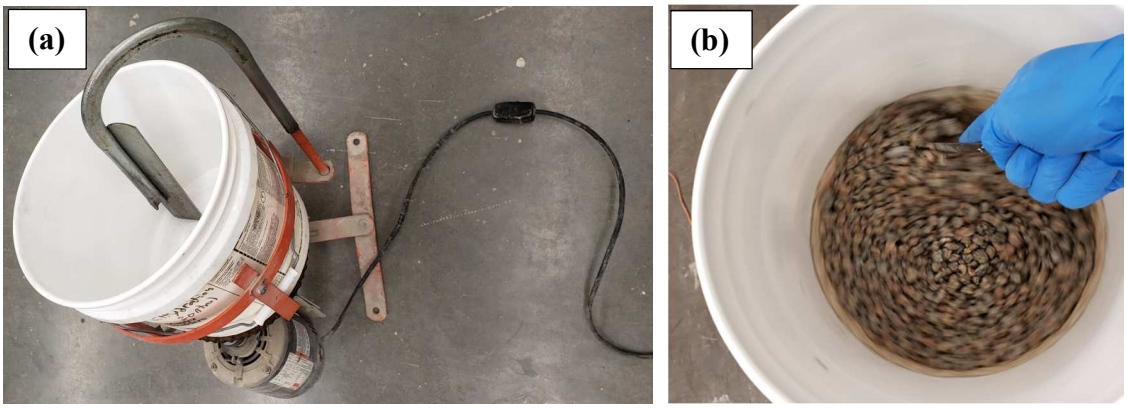

Figure 3.7: Coating setup (a) belt drive fan and blower motor, and (b) mixing of PCM-LWA and coating material

3.4.3. Leakage test for TESA

The leakage test of TESA was carried out as proposed by Hasanabadi et al. (2021). About 50 g of TESA (control and coated) was dispersed on a 70 mm diameter circle drawn on a filter paper, see Figure 3.8a, then placed in an oven at 80 °C for 1 h, see Figure 3.8b. After that, TESA and filter paper was weighed, and TESA was removed from the filter paper, and then the mass loss was estimated. A photograph of the filter paper was taken before, during, and after the test.

Figure 3.8: Leakage test, (a) drawn circle on a filter paper, and (b) control and coated TESA in an oven

3.5. Production of TESA concretes

3.5.1. Production of TESA concrete cubes

Table 3.5 shows the mix design used to make concrete samples in this research. The materials utilized were deionized water, cement, sand, limestone aggregates, and expanded clay. TESA concretes such as RMK 1, RMK 2, and RMK 3 were made of expanded clay (LWA) and PCMs. The LWA was impregnated with paraffin wax (PW) for RMK 1, a blended paraffin wax with soybean oil (PWSO) for RMK 2, and blended coconut oil with soybean (COSO) for RMK 3, respectively. These TESA were coated with latex before the production of concrete samples. ASTM C305-06 was used to mix concrete. Then, it was cast into a mold (152x157.2x156 mm^3), as shown in Figure 3.9, and covered with a plastic sheet for 24 h. Then, concrete was removed from the mold and placed in the curing room (100% relative humidity) for 14 days. Then, concrete cubes were dried in the environmental chamber (at 23.2±2 °C and 50% relative humidity) for 14 days. These samples were cast in molds containing t-wires thermocouples developed in this study, as shown in Figure 3.9.

Table 3.5: Mix design

Condition	Abs	SG	Cement	Sand	LMT	EC	TESA	Water
	%		(Kg/m^3)					
Control 1	0.80	2.72	3000	2379	3568	-	-	1529
Control 2	17.94	1.26	3000	2379	-	1677	-	1801
RMK 1	0.67	1.41	3000	2379	-	-	1882	1513
RMK 2	3.36	1.38	3000	2379	-	-	1840	1562
RMK 3	1.85	1.37	3000	2379	-	-	1826	1534

Note: WA and SG represent water absorption and specific gravity, respectively. EC: expanded clay LWA, LMT: limestone aggregate.

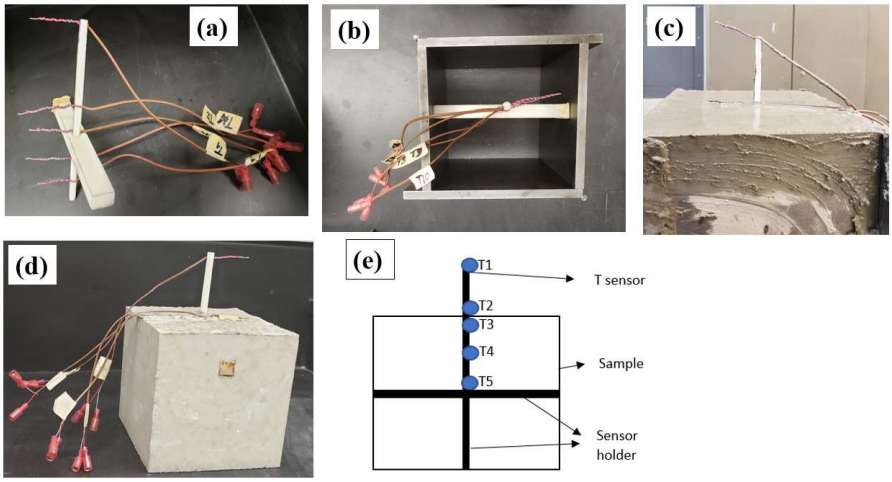

Figure 3.9: Temperature profile sample set-up, (a) thermocouples, (b) mold, (c) freshly concrete casted, (d) dry concrete, and concrete and location of t-wire thermocouples.

3.5.2. Thermal conductivity and compressive strength of concretes

The thermal conductivity was performed to determine the ability of controls (EC and LMT) and TESA-concretes (50x50x50 mm^3) to conduct heat, as shown in Figure 3.10. According to C-Therm Trident's manual, this test was carried out, and it conformed to the ASTM D7984. Thus, the thermal joint compound was painted on a single side of the specimen before placing it on the MTPS sensor. Then the test consisted of placing a metallic block of 500 grams (g) on the sample before collecting the readings. After that, the same samples were tested for compressive strength according to ASTM C109 (2008). Every test was performed in triplicate.

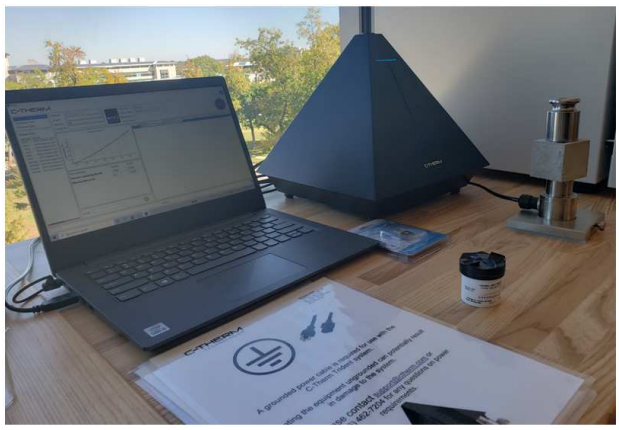

Figure 3.10: C-Therm Trident setup for thermal conductivity test of concrete cubes (50 x 50 x50 mm^3)

3.5.3. Temperature profile of TESA concrete cubes

The thermocouples connected to the CR1000 and multiplexer recorded the temperature profile on the specimens placed on a flat surface on the roof. Five concrete samples, namely the controls (LMT and EC) and TESA (PW, PWSO, and COSO), were tested in this study. The average size of samples was 152x157.2x156 mm3. The sensor holder and thermal insulations were nylon rods and polystyrene foam. The thermal couple sensors were placed inside and outside the specimens at different thicknesses, as shown in Figure1. The distance between sensors was 67.76 mm from T1 to T2. 25.26 mm from T2 to T3; 25.26 mm from T3 to T4; 25.26 mm from T4 to T5; and 74.29 mm from T5 to T6. Nothing was separating the layers, but they were defined by the locations of thermocouples throughout a concrete cube, as shown in Figure 3.11.

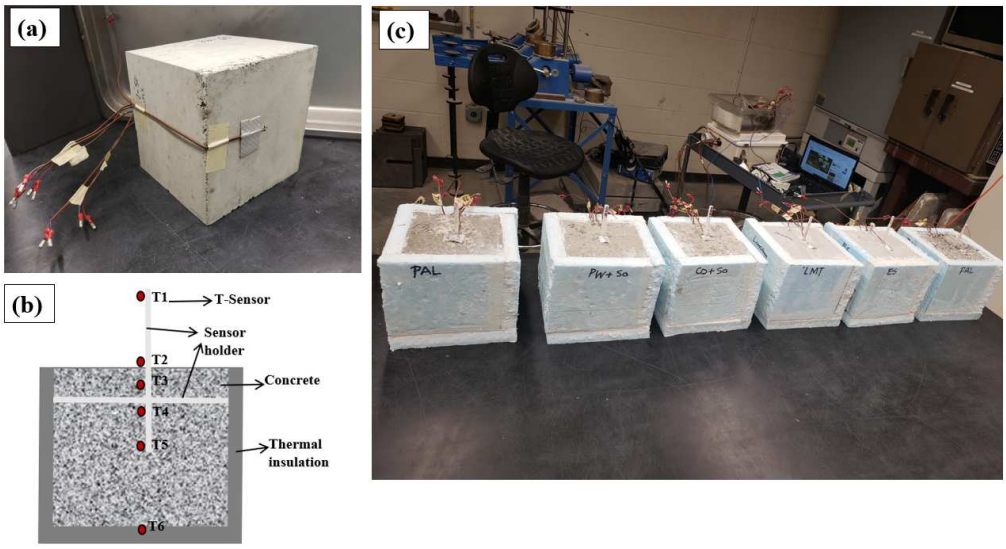

Figure 3.11: Concrete cubes, (a) t-wire #6 (T6) placed at the bottom of the concrete cube, (b) representation of insulated concrete cube with thermocouples, and (c) one-dimension surface area of concrete cubes

The thermocouples (from T1 to T6) were connected to a datalogger CR1000/ multiplexer and to the computer [software PC 400 4.7–shortcut] to collect the temperature profiles of specimens every 5 min, as shown in Figure 3.12. The temperature of samples was recorded during the summer and winter seasons in Kansas City, Missouri, United States of America.

Figure 3.12: Connection of the concrete cubes to the CR1000/Multiplexer and to the computer

Figure 3.13 shows the set-up of the field test during summer. Thus, the temperature profile of samples was recorded within ten days from August 26th to September 5th, 2021, in Kansas City, Missouri, United States of America. During this period, specimens' peak temperatures (daytime) were in a similar range, and the lowest (nighttime) were also in a similar capacity. Therefore, the present study only reported the temperature profiles recorded for one day, from August 26th at 09:00:00 to August 27th at 20:45:00, 2021, during summer. The weather Underground Joe's Data Center provided the air temperature, wind speed, and dew point (Paseo West Station, 2021).

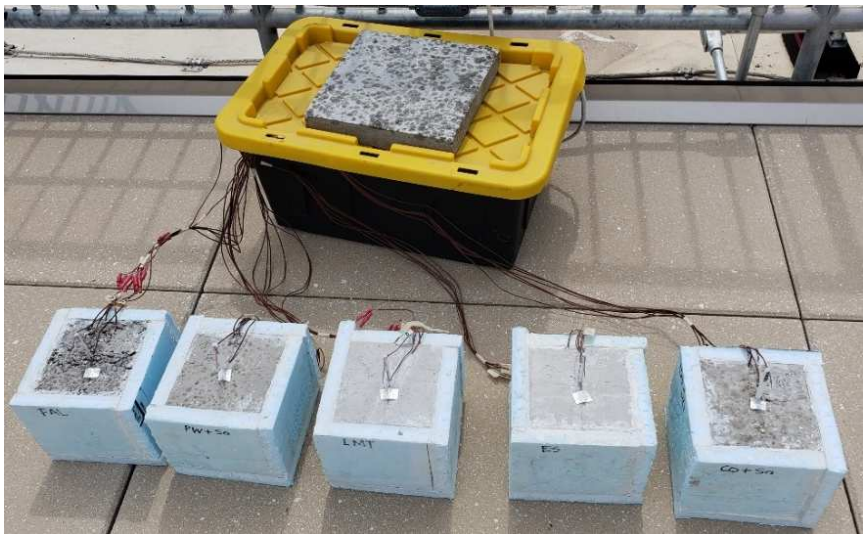

Figure 3.13: Experimental set-up of concrete cubes during summer field test

As depicted in Figure 3.14, the temperature profile of control 1, control 2, RMK 1, RMK 2, and RMK 3 were recorded in the winter season from February 9th to 16th, 2022, in Kansas City, Missouri, United States. The air temperature, wind speed, and dew point were obtained from the thermal data station HOBO RX3000 Advance Remote Weather Station operating at the exact location where the concrete field tests were performed.

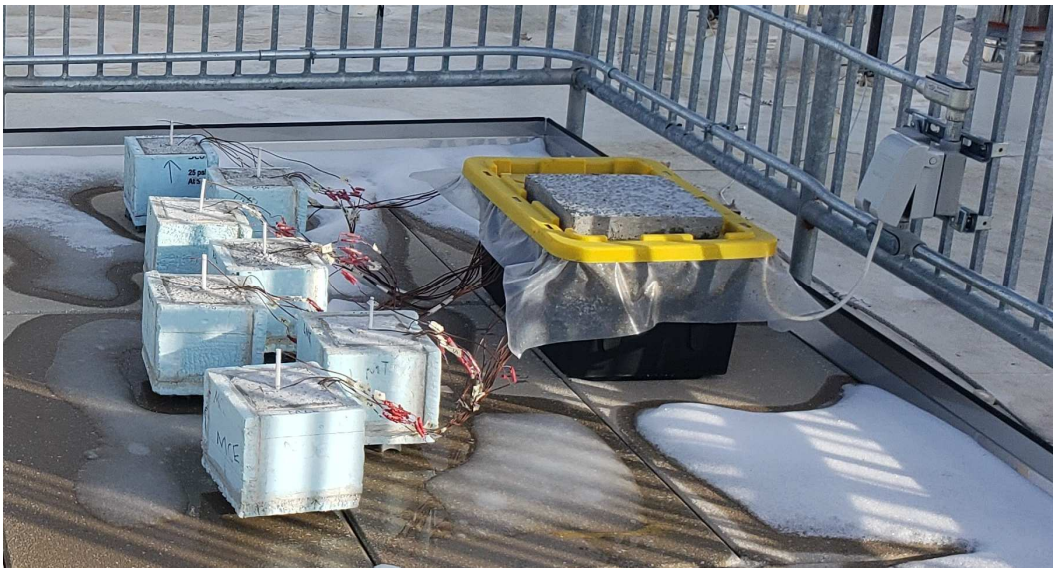

Figure 3.14: Experimental set-up for winter field test

3.5.4. Heat stored and discharged equation

The thermal performance of concrete consisted of charging, storing, and discharging heat into and out of the concrete specimens. In summer, concrete samples' actual field thermal performance was investigated from August 26th to September 5th, 2021, as described in section 5.3.4 (chapter 5). Whereas, in winter, the actual field test of concrete specimens was carried out from February 9th at 08:05 a.m. to February 16th at 07:20 a.m., 2022; in Kansas City, Missouri, United States of America, as described in section 6.3.3 (chapter 6).

CHAPTER 4: ASSESSMENT OF LOW-COST ORGANIC PHASE CHANGE MATERIALS FOR IMPROVING INFRASTRUCTURE THERMAL PERFORMANCE

4.1. Abstract

The literature has recently investigated the use of different phase change material (PCM) types and their incorporation techniques into cement-based materials (CBMs). The outcome of such analysis has demonstrated similar negative and positive impacts on the overall performance of CBMs. So, it is challenging for the researchers to select one PCM type or incorporate a technique over the other. But, if appropriate PCMs and means of integration are employed, they can minimize these undesirable properties of PCMs on the CBMs. This study investigates the application of mixtures of ratios of 50 weight percent (wt%) of coconut oil and soybean oil (COSO) and paraffin wax and soybean oil (PWSO) as blended organic-organic PCMs. These PCMs and paraffin wax (PW) were vacuum impregnated into expanded clay lightweight aggregate (LWA) to produce thermal energy storage aggregates (TESA). The differential scanning calorimetry (DSC) analysis of the as-received PW or prepared PWSO and COSO or after multiple thermal cycles showed high thermal latent heat of fusions necessary to store a large quantity of heat. A wide range of melting points could be suitable for different degrees of phase transitions. Vacuum impregnated TESA showed PCMs absorption capacity of 30.20% for PW, 28.00% for PWSO, and 27.42% for COSO. Moreover, to prevent leakage, the TESA was coated with latex. The application of low-cost/widely available PCMs/TESA, developed in this study, can be beneficial for improving the thermal infrastructure performance in developed/developing countries in different weather conditions.

Keywords: Phase change material, differential scanning calorimetry, vacuum impregnation, absorption capacity, thermal energy storage aggregates, leakage

4.2. Introduction

As the global population increases, so does the need for power (Kalombe, Ojumu et al. 2020). Higher consumption of fossil fuels has led to higher emissions of CO_2 and other greenhouse gases, which contribute to climate change (Frigione, Lettieri et al. 2019). Thermal energy storage (TES) is a valuable tool for improving energy efficiency and increasing energy savings in buildings (Frigione, Lettieri et al. 2019, Al-Absi, Isa et al. 2020). TES stores the existing thermal energy to reuse it during its shortage. The most significant value of TES is that it can solve the mismatch between the supply and demand of energy (Al-Absi, Isa et al. 2020). As an illustration, solar energy can be stored for heating the cold at night during the day. This cycle continues with the coolness during the night, and this coolness can use for cooling the warm of the day (Iten, Liu et al. 2016). Latent heat thermal energy storage (LHTES) is the most attractive approach due to its high storage capacity and minor temperature variations from storage to retrieval compared to thermal sensible heat or chemical heat methods (Kenisarin, Mahkamov et al. 2020).

Phase change materials (PCMs) used for LHTES systems utilize solid-liquid transitions and can be classified into three main types: organic, inorganic, and eutectic (Amaral, Vicente et al. 2017). Organic PCMs have continuous melting and freezing without phase isolation or degradation. Organic PCMs are chemically stable, do not have supercooling, are non-corrosive, and are recyclable (Zeinelabdein, Omer et al. 2018). Organic PCMs consist of paraffin and non-paraffin materials, including fatty acids, sugar alcohols, and glycols subdivisions (Zeinelabdein, Omer et al. 2018). Regardless of the different PCMs for more wide-spread application, materials should be non-toxic, commercially available, low-cost, environmentally friendly, and recyclable.

In practice, the mentioned properties are not fully met by most PCMs (Tyagi, Kaushik et al. 2011, Al-Absi, Isa et al. 2020, Faraj, Khaled et al. 2020). PCMs can be integrated into building materials using direct incorporation, immersion, impregnation, micro-encapsulation, shape stabilized PCM, or form-stable composites. However, the most significant problems with PCM incorporation are leakage, evaporation, degradation, and loss of the PCM to the outer environment (Jayalath, Mendis et al. 2011, Pielichowska and Pielichowski 2014, Farnam, Krafcik et al. 2016).

Numerous studies have suggested impregnating PCM into highly absorptive lightweight aggregate (LWA) as an efficient technique to incorporate PCM into cement-based materials. However, most reported research groups have developed a particular operating procedure to integrate and to characterize PCMs into concrete, which is sometimes difficult to replicate due to the lack of standard procedures. For instance, Farnam et al. (2016) reported soaking graded 4.475 mm, expanded shale in paraffin, and methyl laurate at ambient temperature and vacuum conditions for 72 hours. Then, a centrifuge was used to remove the PCM on the surface of LWAs to reach the saturated-surface-dry (SSD) condition. Their results showed 23% and 13% of PCMs absorbed into LWAs using vacuum and ambient conditions, respectively (Farnam, Krafcik et al. 2016). However, Mohseni et al. (2019) impregnated PCM into LWA by soaking aggregates in a melted solution of paraffin, and vacuumed for 30 min at a pressure of 0.1 MPa until no visible air bubbles were seen emanating from the LWA. Then the PCM-LWA was placed in the refrigerator (at 4 °C) to allow the PCM to solidify, resulting in 24.4% of PCM absorbed by the LWA (Mohseni, Tang et al. 2019). Sukontasukkul et al. (2020) reported paraffin (melting temp 57-59.9 °C) and polyethylene glycol (melting temp 42–46 °C) impregnated into aggregates in an oven at a temperature of 120 °C for 8 h. The PCM absorbed by LWAs was 17.8 % and 23.5% for paraffin and polyethylene glycol, respectively. For both vacuum and non-vacuum impregnation techniques,

heating maintained PCMs temperatures above the melting point to reduce viscosity and allow PCM to better penetrate inside the aggregates (Sukontasukkul, Sangpet et al. 2020). Although many reported different approaches to impregnate LWA with PCMs, most utilized paraffin. Meanwhile, there are thousands of PCMs with considerable melting and solidification processes that could significantly improve the thermal performance of building materials such as concrete. For example, biobased PCMs or food-grade materials such as palm kernel oil, palm oil, coconut oil, and soybean oil which have been used mainly in heating, ventilation and air-conditioning (HVAC) prototype systems with a thermal energy storage module (Dhamodharan and Bakthavatsalam 2020, Safira, Putra et al. 2020, Okogeri and Stathopoulos 2021), could also be utilized to produce PCM-LWA.

In the previous studies, the surface of the impregnated LWA or PCM-LWA has been coated with anti-bleeding materials to prevent leakage and enhance thermal conductivity. Memon et al. (2015) immersed PCM-LWA in a mixture of epoxy and graphite for 5 min; and then the coated materials were dusted with silica fume in single and double-layer procedure (Memon, Cui et al. 2015). The coated PCM-LWA were stored for seven days allowing the epoxy to cure before producing concrete (Mohseni, Tang et al. 2019). Nizovtsev et al. (2019) coated the surface of PCM-LWA with a thin protective layer of varnish (Nizovtsev, Borodulin et al. 2019). Kakar et al. (2019) used epoxy glue to coat the PCM-LWA. Then, 10 min later, the ordinary Portland cement was used to cover the glue. After 10 h, the coating material was separately applied a second layer of glue and cement on the surface of the PCM-LWA (Kakar, Refaa et al. 2019). Hasanabadi et al. (2021) used a layer of polystyrene to coat the PCM-LWA composite to prevent leakage. Based on several types of coating materials used in order to avoid leakage of PCM from the impregnated LWA, it could be said that the majority of coating materials used to increase the cost of the process

and makes it less feasible for PCM-LWA production at a larger scale (Hasanabadi, Sadrameli et al. 2021). Thus, the selection of anti-bleeding materials is an area of research requiring further investigations.

Most of the literature regarding PCMs in concrete has focused on using paraffin impregnated in LWA (Farnam, Krafcik et al. 2016, Farnam, Esmaeeli et al. 2017, Nizovtsev, Borodulin et al. 2019, Qu, Chen et al. 2020, Sukontasukkul, Sangpet et al. 2020). However, other PCMs could be suitable for specific applications. The utilization of coating materials and conductive powder increases the overall cost and sometimes weakens the PCM performance. The micro-cracks occur in PCM-LWA concretes due to the extra water absorbed by PCM-LWA due to the lack of proper coating, which could wet the cement particles and lead to additional hydration products, thus causing internal stress (Šavija 2018, Drissi, Ling et al. 2019). Also, biobased PCMs have only been utilized in air conditioning systems (Okogeri and Stathopoulos 2021). This paper proposes a couple of specific lab-made organic PCMs and a procedure for impregnating PCMs in expanded clay LWA to create PCM-LWA. The developed PCMs and PCM-LWAs are analyzed to determine the thermal properties and leakage capacity, respectively.

4.3. Methodology

4.3.1. Materials and production

This study utilized low-cost and readily available organic PCMs, including paraffin wax (PW), soybean oil (SO), red palm oil (PO), and coconut oil (CO). The porous LWA used was expanded clay supplied by Arcosa (Baton Rouge, LA). The present project used the coating materials consisting of latex (concrete bonding adhesive/acrylic fortifier), acrylic (generic coating in xylene type 1), epoxy, and paste (water/cement ratio of 0.75).

4.3.2. Differential scanning calorimetry (DSC)

DSC measures temperatures and heat flow associated with thermal transitions in a material (TA Instruments 2022). DSC techniques measure properties such as glass transitions, cold (crystallization), phase changes, melting, crystallization, product stability, cure/cure kinetics, and oxidative stability. DSC technology significantly improves baseline flatness, transition resolution, and sensitivity. It allows direct heat capacity measurement and makes the analytical experiments faster and more accurate (TA Instruments 2022).

In this study, the DSC 2500 (manufactured by TA instruments) was used to determine crystallization and melting temperatures, and latent heat of fusion. During the test, PCMs were poured into used Tzero Aluminum Hermetic pans with airtight lids to contain the PCMs. DSC operated between -90 °C to 80 °C, heating/cooling rate of 3 °C/min with 2 min isothermal holds at both minimum and maximum temperatures. This test was performed under an inert nitrogen atmosphere at a 20 mL/min flow rate. The mass of PCMs was 13 ± 2 mg.

After obtaining the thermal properties results of the as-received PCMs, different combinations of PCMs illustrated in Table 4.1 were prepared and investigated to improve melting and crystallization processes across a wider temperature range. Thus, two or three different types of PCMs (in liquid state) were mixed in a beaker using a stirring bar while heating up on a hot plate at about 80 °C for 10 mins. The blended PCMs were allowed to cool and analyzed using DSC.

Table 4.1: PCMs blending proportions

ID name	PCMs (wt.%)
PWCO	PW (50)+ CO (50)
PWSO	PW (50) + SO (50)
COSO	CO (50) + SO (50)
PWCOSO	SO (30) + CO (30) + PW (40)

Note: wt.% stands for weight percent

The durability of the PCMs over time was determined using multiple thermal cycles by placing PCM into a container and placing it in an oven at 80 °C for 6 hrs, then removing to cool at room temperature for 6 hrs for one cycle. After eleven cycles, the PCMs were analyzed using DSC to identify the new melting and solidification points and heat storage capacity.

The thermal expansion test determined the volume change of PCMs after one full cycle. PCMs were heated on a hot plate at about 80 °C for 10 mins, then the melted solution of PCMs was poured into a graduated cylinder, where its initial volume and mass were recorded. Then, the graduated cylinder was put in the freezer set at -23 °C for 120 mins. After that, the thermal expansion was determined using equation (4.1).

$$\beta = \frac{1}{V_o}\frac{\Delta V}{\Delta T} \qquad (4.1)$$

where: β: thermal expansion (1/°C) (or volumetric thermal expansion coefficient), V_o: particular volume measurement (mL), ΔV: change in volume (mL), and ΔT: change in temperature (°C).

4.3.3. Impregnation of PCMs into the expanded clay

The as-received expanded clay LWA was first dried in an oven at 110 °C for 72 hrs. Then, the oven dried LWA was graded 4.75 mm minimum. The graded LWA was blown dry with

compressed air to remove surface and pores dust. Then, a specific quantity of LWA was weighed, poured in the volumetric flask, and vacuumed for 20 mins to further remove the air in the pores.

The impregnation technique consisted of filling the pores of expanded clay LWA with PCMs (in liquid state) using a vacuum pump, as shown in Figure 4.1. After air was entrapped within the LWA's pores were removed, under vacuum pressure at about -860 mbar, for as much as the pump could release (visual judgment). Liquid PCM was then allowed to enter the vacuum chamber, and LWA was submerged in the PCM. Vacuum was applied until no visible air bubbles were seen emanating from the LWA for approximately 30 mins. The air was then allowed to enter the volumetric flask to help force the PCM into the pores of LWA for about 20 mins. Afterwards, the PCM-LWA was vacuum impregnated for an additional 10 mins at a pressure of -860 mbar. The temperature during the entire impregnation process was kept above the melting point of PCM as shown in Figure 4.1a. Afterwards, particles were removed and excess PCM were allowed to drain from the surface of the particles for about 45 seconds (Figure 4.1b). PCM-LWA particles were dried using paper towels to reach saturated surface-dry (SSD) condition (Figure 4.1c) to form TESA (Figure 4.1d). The TESA was stored in the environmental chamber at 23.03±2 °C and 50% relative humidity for seven days before any coating.

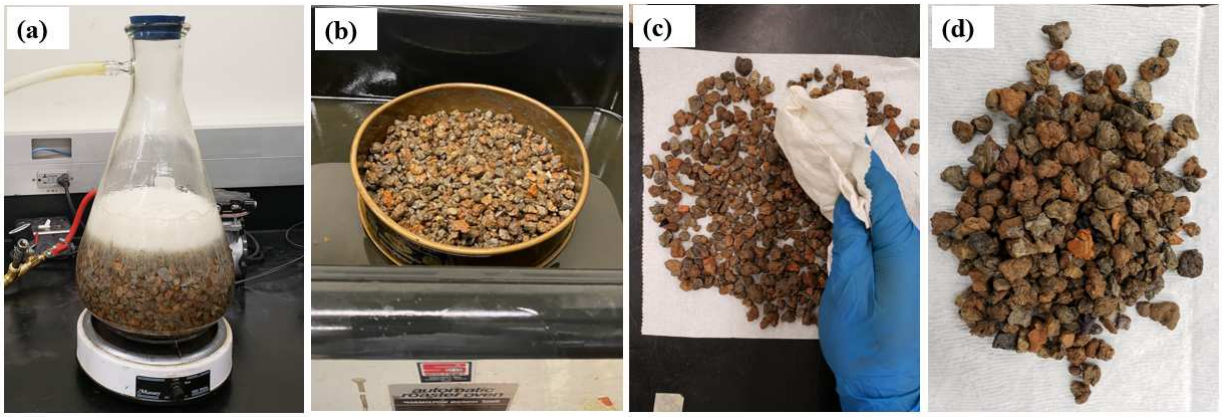

Figure 4.1: Steps for impregnating PCM into expanded clay: (a) impregnation of PCM into LWA's pores, (b) drainage of PCM, (c) SSD process, and (d) TESA as final products.

To prevent leakage of PCMs from TESA, coating materials were applied to the surface. The anti-bleeding materials consisted of cement paste (water to cement ratio of 0.75), low solid latex, acrylic, and two parts epoxies. The quantity of coating material used was equivalent to 10 wt% of the mass of TESA to be coated. Coating materials were poured onto the TESA in a rotating drum and mixed for 10 mins. During this period, a spoon was gently used by hand to ensure a complete coating of all TESA particles and break up agglomerations. The coated-TESA particles were spread out on the surface of a table and left in the air to dry at room temperature for 24 hrs.

4.3.4. Leakage test for TESA

The leakage performance of TESA was carried out as proposed by Hasanabadi et al. (2021). About 50 g of the TESA variations were placed on a 70 mm diameter circle drawn on a filter paper (Figure 4.2a) and placed in an oven at 80 °C for 1 hr (Figure 4.2b). Afterwards the samples and filter paper were weighed, and TESA mass loss estimated. Using PW as reference PCM, it was found that 30.20% of PW was absorbed in LWA through vacuum impregnation to form PW-TESA, which was coated using paste, acrylic, epoxy, and latex to create the coated TESA depicted in Figure 4.2b. After seven days of curing, the PW-TESA coated gained mass estimated at 0.00% for control, 36.67% for paste, 1.67% for acrylic, 10.67 % for epoxy, and 1.67% for latex. The mass gained by PW-TESA was a function of the amount and viscosity of the coating materials applied on TESA. Thus, the higher the viscosity, the higher the mass gained of PW-TESA after coating.

Figure 4.2: Leakage test: (a) drawn circle on a filter paper, and (b) control and coated TESA in an oven

4.4. Results and discussions

4.4.1. DSC analysis results of PCMs

Figure 4.3 shows the DSC analysis results of the as-received PCMs. The freezing process onset and endpoint and latent heat of crystallization were: 55.27 °C and 18.30 °C, and 188.07 J/g for PW; 11 °C and -12.9 °C, and 97.956 J/g for CO; -8.21 °C and -78.34 °C, and 52.139 J/g for SO; 18.21 °C and -20.30 °C, and 23.654 J/g for PO. However, the melting process onset and endpoint and latent heat of fusion were: 22.50 °C and 61.30 °C and 191.3 J/g for PW; 3.48 °C and 29.52 °C, and 101.24 J/g for CO; -53.85 °C and 0.10 °C, and 42.486 J/g for SO; -20.71 °C and 15.20 °C, and 27.261 J/g for PO. Therefore, PW melted at a high temperature and had a high latent heat of fusion followed by CO, SO, and then PO, as depicted in Figure 4.3. Thus, the DSC analysis results provided a large diversity of melting point ranges, in good agreement with the values reported in the literature (Srivastava, Semwal et al. 2017, Safira, Putra et al. 2020, Faraj, Khaled et al. 2021).

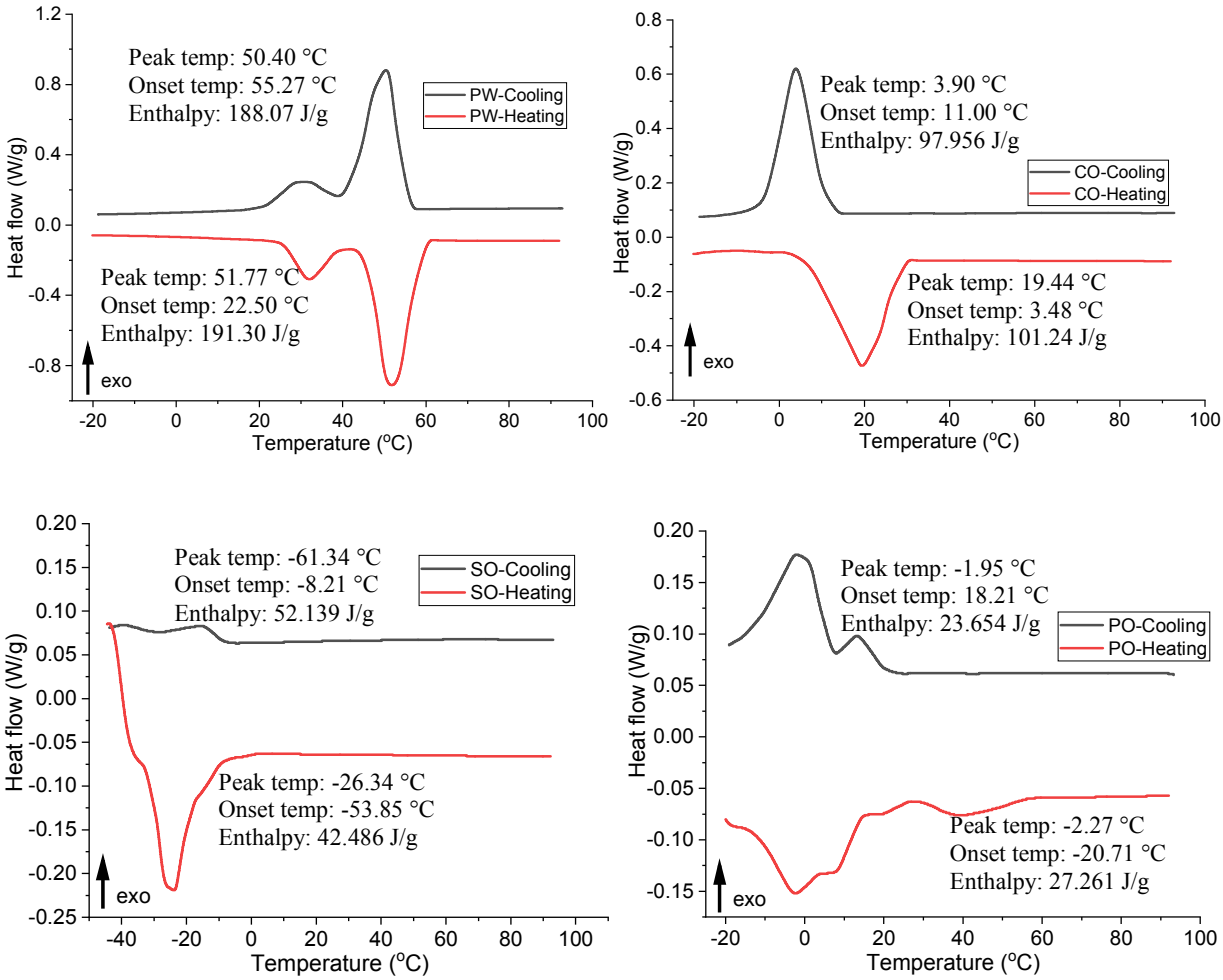

Figure 4.3: DSC analysis results of as-received PCMs

However, inorganic PCMs are known to have shape phase transition (Chandel and Agarwal 2017), whereas organic PCMs have impurities, as indicated by PW's first small humped peak (Figure 4.3). Based on the results reported in Figure 4.3, PCMs with intermediate thermal properties were developed by blending PW, CO, and SO. Among those, PO had the lowest latent heat of fusion; thus, it was not considered for further investigation. The preparation of each blended PCMs resulted in a homogenous mixture. Figure 4.4 shows the DSC analysis results for blended PCMs. It was found that the freezing process onset and endpoint and heat of solidification were: 50.31 °C and 4.11 °C, and 136.50 J/g for PWCO; 53.08 °C and 10.26 °C, and 102.76 J/g for PWSO; 50.94 °C and -17.45 °C, and 104.94 J/g for PWCOSO; 7.55 °C and -65.08 °C, and 89.592

J/g for COSO. Meanwhile, the melting process onset and endpoint and latent heat of fusion were: -16.23 °C and 57.39 °C, and 129.00 J/g for PWCOSO; 3.25 °C and 57.43 °C, and 127.67 J/g for PWCO; 7.52 °C and 58.72 °C, and 103.46 J/g for PWSO; -30.63 and 25.46 °C, and 75.676 J/g for COSO, as depicted in Figure 4.4.

The blend PWCOSO peak was broad and representative of each PCM's thermal properties, indicating the mixture's heterogeneity. A similar observation was made for PWCO. Thus, the organic PCMs (PW, CO, and SO) were easily blended and provided thermal properties of new organic-organic PCMs. It was noticed that: (i) when PW was mixed with CO, or SO, the melting temperature range and latent heat of fusion decreased, whereas the freezing temperature range increased compared to the as-received PW; (ii) when CO was mixed with PW, the melting and freezing temperature ranges and latent heat of fusion were significantly increased for CO, in contrast with CO+SO blend; (iii) when SO was mixed with PW or CO, the blended PCMs reduced the freezing temperature range. In contrast, the melting temperature increased significantly, and the heat of fusion considerably decreased. Depending on the application of PCMs in building or construction, the thermal properties provided by DSC analysis for PWSO and COSO were in the range for hot and cold in different regions around the world. Thus, PWSO and COSO were investigated further in this study.

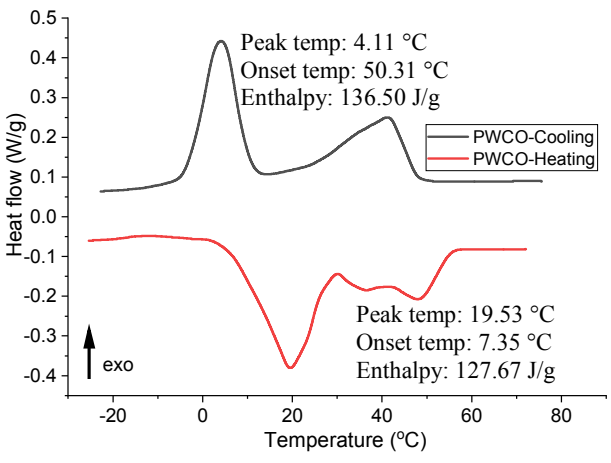

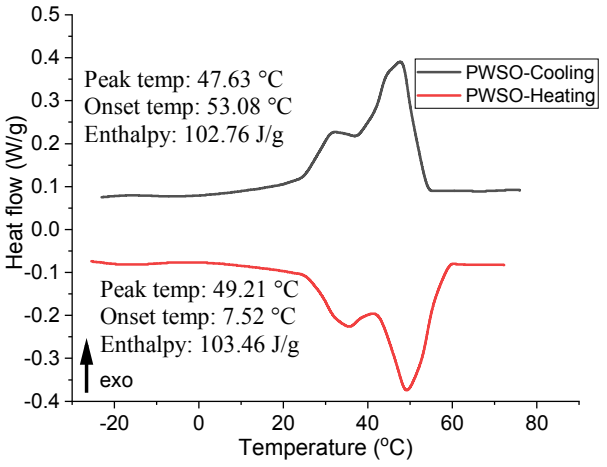

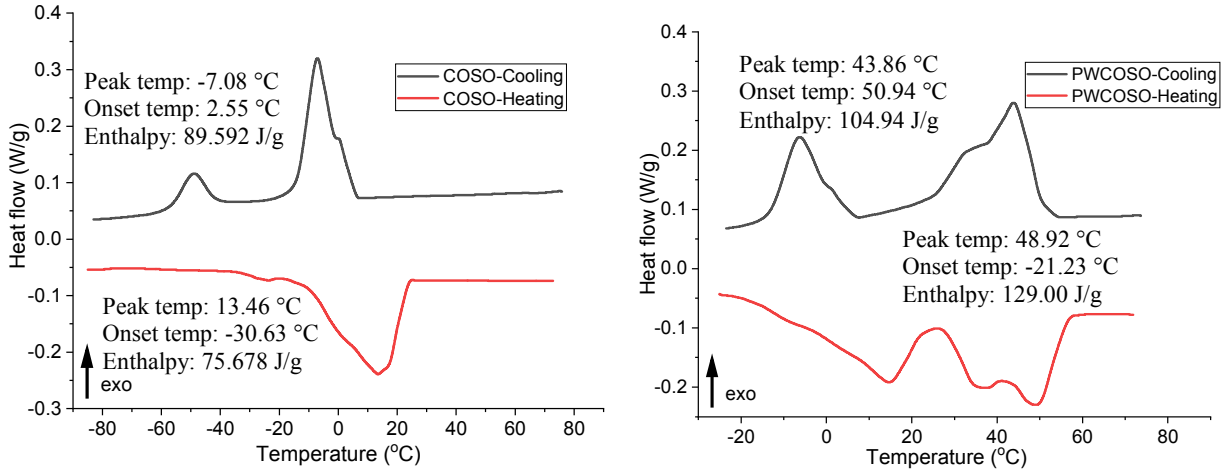

Figure 4.4: DSC analysis results of blended PCMs thermal properties

Figure 4.5 shows the DSC analysis results of eleven thermal cycles. There was a significant reduction in latent heat of fusion for COSO and PWSO, except that of PW increased. At the same time, there was an increase in the peak melting temperature of PW, PWSO, and COSO between the as-received and the multiple cycles PCMs. As depicted in Figure5, the freezing process onset and endpoint and heat of crystallization were: were 6.72 °C and -60.22 °C, and 67.958 J/g for COSO; 54.24 °C and 12.30 °C with 76.118 J/g for PWSO; 54.22 °C and 15.12 °C; and 199.87 J/g for PW. Whereas the melting process onset and endpoint and latent heat of fusion were: 22.56 °C and 63.31 °C, and 197.65 J/g for PW; 20.24 °C and 62.40 °C, and 83.404 J/g for PWSO; -10.27 °C and 25.02 °C, and 63.068 J/g for COSO, as depicted in Figure 4.5.

The experimental procedure developed in this study, reflected the extreme or/and worst cases that could happen if the PCMs were constantly exposed to 80 °C for 6 hrs. The PCMs were cooled at room temperature for 6 hours repeatedly eleven times. The conclusion was that all analyzed PCMs tended to lose their latent heat storage capacity as the thermal cycles increased (Rathod and Banerjee 2013, Che, Chen et al. 2018, Rathod 2018, Kahwaji and White 2019, Yang, Jin et al. 2021), which was the case in this project. Except for PW that increased in melting and solidification points after multiple cycles.

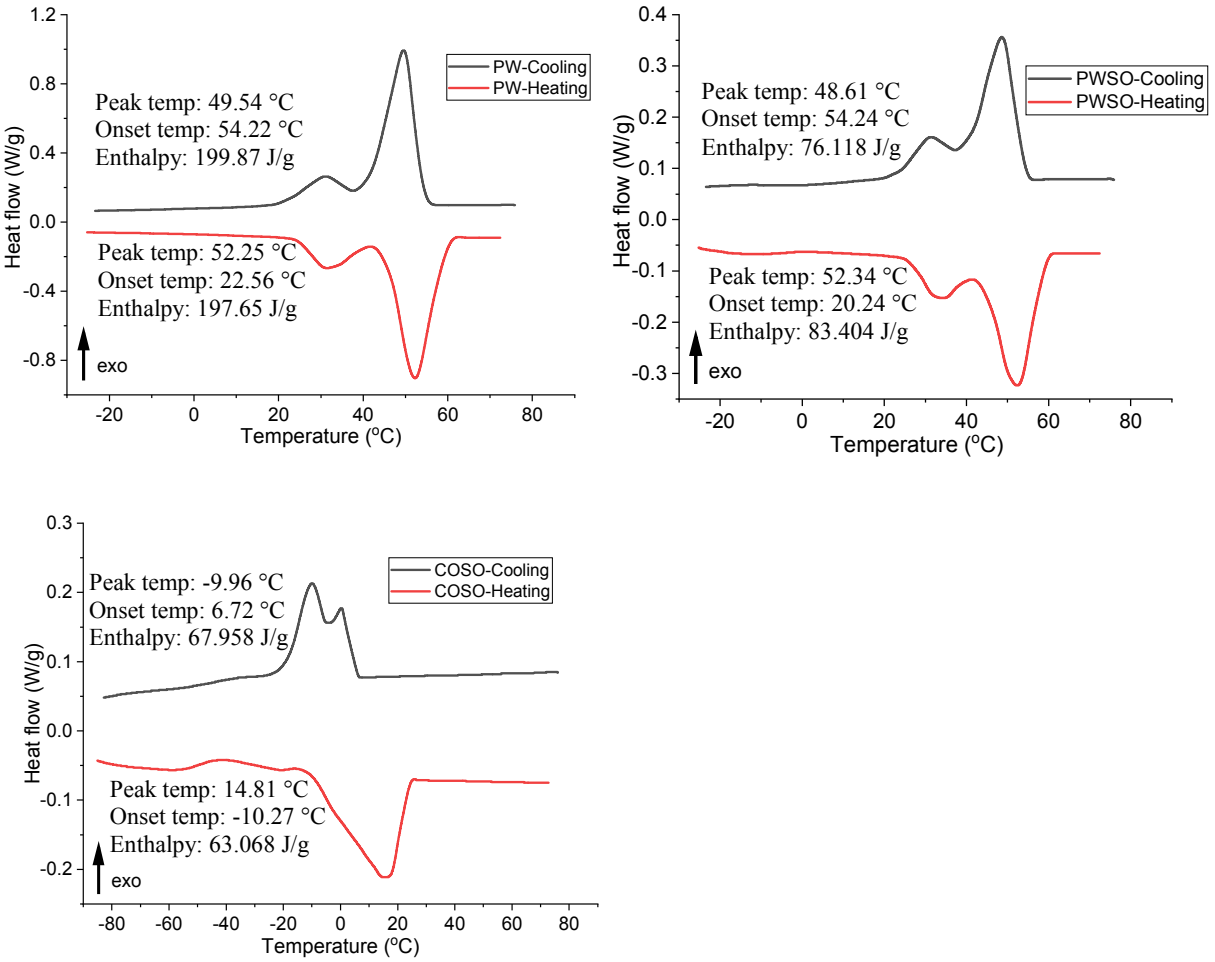

Figure 4.5: DSC analysis results of thermal cycle tests of PW, CO, and PWSO

However, the DSC results reported in Figure 3-5 were single run of heating and cooling of PCMs. Therefore, for the purpose repeatability analysis, the DSC tests of each PCMs were run in triplicate and the results were reported in Table 4.2. Table 4.2 summarizes the thermal properties of organic PCMs, namely paraffin wax and fatty acidic (palm oil, soybean oil, and coconut oil) characterized in this study. Based on the results presented in Table 4.2, CO, SO, and PW were in the range of potential application for cold and hot temperature conditions with a considerable latent heat thermal energy storage capacity. Thus, it was necessary to develop PCMs with intermediate thermal properties that might respond to the need for thermal energy-saving or thermal insulation for cold or hot temperatures building materials. As depicted in Table 4.2, after multiple thermal

cycling of PCMs, it was found that the latent heat of fusion and latent heat of crystallization were: (i) reduced by 37.07% and 50.34% for COSO; (ii) reduced by 4.08% and 4.81% for PWSO; and (iii) increased by 2.08% and 2.40% for PW, respectively, when compared them to the as-received PW or blended PWSO and COSO before thermal cycling processes. Although there is no common standard for thermal cycling tests available in the literature, it has been reported in the literature that when PCMs undergo multiple thermal cycles, there is always a decrease in melting point and latent heat of fusion capacity (Rathod and Banerjee 2013, Ferrer, Solé et al. 2015, Kurdi, Almoatham et al. 2021, Majo, Sanchez et al. 2021). Similar observations were made for COSO and PWSO. The detection and identification of product degradation have been reported to be a difficult task with chemical characterization methods such as Fourier-transform infrared spectroscopy (FT-IR) or nuclear magnetic resonance spectroscopy (NMR) because of detection limits (Majo, Sanchez et al. 2021).

Meanwhile, there was an increase in melting point and latent heat of fusion for PW. PW is a mixture of several linear alkyl hydrocarbons (Kurdi, Almoatham et al. 2021) with good thermal and chemical stability after many thermal cycles (Rathod and Banerjee 2013). However, no research has been reported on the increase of thermal properties of PW. Table 4.2 depicts the increase of melting point and latent heat of fusion after eleven thermal cycles of PW achieved in this study. Thus, the PW behaviors could be attributed to its initial chemical properties and the procedure developed in this study which was an exciting finding.

As shown in Table 4.2, these results were significant in determining the temperature range of freezing/melting and the latent heat of fusion to identify potential applications for different regions and climates. It could be said that PW could be utilized in hot weather regions due to its high melting point and high latent heat storage. Followed by the PWSO, which could be used in

cool weather; lastly, the COSO could be used in cold-weather regions due to its low melting process.

Table 4.2: Summary of thermal properties of PCMs obtained from the DSC analysis in triplicate

		Melting process			Solidification process		
Conditions	PCMs	Latent heat (J/g)	Onset (°C)	Peak (°C)	Latent heat (J/g)	Onset (°C)	Peak (°C)
As received	PW	191.37±3.4	23.21±0.3	52.07±0.3	192.60±5.4	56.06±1.6	49.75±0.6
	CO	97.70±5.0	-0.54±4.3	19.88±0.6	93.07±6.9	15.18±0.1	2.95±1.3
	SO	49.77±3.1	-53.99±2.2	-24.51±0.4	14.31±0.5	-6.04±0.4	-17.00±0.1
	PO	42.19±0.9	-26.76±0.4	2.35±0.7	40.21±1.1	19.76±1.1	-0.12±0.7
Blended	PWCOSO	122.88±5.9	-17.88±0.9	49.64±0.9	102.09±2.9	52.30±3.3	44.88±1.4
	PWCO	162.75±0.9	-10.84±0.7	49.76±0.3	153.57±2.9	54.40±0.4	47.60±0.4
	PWSO	95.50±1.2	17.89±0.5	51.30±0.9	92.91±0.4	54.88±0.3	48.91±0.8
	COSO	74.24±1.34	-27.69±4.7	13.64±0.2	65.52±20.9	8.62±3.1	-7.30±0.2
Thermal cycle	PW	195.35±2.6	20.50±2.7	51.57±0.6	197.22±2.6	55.27±1.0	49.51±0.3
	PWSO	91.60±11.6	10.49±7.2	51.70±0.9	88.44±17.4	55.29±0.1	48.90±0.4
	COSO	46.72±1.5	-1.18±0.6	18.29±0.1	32.54±1.2	14.01±3.9	-5.48±0.2

The volumetric thermal expansion coefficient (β-value) of PW, PWSO, and COSO calculated was 3.43 $x10^{-5}$ $°C^{-1}$, 6.88 $x10^{-5}$ $°C^{-1}$, and 7.23 $x10^{-5}$ $°C^{-1}$, respectively. The results indicated that the β-value of PW, PWSO, and COSO increased in small increments when it melted, and it decreased when it froze. Also, the β-value was different for each PCM type; thus, depending on the kinds of PCM, the β-value effects could have a significant impact on the thermal energy stored during melting. Depending on the thermal properties of PCMs, melting and solidification process per unit mass of the PCM take longer when the air void is present. Moreover, due to the thermal properties of PCMs and the lack of convective effects, the solidification process is much slower than the melting process. In other words, due to the expansion of the PCM during the melting process, the volume percentage of the air void decrease, whereas during the solidification,

the PCM contracts and the air void expand (Elmozughi, Solomon et al. 2014, Santiago Acosta, Otero et al. 2019, Sun, Li et al. 2021). However, no change in mass or evaporation was observed during phase change transitions (melting or freezing) of the PCMs throughout the trial.

4.4.2. Leakage of TESA

The purpose of producing TESA was to utilize it to produce thermal efficient concretes or for any other applications. Once the TESA was made, cured, and coated, a bleeding test was performed to determine the best coating material for TESA. Figure 4.6 shows the leakage results of TESA made of PW (control) and TESA coated with the paste. It was visually observed that PW-TESA coated with paste leaked the least, and the control sample leaked the most. After the leakage test, the mass loss of coated TESA samples was 0.116% for latex, 0.120% for epoxy, 0.167% for control, 0.278% for paste, and 0.311 for acrylic. The mass loss was equivalent to the total leakage or evaporation of the coating materials applied on TESA particles. Based on these results, all the coating materials can be used for TESA since less than 0.5% leakage was obtained. However, depending on the applications of TESA, other parameters such as chemical reaction with PCMs and LWA, durability, tenacity, and cost involved to make a coated TESA could be considered in selecting the appropriate coating material.

Therefore, latex can be considered the best coating material for TESA based on the visual judgment (leak spot on the filter paper) and mass loss results obtained. Other coating materials cannot be considered for several reasons for each case. For instance: (i) for PW-TESA coated with epoxy, the TESA particles were stuck or glued to each other, separating them manually or using them as they were during the mixing of fresh concrete; it would cause them to be broken down and destroyed the coating and caused leakage; (ii) for PW-TESA coated with paste showed no leak spot on the filter paper after the leakage test. Still, a mass loss was obtained, attributed to the

evaporation of water present in the paste during the release of the heat from the melted PCM inside the TESA. This water would reduce the thermal conductivity of the TESA, and the paste would have dissolved or broken down the coated layer during the mixing of fresh concrete. (iii) TESA coated with acrylic showed the highest leakage; this could be attributed to the chemical reactions between the acrylic and PW-TESA. Also, the heat in the oven during the leakage test catalyzed an accumulation of the silica and alumina in the LWA, which destroyed the coating layer. (iv) PW-TESA without coating material or the control showed high leakage. Therefore, PW-TESA was not considered for further investigation in this project because the melted PCM in the TESA would have flown and negatively affected concrete's mechanical and durability properties. Therefore, as mentioned earlier, latex showed promising results to be considered as the best coating material. Next, a series of experiments was carried out to determine the optimal amount of latex to coat TESA. The amount of latex was estimated to be equivalent to 10 wt% of the mass of TESA.

Figure 4.6: Leakage results for: (a) PW-TESA control, and (b) PW-TESA coated with the paste

Aforementioned, PW, PWSO, and COSO were selected as the most suited PCMs for TESA production. Therefore, PWSO and COSO were impregnated separately into the expanded clay and

coated with latex. After impregnating the LWA, the percentage absorption of PCMs were 28.00% and 27.42% for TESA made with PWSO and COSO. After coating with latex and being cured for seven days, the mass gained by TESA produced of PWSO and COSO was 1.56% and 1.03%, respectively. Then, the leakage test results showed a mass loss of 0.16% and 0.08% for TESA made of PWSO and COSO, respectively.

4.4.3. Potential application

Organic PCMs with a high melting process (PW and PWSO) and low freezing process (COSO) can be used in different applications, including manufacturing building materials. Three types of TESA were produced: TESA-PW, TESA-PWSO, and TESA-COSO. The water absorption and specific gravities were 17.94% and 1.26 for expanded clay LWA, 0.67% and 1.41 for PW-TESA, 1.85% and 1.37 for PWSO-TESA, and 3.36% and 1.38 for COSO-TESA. Therefore, TESA could be an excellent replacement for traditional LWA in the building industry. Thus, as depicted in Figure 4.7, TESA can produce concrete, including roof tiles, floor tiles, ceilings, walls, pavement, bridge decks, etc. Three types of TESA can be made and tested during summer to identify if it improves the thermal inertial of the build materials or in winter to determine if it creates a delay in freeze cycles of concrete pavements.

Due to the low cost of the proposed materials, construction industries can utilise building materials made of TESA in developed/developing countries. Thus, every class of the population (rich, middle, or inferior) can afford this type of building materials. However, as the nature of TESA is to absorb heat, it may result in a reduced curing temperature for the freshly mixed concrete. With that, TESA may promote low heat of hydration, prevent thermal distress and cracking within thick sections, and low early strength (it causes a delay in early strength gain).

Such behavior may be a disadvantage in specific applications, such as cold weather concreting, post-tensioning, etc.

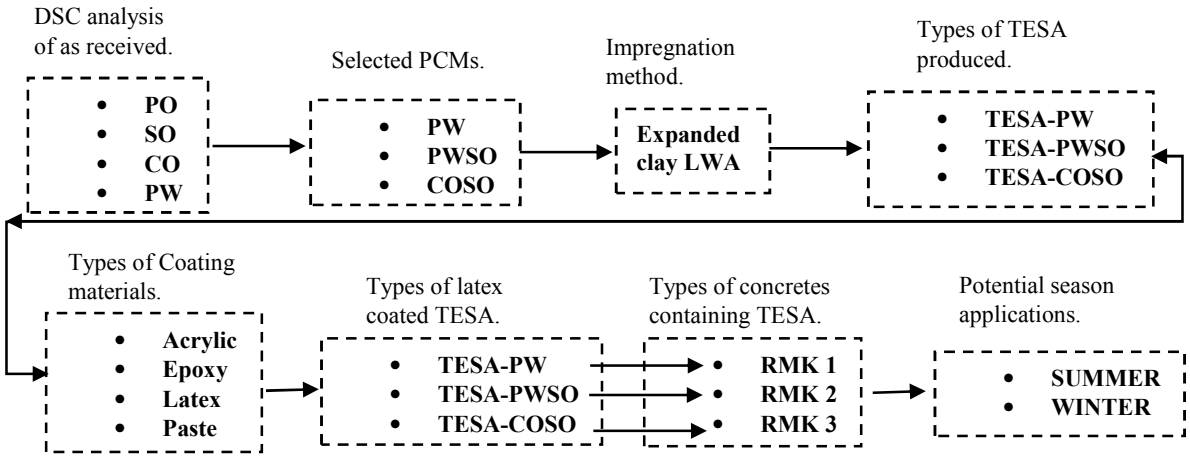

Figure. 4.7: Potential application of TESA

4.5. Conclusion and recommendations

The present study successfully created a process of integrating food-grade materials as PCMs into expanded clay LWA to form TESA. This study confirms the viability of the application of PCMs or the developed TESA in different weather zones for several applications. Due to the melting and solidification processes made out of a blend of COSO, PWSO, or PW. The summary of the achieved results in this work is highlighted below:

1) PCMs with low, medium and high thermal properties were developed and characterized. PCMs with a high melting process were in the order from PW, PWSO, to COSO. Even after eleven manual thermal cycles at 80 °C for 6 hours, these PCMs still had better melting processes. This test was performed to show the worst scenario that could have happened to the PCMs when exposed to a constant high temperature for a prolonged duration.
2) The three PCMs were vacuum impregnated into LWA, and the absorption capacity was 30.20% for PW-TESA, 28.00% for PWSO-TESA, and 27.42% for COSO-TESA particles.

Then, TESA was coated with latex using 10 wt% of the mass of TESA. Not many spots of leaks on the filter paper were observed during the leakage test, but after the test, the mass loss of the TESA particles was equivalent to 0.08% for COSO-TESA, 0.116% for PW-TESA, and 0.160% for PWSO-TESA.

The thermal performance of the three types of TESA would depend on the melting and solidification processes of the PCMs used to make the TESA. Thus, the DSC analysis obtained results would influence the selection of the types of PCMs and TESA before applying them to different industries, including building, pavement, solar panels, or air conditioning systems to enhance the thermal performance in those applications. Also, the materials utilized in this research, such as LWA, PCMs, or latex, can be found in developed/developing countries and are environmentally friendly and widely available at a low cost. Therefore, the outcome of the present study recommends investigating the potential applications of the developed/characterized PCMs or/and TESA in this work.

4.6. Reference

Al-Absi, Z. A., M. H. M. Isa and M. Ismail (2020). "Phase change materials (PCMs) and their optimum position in building walls." Sustainability (Switzerland), MDPI. **12**.

Amaral, C., R. Vicente, P. A. A. P. Marques and A. Barros-Timmons (2017). "Phase change materials and carbon nanostructures for thermal energy storage: A literature review." Renewable and Sustainable Energy Reviews **79**: 1212-1228.

Che, H., Q. Chen, Q. Zhong and S. He (2018). "The effects of nanoparticles on morphology and thermal properties of erythritol/polyvinyl alcohol phase change composite fibers." E-Polymers, European Polymer Federation. **18:** 321-329.

Dhamodharan, P. and A. K. Bakthavatsalam (2020). "Experimental investigation on thermophysical properties of coconut oil and lauryl alcohol for energy recovery from cold condensate." Journal of Energy Storage, Elsevier Ltd. **31**.

Drissi, S., T. C. Ling, K. H. Mo and A. Eddhahak (2019). "A review of microencapsulated and composite phase change materials: Alteration of strength and thermal properties of cement-based materials." Renewable and Sustainable Energy Reviews, Elsevier Ltd. **110:** 467-484.

Elmozughi, A. F., L. Solomon, A. Oztekin and S. Neti (2014). "Encapsulated phase change material for high temperature thermal energy storage - Heat transfer analysis." International Journal of Heat and Mass Transfer, Elsevier Ltd. **78:** 1135-1144.

Faraj, K., M. Khaled, J. Faraj, F. Hachem and C. Castelain (2020). "Phase change material thermal energy storage systems for cooling applications in buildings: A review." Renewable and Sustainable Energy Reviews, Elsevier Ltd. **119**.

Faraj, K., M. Khaled, J. Faraj, F. Hachem and C. Castelain (2021). "Experimental study on the use of enhanced coconut cil and paraffin wax phase change material in active heating using advanced modular prototype." Journal of Energy Storage, Elsevier Ltd. **41**.

Farnam, Y., H. S. Esmaeeli, P. D. Zavattieri, J. Haddock and J. Weiss (2017). "Incorporating phase change materials in concrete pavement to melt snow and ice." Cement and Concrete Composites, Elsevier Ltd. **84:** 134-145.

Farnam, Y., M. Krafcik, L. Liston, T. Washington, K. Erk, B. Tao and J. Weiss (2016). "Evaluating the use of phase change materials in concrete pavement to melt ice and snow." Journal of Materials in Civil Engineering, American Society of Civil Engineers (ASCE). **28:** 04015161.

Ferrer, G., A. Solé, C. Barreneche, I. Martorell and L. F. Cabeza (2015). "Review on the methodology used in thermal stability characterization of phase change materials." Renewable and Sustainable Energy Reviews, Elsevier Ltd. **50:** 665-685.

Frigione, M., M. Lettieri and A. Sarcinella (2019). "Phase change materials for energy efficiency in buildings and their use in mortars." Materials, MDPI AG. **12**.

Hasanabadi, S., S. M. Sadrameli and S. Sami (2021). "Preparation, characterization and thermal properties of surface-modified expanded perlite/paraffin as a form-stable phase change composite in concrete." Journal of Thermal Analysis and Calorimetry, Springer Science and Business Media B.V. **144:** 61-69.

Iten, M., S. Liu and A. Shukla (2016). "A review on the air-PCM-TES application for free cooling and heating in the buildings." Renewable and Sustainable Energy Reviews **61**: 175-186.

Jayalath, A., P. Mendis, R. Gammampila and L. Aye (2011). "Applications of phase change materials in concrete for sustainable built environment : a review." Construction and Building Materials, Elsevier Ltd. **120:** 408-417.

Kahwaji, S. and M. A. White (2019). "Edible oils as practical phase change materials for thermal energy storage." Applied Sciences (Switzerland), MDPI AG. **9**.

Kakar, M. R., Z. Refaa, J. Worlitschek, A. Stamatiou, M. N. Partl and M. Bueno (2019). "Impregnation of lightweight aggregate particles with phase change material for its use in asphalt mixtures." International Symposium on Asphalt Pavement & Environment, Springer.

Kalombe, R. M., V. T. Ojumu, C. P. Eze, S. M. Nyale, J. Kevern and L. F. Petrik (2020). "Fly ash-based geopolymer building materials for green and sustainable development." Materials **13**: 1-17.

Kenisarin, M. M., K. Mahkamov, S. C. Costa and I. Makhkamova (2020). "Melting and solidification of PCMs inside a spherical capsule: A critical review." Journal of Energy Storage **27**.

Kurdi, A., N. Almoatham, M. Mirza, T. Ballweg and B. Alkahlan (2021). "Potential phase change materials in building wall construction—a review." Materials, MDPI. **14**.

Majo, M., R. Sanchez, P. Barcelona, J. Garcia, A. I. Fernandez and C. Barreneche (2021). "Degradation of Fatty Acid Phase-Change Materials (PCM): New Approach for Its Characterization." Molecules **26**(4).

Memon, S. A., H. Z. Cui, H. Zhang and F. Xing (2015). "Utilization of macro encapsulated phase change materials for the development of thermal energy storage and structural lightweight aggregate concrete." Applied Energy, Elsevier Ltd. **139:** 43-55.

Mohseni, E., W. Tang and S. Wang (2019). "Development of thermal energy storage lightweight structural cementitious composites by means of macro-encapsulated PCM." Construction and Building Materials, Elsevier Ltd. **225:** 182-195.

Nizovtsev, M. I., V. Y. Borodulin, V. N. Letushko, V. I. Terekhov, V. A. Poluboyarov and L. K. Berdnikova (2019). "Heat transfer in a phase change material under constant heat flux." Thermophysics and Aeromechanics, Kutateladze Institute of Thermophysics SB RAS. **26:** 313-324.

Okogeri, O. and V. N. Stathopoulos (2021). "What about greener phase change materials? A review on biobased phase change materials for thermal energy storage applications." International Journal of Thermofluids, Elsevier B.V. **10**.

Pielichowska, K. and K. Pielichowski (2014). "Phase change materials for thermal energy storage." Progress in Materials Science, Elsevier Ltd. **65:** 67-123.

Qu, Y., J. Chen, L. Liu, T. Xu, H. Wu and X. Zhou (2020). "Study on properties of phase change foam concrete block mixed with paraffin / fumed silica composite phase change material." Renewable Energy, Elsevier Ltd. **150:** 1127-1135.

Rathod, M. K. (2018). "Phase Change Materials and Their Applications." Phase Change Materials and Their Applications, InTech.

Rathod, M. K. and J. Banerjee (2013). "Thermal stability of phase change materials used in latent heat energy storage systems: A review." Renewable and Sustainable Energy Reviews. **18:** 246-258.

Safira, L., N. Putra, T. Trisnadewi, E. Kusrini and T. M. I. Mahlia (2020). "Thermal properties of sonicated graphene in coconut oil as a phase change material for energy storage in building applications." International Journal of Low-Carbon Technologies, Oxford University Press. **15:** 629-636.

Santiago Acosta, R. D., J. A. Otero, E. M. Hernández Cooper and R. Pérez-Álvarez (2019). "Thermal expansion effects on the one-dimensional liquid-solid phase transition in high temperature phase change materials." AIP Advances **9**(2).

Šavija, B. (2018). "Smart crack control in concrete through use of phase change materials (PCMs): A review." Materials, MDPI AG. **11**.

Srivastava, Y., A. D. Semwal, V. A. Sajeevkumar and G. K. Sharma (2017). "Melting, crystallization and storage stability of virgin coconut oil and its blends by differential scanning

calorimetry (DSC) and Fourier transform infrared spectroscopy (FTIR)." J Food Sci Technol **54**(1): 45-54.

Sukontasukkul, P., T. Sangpet, M. Newlands, D. Y. Yoo, W. Tangchirapat, S. Limkatanyu and P. Chindaprasirt (2020). "Thermal storage properties of lightweight concrete incorporating phase change materials with different fusion points in hybrid form for high temperature applications." Heliyon, Elsevier Ltd. **6**.

Sun, Z., L. Li, X. Cheng, J. Zhu, Y. Li and W. Zhou (2021). "Thermal Properties and the Prospects of Thermal Energy Storage of Mg-25%Cu-15%Zn Eutectic Alloy as Phase Change Material." Materials (Basel) **14**(12).

TA Instruments' DSC Technology, Available at: https://www.tainstruments.com/products/thermal-analysis/differential-scanning-calorimeters/ Access on June 1st, 2022.

Tyagi, V. V., S. C. Kaushik, S. K. Tyagi and T. Akiyama (2011). "Development of phase change materials based microencapsulated technology for buildings: A review." Renewable and Sustainable Energy Reviews. **15:** 1373-1391.

Yang, L., X. Jin, Y. Zhang and K. Du (2021). "Recent development on heat transfer and various applications of phase-change materials." Journal of Cleaner Production, Elsevier Ltd. **287**.

Zeinelabdein, R., S. Omer, E. Mohamed and G. Gan (2018). "Free cooling using phase change material for buildings in hot-arid climate." International Journal of Low-Carbon Technologies, Oxford University Press. **13:** 327-337.

CHAPTER 5: PERFORMANCE INVESTIGATION OF LOW-COST PCM-MODIFIED CONCRETE IN HIGH OPERATING TEMPERATURE CONDITIONS

5.1. Abstract

The extent of energy economization of the structure depends on the thermal envelope performance. Thus, creating building materials capable of enhancing energy efficiency in the buildings is crucial. This study investigates the thermal performance of low-cost phase change materials (PCMs)-modified concrete in high operating temperature conditions. This approach has not been made previously to the best of the authors' knowledge. Three types of thermal energy storage aggregates (TESA) containing paraffin wax (PW), blended coconut oil with soybean oil (COSO), and blended paraffin wax with soybean oil (PWSO) were evaluated when utilized in concrete for thermal conductivity, compressive strength, and heat storage. The results showed that TESA concrete had better thermal performance due to the sensible and latent heat behavior of phase change materials (PCMs) impregnated in the expanded lightweight aggregate (LWA). TESA enhanced the thermal conductivities but slightly decreased the compressive strength of concrete compared to the control. However, at the top surface layer of concrete, about 25 mm thick, TESA concrete stored a large quantity of heat due to sensible and latent heat mechanisms occurring during the absorption of sunlight; thus, TESA concrete provided higher thermal insulation than the control sample. Consequently, TESA may control and minimize the temperature fluctuation in concrete and can be utilized to enhance the thermal inertia of buildings in high operating temperature applications such as in high seasons or tropical climates.

Keywords: Phase change materials, Thermal energy storage aggregates, Heat absorption, Thermal insulation, High operating temperature

5.2. Introduction

The change in living standards and comfort demands for cooling in hot regions and heating in cold ones have caused an increase in energy demand in the construction and building industry. However, the energy obtained from fossil fuels is limited, and their use has been held responsible for climate changes and environmental pollution (Kalombe, Ojumu et al. 2020). The utilization of thermal energy storage by phase change materials (PCMs) increases in interest for construction and building applications (Zhou, Zhao et al. 2012). A PCM usually absorbs and releases thermal energy 5–14 times more than other storage materials such as water or rock (Vakhshouri 2021). Heat absorption occurs when PCM undergoes phase transitions (Marani and Nehdi 2019). The utilization of PCMs covers several fields, including applications requiring a wide temperature range from -20 °C to 200 °C for heating, cooling, and hybrid mixing of heating and cooling (Faraj, Khaled et al. 2020). PCMs experience sensible and latent heat processes based on the instantaneous PCM temperature compared to the melting and solidification range (Faraj, Khaled et al. 2020). The introduction of PCMs improves the thermal properties of building materials, such as thermal mass, thermal inertia, and specific heat capacity (Sivanathan, Dou et al. 2020, Liao, Zeng et al. 2021). The thermal inertia, also known as time lag and decrement factor, is one of the essential parameters to estimate the thermal performance of the buildings (Zhou, Zhao et al. 2012). Designing a heat storage system is a complex task since it is not restricted to the system's thermal performance only but involves considering the cost, safety, and sustainability of materials used and processes employed (Sivanathan, Dou et al. 2020, Liao, Zeng et al. 2021).

Lightweight concrete with enhanced thermal inertia dramatically improves the thermal behavior of the envelope, thus allowing a better performance during the hot season, which has been, to date, a critical challenge for traditional lightweight insulation. This integrated approach

leads to a significant reduction in the energy used for cooling. Particularly in temperate climates, it might obviate the need for active air conditioning (AC) systems in many cases (Bamonte, Caverzan et al. 2017). Lightweight aggregates (LWA) are used as internal reservoirs to supply the extra water needed by the cementitious components of the concrete during their hydration processes. Due to their porous nature and reasonably high absorption capacity, thus, the LWA can also be filled with other materials, such as PCMs (Bentz and Turpin 2007). Many PCMs, such as paraffin, have a low thermal conductivity; embedding them in a more thermally conductive material such as LWA will enhance the necessary heat transfer between the PCM and the bulk concrete (Bentz and Turpin 2007). The presence of PCMs can considerably reduce the temperature rise and cool-down rate in the first 24 hrs following placement of freshly mixed concrete, provided the PCM melting temperature is chosen suitably (She, Wei et al. 2019).

The process of integrating PCMs into LWA, known as impregnating or soaking to produce PCM-LWA, have been reported by many authors. Previously, LWA had been impregnated with PCMs such as butyl stearate, dodecanol, polyethylene glycol, tetradecanol, paraffin, and dimethyl sulfoxide (Hawes, Banu et al. 1992); polyethylene glycols, octodecimo, and paraffin wax (Bentz and Turpin 2007); paraffin oil and methyl laurate (Farnam, Krafcik et al. 2016); octadecane (Min, Kim et al. 2017); paraffin and polyethylene glycol (Sukontasukkul, Sangpet et al. 2020); nonacosane (Nizovtsev, Borodulin et al. 2019); and paraffin (Qu, Chen et al. 2020). The developed PCM-LWA were coated with different coating materials to prevent leakage (Liu, Wang et al. 2017, Kakar, Refaa et al. 2019, Sukontasukkul, Sangpet et al. 2020). In terms of the performance of PCM-LWA, it has been shown that incorporating PCM-LWA to make cement-based materials helped increase the workability, lower the moisture absorption, and improve the thermal properties of concrete. Thus, the thermal conductivity and specific heat depend strongly on the state of PCM

(Sukontasukkul, Sangpet et al. 2020). The coating materials reduced the water absorption and drying shrinkage of PCM-LWA concrete because of the reliable coating system and the PCM contribution in reducing thermal cracks during the hydration process (Liao, Kumar et al. 2019, Mohseni, Tang et al. 2019). PCMs used in the production of concrete controlled temperature related to cracking. PCMs can offset temperature changes and reduce gradients in concrete structures through their ability to capture heat. But they can also influence concrete properties (Šavija 2018). Thus, PCM-LWA concrete decreased by 40% in compressive strength (Hasanabadi, Sadrameli et al. 2021). Therefore, it becomes possible to reduce the peak values of the heat flux passing through the concrete material and limit the material temperature range during heating for a long time, reducing the energy consumption by lowering the indoor temperature (Nizovtsev, Borodulin et al. 2019, She, Wei et al. 2019).

The studies mentioned above utilized similar types of PCMs. Organic PCMs, particularly paraffin, seem to be one of the most suitable latent heat storage materials used in concrete. Impregnating paraffin into LWA still has negative impacts on the properties of concrete. Thus, it is essential to explore other types of organic PCMs and develop a simple process to integrate them into concrete. Therefore, if appropriate PCMs and means of integration are employed, they can minimize these undesirable properties. This study investigates the thermal inertia of concrete cubes made of thermal energy storage aggregates (TESA) for the first time during the summer of 2021. In the previous work of the authors (Kalombe, Sobhansarbandi, and Kevern 2022a) the TESA consisted of expanded clay LWA impregnated with paraffin wax, blended coconut oil with soybean oil, or blended paraffin wax with soybean oil coated with latex was investigated, yielding to the absorption capacity of 30.20% for PW-TESA, 28.00% for PWSO-TESA, and 27.42% for COSO-TESA particles. In this study, TESA concrete is tested for compressive strength and

thermal conductivity, then evaluated for temperature profiles and heat storage capacity during the field tests.

5.3. Methodology

5.3.1. Materials and material production

The materials consisted of expanded clay LWA, limestone, water, cement, sand, and TESA made up of PW, PWSO, and COSO. TESA was produced as reported by Kalombe, Sobhansarbandi, and Kevern 2022. After seven days of curing TESA, the specific gravity and water absorption of TESA were determined according to ASTM C127-15. Then five mix designs were made using a water to cement ratio of 0.5 as depicted in Table 5.1. Then, ASTM C305-06 was used to mix concrete. Then, it was cast into a mold (152x157.2x156 mm^3) and covered with a plastic sheet for 24 hrs. Then, concrete was removed from the mold and placed in the curing room (100% relative humidity) for 14 days. The concrete were dried in the environmental chamber (at 23.2±2 °C and 50% relative humidity) for 14 days.

Table 5.1: Mixture properties

Condition	Abs	SG	Cement	Sand	LST	EC	TESA	Water
	%		(kg/m^3)					
Control 1	0.8	2.72	3000	2379	3568	-	-	1529
Control 2	17.9	1.26	3000	2379	-	1677	-	1801
RMK 1	0.7	1.41	3000	2379	-	-	1882	1513
RMK 2	1.9	1.37	3000	2379	-	-	1826	1534
RMK 3	3.4	1.38	3000	2379	-	-	1840	1562

Note: RMK 1, RMK 2, RMK 3 stands for TESA made with paraffin wax, paraffin wax and soybean oil, coconut oil and soybean oil, Control 1: concrete made limestone aggregate (LST), control 2: concrete made expanded clay (EC) LWA. Abs: water absorption, and SG: specific gravity.

5.3.2. Thermal conductivity and compressive strength of concrete

The thermal conductivity was performed to determine the ability of controls (EC and LMT) and TESA-concrete (50x50x50 mm^3) to conduct heat. The test conformed to the ASTM D7984. Thus, the thermal joint compound was painted on a single side of the specimen before placing it on the MTPS sensor. Then the test consisted of placing a metallic block of 500 grams (g) on the sample before collecting the readings. After that, the same samples were tested for compressive strength according to ASTM C109 (2008).

5.3.3. Temperature profiles

The t-wire thermocouples connected to concrete specimens and to the CR1000 and multiplexer recorded the temperature profile. The specimens were placed on a flat surface on the roof and exposed to the sunlight. Five concrete samples, namely the control 1, control 2, RMK 1, RMK 2, and RMK 3 as indicated in Table 5.1, were tested in this study. The average size of samples was 152x157.2x156 mm^3. Figure 5.1 shows the samples' set-up configuration. The sensor holder and thermal insulations were nylon rods and polystyrene foam, respectively. The t-wire thermocouples (error = ± 1 °C) were placed inside and outside the specimens at different thicknesses such as 68 mm from T1 to T2; 25 mm from T2 to T3; 25 mm from T3 to T4; 25 mm from T4 to T5; and 74 mm from T5 to T6. Nothing was separating the layers, but they were defined by the locations of thermocouples throughout a concrete cube, as shown in Figure 5.1. The thermocouples (from T1 to T6) were connected to a datalogger CR1000/ multiplexer and software PC 400 4.7–shortcut to collect the temperature profiles of specimens every 5 min. The datalogger error is estimated at ± 0.1 °C over 0 to 40 °C, ± 0.3 °C from –25 to 50 °C, and ± 0.8 °C from –55 to 85 °C (Campbell-Scientific 2018). The temperature profile of samples was recorded within ten days from August 26th to September 5th, 2021, in Kansas City, Missouri, United States of America.

During this period, specimens' peak temperatures (daytime) were in a similar range, and the lowest (nighttime) were also in a similar range. Therefore, the present study only reported the temperature profiles recorded for one day, from August 26th at 09:00:00 to August 27th at 20:45:00, 2021, in summer.

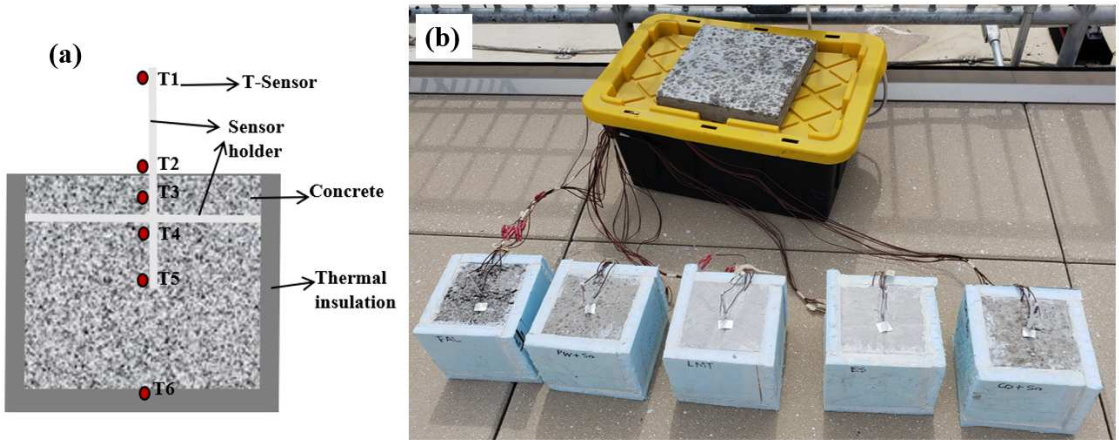

Figure 5.1: Concrete set-up of the sample: (a) thermocouples location and thermal insulation, (b) summer field test

5.3.4. Heat storage

The thermal performance of concrete consisted of absorbing or charging, storing, and discharging heat into and out of the concrete specimens. Thus, the present study determined the maximum energy stored by a sample at the air peak temperature using the scenario depicted in Figure 5.2.

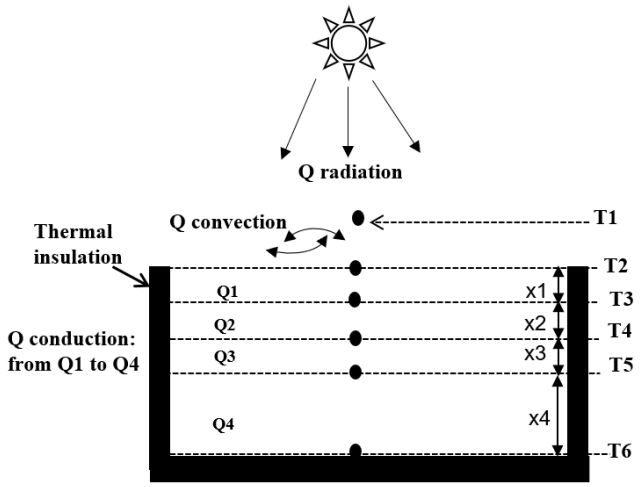

Figure 5.2: Samples' set-up containing t-thermocouple wires to estimate the heat storage

As shown in Figure 5.2, the specimen was exposed to sunlight. Once the sunlight was absorbed, heat flew into and out of the surface, which was considered as heat lost by radiation to the sample according to the Stefan-Boltzmann's law represented by equation (5.1):

$$Q_{Rad} = \varepsilon \, \delta \, A \, t \left(T_2^4 - T_{sky}^4\right) \qquad (5.1)$$

where, Q_{Rad}: the heat of radiation [Joules (J)], δ: Stephan-Boltzmann's constant (5.6703 x 10^{-8} W/m^{2}K^4), ε: emissivity, A: surface area of the specimen (m^2), t: time (second), T_2: temperature on the surface of the sample (K^4), and T_{sky}: peak temperature (K^4). Since for all tangible objects, emissivity is also a function of wavelength (Mike 2018). This study assumed that concrete samples were in thermal equilibrium with the air peak temperature, such as steady-state conditions, and no net heat transfer. Thus, the absorptivity was equal to the emissivity (Mike 2018). The emissivity was determined as reported by Albatayneh et al. (2020), defined in equation (5.2):

$$\varepsilon = \left[0.787 + 0.767 \times \ln\left(\frac{\text{Dew point temperature}}{273}\right)\right] + 0.0224N - 0.0035N^2 + 0.00028N^3$$

(5.2)

where N: is the opaque sky cover, assumed to be 0.5 in this research (Albatayneh, Alterman et al. 2020). Dewpoint temperature obtained from Joe's Data Center (WheatherUnderground 2022). Then, the sky temperature was determined using equation (5.3) (Nowak 1989):

$$T_{sky}(\text{kelvin}) = 0.0553\ (T_{air})^{1.5} \qquad (5.3)$$

where T_{air}: air temperature obtained from Joe's Data Center. The heat transfer by convection took place in the air on top of the sample's surface. The heat transfer by convection took place in the air on top of the sample's surface. Newton's law is represented in equation (5.4):

$$Q_{Conv} = A\ t\ h_{Conv}(T_2 - T_{air}) \qquad (5.4)$$

where Q_{Conv}: the heat of convection (J), T_{air}: air temperature (K), T_2: temperature (K) of the surface of the concrete sample (K), h $\left(\frac{W}{m^2K}\right)$: convective heat transfer coefficient and was determined using equation (5.5) for wind speed less than five m/s (Defraeye, Blocken et al. 2011).

$$h\ \left(\frac{W}{m^2K}\right) = (4 \times U) + 5.6 \qquad (5.5)$$

where U: wind speed (m/s). The heat transfer through conduction of the sample was determined per layer from the surface (T2) to the center (T5). Thus, for the first, equation (5.6) or modified Fourier's law was utilized:

$$Q_{Cond} = \frac{K\ At\ (T_2 - T_3)}{x_1} \qquad (5.6)$$

where Q_{Cond}: heat transfer by conduction (J), K: thermal conductivity (W/mK) of the concrete specimen at ambient temperature, T3: temperature (K) 25.26 mm from the surface deep-down in the sample and x_1: thickness (m) as the first layer. After that, equation (5.7) for the

conservation of energy for a dry surface was used to determine the energy stored in the sample (Melvin Pomerantz 2000):

$$Q_{storage}(J) = Q_R + Q_{Conv} - Q_{Cond} \qquad (5.7)$$

The assumptions taken into consideration for this study are: i) all concrete samples were steady-state, ii) one-dimensional conduction, and iii) constant thermal conductivity. As depicted in Figure 5.2, the energy storage was determined per layer from x_1 to x_3 at a specific time of the day. However, when the temperature reached in the TESA concrete samples was equivalent to the melting process of the PCM in the TESA. The mass of PCM (m) and latent heat of fusion (H) in the concrete, expressed as "m × H," were added to the equation of heat stored calculation (Fernandes, Manari et al. 2014). Otherwise, "m × H" was not considered in the equation. The heat stored at each layer was determined as follows:

Energy stored in layer one is represented by q_1 in equation (5.8):

$$q_1 \ (J) = Q_{Rad} + Q_{Conv} - \frac{k\,A\,t\,(T_2 - T_3)}{x_1} + (m \times H)_{PCM} \qquad (5.8)$$

Considering $Q_{Rad} + Q_{Conv} = Q$

Energy stored in layer two was q_2 in equation (5.9):

$$q_2 \ (J) = Q - q_1 - \frac{k\,A\,t\,(T_3 - T_4)}{x_2} + (m \times H)_{PCM} \qquad (5.9)$$

Energy stored in layer three was q_3 in equation (5.10):

$$q_3 \ (J) = Q - q_1 - q_2 - \frac{k\,A\,t\,(T_4 - T_5)}{x_3} + (m \times H)_{PCM} \qquad (5.10)$$

The total energy stored by the specimen from the surface (T2) to the center (T5) was calculated using equation (5.11):

$$Q_{storage}(J) = q_1 + q_2 + q_3 \qquad (5.11)$$

5.4. Results and discussions

5.4.1. Thermal conductivity and compressive strength

Table 5.2 shows the thermal conductivity (k-value) and compressive strength of concrete cubes. This research found that control 1 had the highest k-value. Thus, control 2, RMK 1, RMK 2, and RMK 3 could provide better thermal insulation in building materials at a low cost since materials used to produce TESA are widely available worldwide at a low price. Therefore, adding conductive materials to TESA would increase its production cost. However, instead of using the conductive powder materials while impregnating the LWA, that would interfere with the PCMs in the pores of LWA and affect the thermal properties of PCMs. The conductive powder materials could be added to the mix design as part of the concrete component to increase the overall thermal conductivity if a higher k-value is necessary for a specific application.

On the other hand, the specimen with the highest compressive strength was made of control 1, followed by control 2, RMK 1, RMK 3, and RMK 2. Since the nature of TESA was to absorb heat, it might have resulted in a reduced curing temperature for the concrete. TESA might have absorbed the heat generated by the exothermic hydration reaction. Perhaps resulting in a lower degree of hydration than ordinary Portland cement (OPC) mixed without PCM such as LMT and EC (Hunger, Entrop et al. 2009, Sharma, Neithalath et al. 2013). With that, TESA might have promoted low heat of hydration, preventing thermal distress and cracking within thick sections, and low early strength. That might have been a disadvantage in specific applications, such as cold

weather concreting, post-tensioning, etc. Thus, TESA might have created excessive retardation, promoting plastic shrinkage cracking. The remediation of these issues would consist of using pozzolans (i.e., fly ash, silica fume, etc.). The $Ca(OH)_2$ becomes less soluble C-S-H when pozzolanic materials are added. The strength and durability of the concrete are thereby improved to a considerable degree. Then, rendering the PCMs more stable in such a concrete reduced the detrimental effects of $Ca(OH)_2$ (Hawes, Banu et al. 1992). However, specifications may limit the percent substitution of cement with pozzolans based on durability issues with deicing chemicals (ACI 301 recommendation). Also, when appropriately used, admixture can increase early strength ultimate strength, accelerate setting time, and increase workability.

Moreover, the maturity method may be performed using TESA concrete to estimate strength. Concrete's temperature multiplied by the time the concrete is maintained at that temperature is maturity. Also, the water to cement ratio (w/c) of 0.5 was high to expect a high strength; thus, lowering the w/c ratio could have improved the compressive strength of TESA-concrete.

Table 5.2: Thermal conductivity and compressive strength of TESA-concrete

Concrete cubes	Thermal conductivity (W/m °C)	Compressive strength (MPa)
Control 1	0.962 ± 0.004	40.2 ± 1.8
Control 2	0.318 ± 0.002	34.3 ± 1.6
RMK 1	0.655 ± 0.002	29.5 ± 0.8
RMK 2	0.495 ± 0.003	24.7 ± 0.8
RMK 3	0.289 ± 0.002	24.9 ± 0.3

5.4.2. Temperature profiles of concrete

Figure 5.3 shows the temperature profile of five different concrete specimens recorded from morning to the following day in the summer of 2021 in Kansas City, Missouri, USA. The air peak temperature was 36.50 °C, recorded and reported by Paseo West, Joe's Data Center (WheatherUnderground 2022). However, the air temperature was striking through the sample and represented by T1 in Figure 5.2. On the sample, T1 was recorded using the thermocouples located at 68 mm from the surface of the specimens (T1) was about 39.29 °C. T1 was a combination of heat transfer through radiation from the sun, the heat flow in the air due to convection and the heat reflected from the samples to the atmosphere.

In contrast, the temperature on the surface and within the specimens varied depending on the types of aggregate. The latent heat storage capacity of the PCMs impregnated into LWA and the thermal conductivity of the concrete samples. Figure 5.3 indicates that the charging and storage of heat occurred during the daytime. The temperature was high at the surface (T2) and low within the samples from T3 to T6.

Meanwhile, heat discharge or heat loss occurred at nighttime. The temperature was higher at the bottom and within the sample from T6 to T3. And lower at the surface (T2) of the specimen. Thus, three cycles of charging, storage, and discharging occurred as the temperature changed with time. The peak temperature during the daytime was about 50.49 °C for RMK 1, 47.82 °C for RMK 3, 46.58 °C for RMK 3, 45.99 °C for control 2, and 45.40 °C for control 1. However, Table 5.3 shows concrete samples' peak temperatures at T2 and T5 at the peak air temperature.

As shown in Figure 5.3, the results indicated that TESA provided wide and noticeable thermal insulation compared to control samples. Thus, the phase change transition occurs when

PCMs melted or underwent latent and sensible heat. Also, the higher porosity of expanded clay LWA impacted the thermal insulation of concrete compared to control 1.

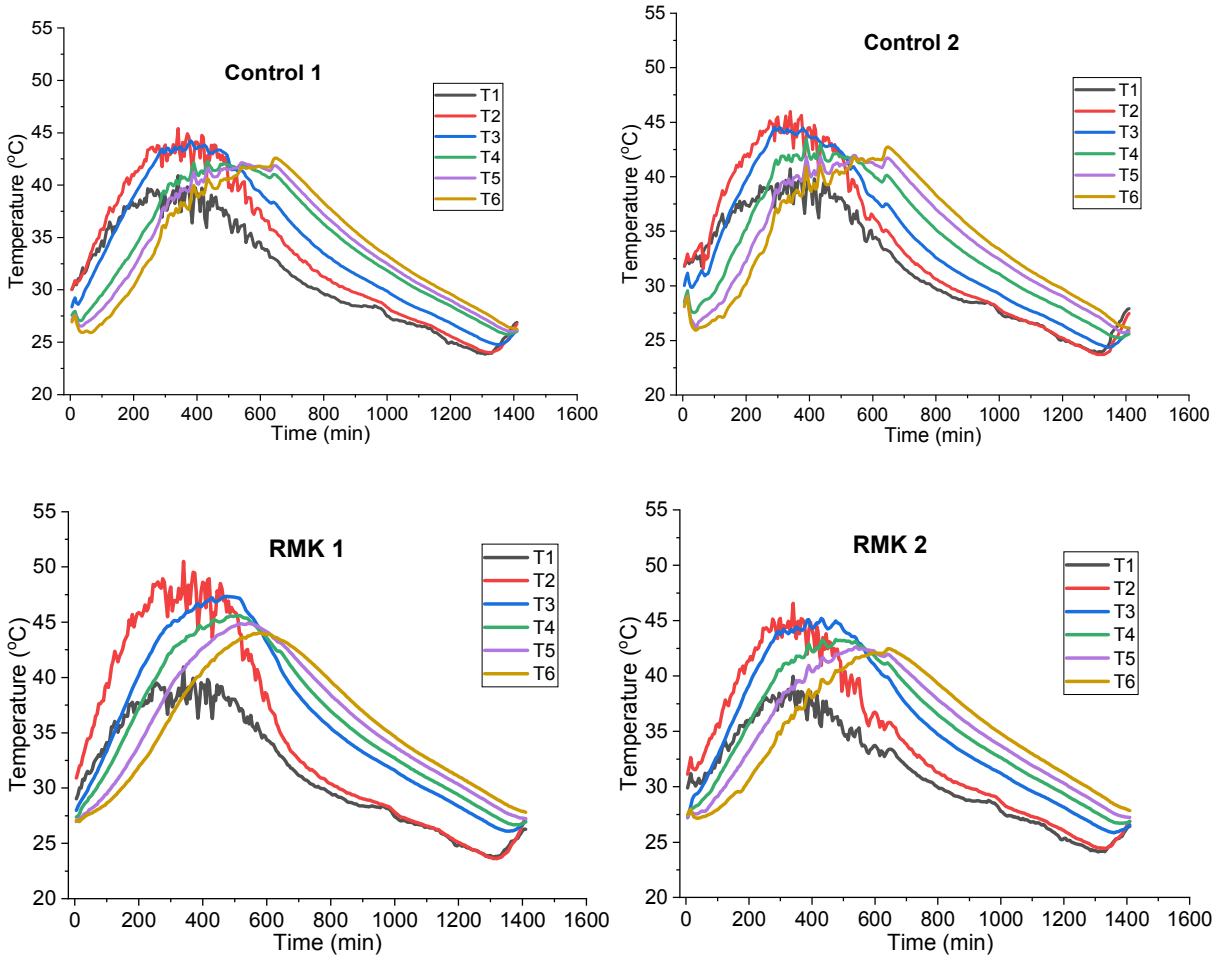

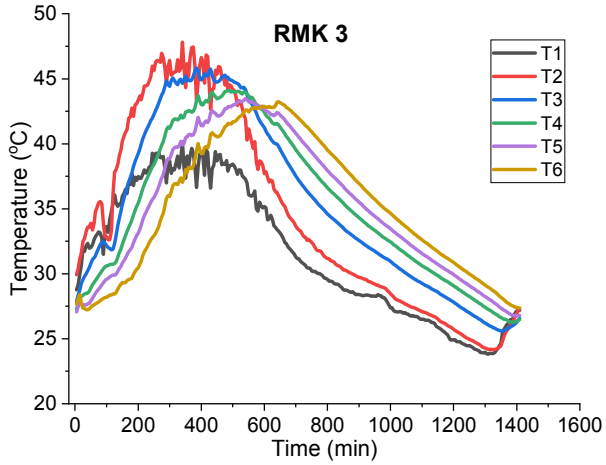

Figure 5.3: Temperature profiles of all concrete cubes made with and without TESA from the air, surface to the bottom of the concrete samples

Table 5.3: Samples' surface (T2) and middle temperatures (T5) at 2 p.m. August 26th, 2021

Samples	T2	T5
	°C	
Air temperature	36.5	
Control 1	42.3	37.98
Control 2	44.11	38.74
RMK 1	46	39.47
RMK 2	43.5	38.01
RMK 3	45.28	39.14

Figure 5.4 provides the temperature profile from the surface T2 to the center T5 at a thickness of about 76 mm through the concrete samples. As shown in Table 5.3, the air peak temperature was 36.5 °C during the daytime, according to Joe's Datacenter – Paseo West- Kansas City, Missouri (WheatherUnderground 2022). However, each sample had a particular temperature at the same test time. The temperature profile showed the following temperatures: (i) control 1's temperature was 42.3 °C at the surface T2 and 37.98 °C at the center T5. The sample had a retardation of 4.32 °C between the surface and the center. (ii) control 2's temperature was 44.11

°C at T2 and 38.74 °C at T5. The temperature difference was 5.37 °C. Control 1 and control 2 showed temperature differences of about 1.05 °C from the surface to the center of the samples during the tests. Although, based on each sample's thermal conductivity, control 1 was expected to absorb more heat and record a higher temperature throughout the sample than control 2. However, this was not the case because limestone, as a rock with no cavities, could not keep much heat for a longer time as expanded clay did. Therefore, the porosity of expanded clay played a significant role in storing sensible heat regardless of its lower thermal conductivity. Thus, control 2 provided good thermal insulation and retardation for heat to penetrate the sample than control 1. Therefore, to enhance the thermal performance of concrete produced using expanded clay, PCMs were impregnated into expanded clay to form TESA (Kalombe, Sobhansarbandi, and Kevern 2022a). These PCMs were expected to absorb and store a significant amount of sensible and latent heat, then reflect high temperatures depending on their latent heat capacities at the surface of the concrete.

(iii) RMK 1's temperature was 46 °C at T2 and 39.37 °C at T5. The temperature difference was equivalent to 6.53 °C. Thus, PW provided better thermal insulation between the surface and the center of the sample due to its higher latent heat of fusion and higher melting point (Kalombe, Sobhansarbandi, and Kevern 2022a). PW retarded the penetration or/and movement of heat deep into the sample compared to control samples. A similar observation was made for (iv) RMK 2, the temperature at T2 was 43.5 °C, and 38.01 °C at T5, and the temperature interval was 5.49 °C. Based on these results, RMK 2 provided better thermal insulation than the control samples, but the temperature intervals were lower than RMK 1. The difference in temperature between RMK 1 and RMK 2 was attributed to the melting process of PW, which was higher than that of PWSO (Kalombe, Sobhansarbandi, and Kevern 2022a). (v) RMK 3's temperature was 45.28°C at T2 and

39.14 °C at T5, and a temperature difference of 6.14 °C. Thus, COSO was able to enhance the thermal performance of the concrete by providing a higher temperature interval between the surface and the center of the specimen. The thermal performance of RMK 3 was better than control samples, and RMK 2, except for RMK 1.

Figure 5.4 reveals that the melting points (MP) and latent heat of fusion (LHF) played a significant role in the thermal insulation of concrete. The higher the MP and LHF of PCMs, the better the thermal performance of TESA for concrete production in high operating temperature such as summer or tropical climates.

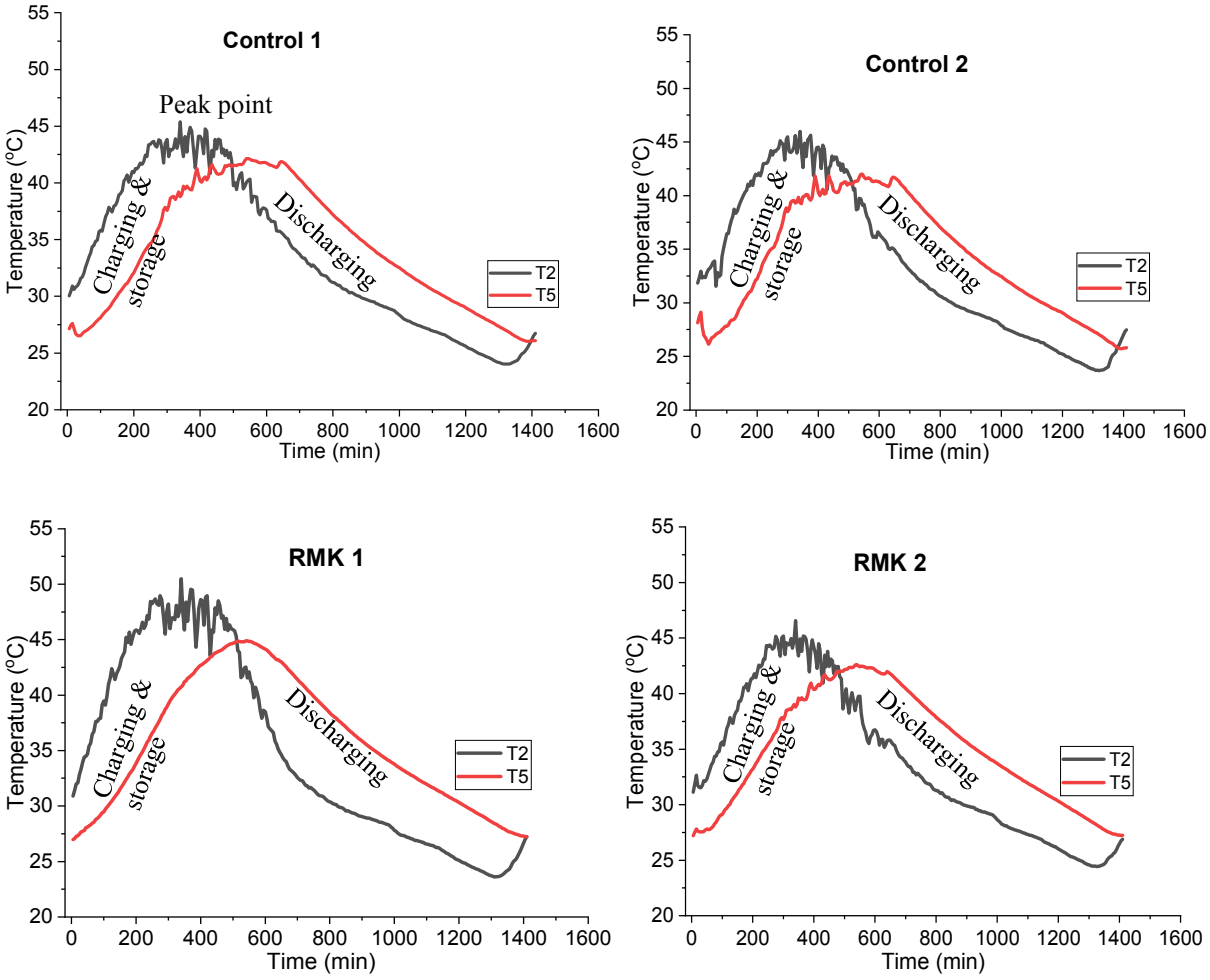

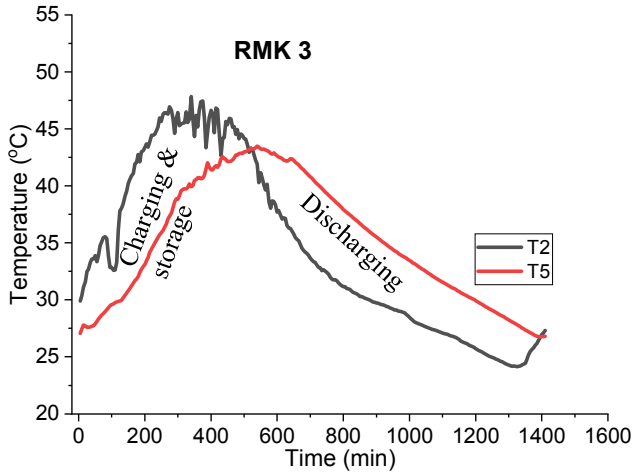

Figure 5.4: Temperature profiles of all concrete cubes containing TESA and controls

5.4.3. Heat storage

This study estimated the heat stored by concrete samples at the air peak temperature of 36.5 °C. Table 5.4 reports the heat stored by five different concrete specimens with an average surface area of 23790 ± 147.6 mm^2. The heat storage capacity was estimated from the surface (T2) to the center (T5) of concrete samples. The thickness was equivalent to 75 mm deep into the sample. Table 5.4 indicates the surface top layer (T2 to T3) estimated at 25 mm thick in the specimen stored a large amount of heat. The concrete samples with low thermal conductivity kept more heat than those with higher thermal conductivity. From T2 to T3, the concrete specimens with the most significant heat stored were RMK 1, RMK 3, and RMK 2, then control 2 and control 1. The difference in heat storage capacity was attributed to the quantity of PCMs absorbed/contained in TESA and to the sensible and latent heat mechanism experimented by PCMs in TESA concrete. Also, the heat stored by TESA concrete was a function of the exposition time of samples to the sunlight and the variation of temperature until the day reached the peak air

temperature. Therefore, the higher the latent heat of fusion of PCMs, the higher the amount of heat stored, and the better the thermal insulation of TESA concrete.

Control 2 provided specific retardation for the heat to penetrate the sample compared to control 1. The difference was due to expanded clay's porosity, which allowed sensible heat to be developed and stored inside the cavities, thus preventing heat from penetrating directly deep down into the sample as control 1. Whereas control 1, made of limestone as a rock with no cavities or pores, could not provide considerable thermal insulation to concrete. However, control 1 transferred an enormous quantity of heat into the sample (T4-T5), thus providing inadequate or insufficient thermal insulation compared to other concrete specimens, as shown in Table 5.4.

The total heat stored by concrete specimens demonstrated the effect of three types of TESA concrete and two controls, how samples enhanced or diminished the thermal inertia performance of concrete. The results showed that TESA concrete had higher thermal insulation were RMK 1, RMK 3, and RMK 2. When utilized in concrete, TESA worked as a battery analogy for whose energy was dependent on daily temperature fluctuation with time, based on which heat charging, storing, or discharging took place. Based on the achieved results, TESA could minimize the necessity of using air conditioning systems traditionally utilized to cool down the temperature in the buildings or any concrete applications, thus providing cooling infrastructures in equatorial or tropical regions.

Table 5.4: Heat stored from the surface to the center of the concrete samples

Location	Thickness	Control 1	Control 2	RMK 1	RMK 2	RMK 3
Thermocouple	(mm)	(Joules)				
T2 to T3	25	220900	229900	310600	249000	275800
T3 to T4	25	-41900	-9200	-5800	-36700	-3600
T4 to T5	25	40800	2900	11700	6900	3000
Total heat stored	75	219800	223600	316500	219200	275200

5.5. Conclusion and recommendations

In this study, the thermal inertia of concrete produced using LWA impregnated with low-cost and readily available organic PCMs as TESA was investigated as a potential technique to reduce summer cooling needs for buildings and related infrastructure. Heat storage was calculated using a charging/discharging process with environmental conditions, which is analogous to the evaluation of battery charging and releasing under load. This technique allows the comparison of different materials and observation of heat flow into and out of various layers of the bulk sample.

TESA significantly improved the thermal properties of concrete by reducing heat penetration through sensible and latent mechanisms. The thermal conductivity of concrete containing TESA was generally higher than the control mixture. The increased thermal conductivity was attributed to the increased mass (sensible) and melting (latent) process behaviors added to the concrete. Concrete containing TESA had a lower compressive strength than the control mixture containing normal-weight concrete but was not significantly different from the unimpregnated LWA control. TESA concrete stored a considerable quantity of heat in the surface layer (25 mm) compared to the control mixtures. TESA concrete containing PW provided higher

thermal insulation, followed by COSO, then PWSO. Thus, the higher energy storage of concrete was a function of the higher amount of PCMs contained in TESA, the higher melting point, and the latent heat of fusion storage capacity of PCMs.

The performance of RMK 1 and RMK 3 demonstrated that TESA concrete could be utilized to build cooler infrastructure in equatorial or tropical countries. TESA concrete can reduce conventional fossil energy currently used for cooling in hot regions. Thus, minimizing the emission of harmful gases responsible for climate changes and environmental pollution.

5.6. Reference

Albatayneh, A., D. Alterman, A. Page and B. Moghtaderi (2020). "The significance of sky temperature in the assessment of the thermal performance of buildings." Applied Sciences **10**(22).

Bamonte, P., A. Caverzan, N. Kalaba and M. Lamperti Tornaghi (2017). "Lightweight concrete containing phase change materials (PCMs): A numerical investigation on the thermal behaviour of cladding panels." Buildings, MDPI AG. **7**.

Bentz, D. P. and R. Turpin (2007). "Potential applications of phase change materials in concrete technology." Cement and Concrete Composites. **29:** 527-532.

Campbell-Scientific (2018). "Operator's manual CR1000 Datalogger." Utah**:** 1-630.

Defraeye, T., B. Blocken and J. Carmeliet (2011). "Convective heat transfer coefficients for exterior building surfaces: Existing correlations and CFD modelling." Energy Conversion and Management **52**(1): 512-522.

Faraj, K., M. Khaled, J. Faraj, F. Hachem and C. Castelain (2020). "Phase change material thermal energy storage systems for cooling applications in buildings: A review." Renewable and Sustainable Energy Reviews, Elsevier Ltd. **119**.

Farnam, Y., M. Krafcik, L. Liston, T. Washington, K. Erk, B. Tao and J. Weiss (2016). "Evaluating the Use of Phase Change Materials in Concrete Pavement to Melt Ice and Snow." Journal of Materials in Civil Engineering, American Society of Civil Engineers (ASCE). **28:** 04015161.

Fernandes, F., S. Manari, M. Aguayo, K. Santos, T. Oey, Z. Wei, G. Falzone, N. Neithalath and G. Sant (2014). "On the feasibility of using phase change materials (PCMs) to mitigate thermal cracking in cementitious materials." Cement and Concrete Composites, Elsevier Ltd. **51:** 14-26.

Hasanabadi, S., S. M. Sadrameli and S. Sami (2021). "Preparation, characterization and thermal properties of surface-modified expanded perlite/paraffin as a form-stable phase change composite in concrete." Journal of Thermal Analysis and Calorimetry, Springer Science and Business Media B.V. **144:** 61-69.

Hawes, D. W., D. Banu and D. Feldman (1992). "The stability of phase change materials in concrete." Solar Energy Materials and Solar Cells.

Hunger, M., A. G. Entrop, I. Mandilaras, H. J. H. Brouwers and M. Founti (2009). "The behavior of self-compacting concrete containing micro-encapsulated Phase Change Materials." Cement and Concrete Composites. **31:** 731-743.

Kakar, M. R., Z. Refaa, J. Worlitschek, A. Stamatiou, M. N. Partl and M. Bueno (2019). "Impregnation of lightweight aggregate particles with phase change material for its use in asphalt mixtures." International Symposium on Asphalt Pavement & Environment, Springer.

Kalombe, R. M., T. V. Ojumu, V. N. Katambwe, M. Nzadi, D. Bent, G. Nieuwouldt, G. Madzivire, J. Kevern and L. F. Petrik (2020). "Treatment of acid mine drainage with coal fly ash in a jet loop reactor pilot plant." Minerals Engineering, Elsevier Ltd. **159**.

Kalombe, R. M., S. Sobhansarbandi, J. Kevern (2022). "Assessment of low-cost organic phase change materials for improving infrastructure thermal performance." Journal of Cleaner Production, Elsevier Ltd. (Pending).

Liao, W., A. Kumar, K. Khayat and H. Ma (2019). "Multifunctional lightweight aggregate containing phase change material and water for damage mitigation of concrete." ES Materials & Manufacturing.

Liao, W., C. Zeng, Y. Zhuang, H. Ma, W. Deng and J. Huang (2021). "Mitigation of thermal curling of concrete slab using phase change material: A feasibility study." Cement and Concrete Composites, Elsevier Ltd. **120**.

Liu, F., J. Wang and X. Qian (2017). "Integrating phase change materials into concrete through microencapsulation using cenospheres." Cement and Concrete Composites, Elsevier Ltd. **80:** 317-325.

Marani, A. and M. L. Nehdi (2019). "Integrating phase change materials in construction materials: Critical review." Construction and Building Materials, Elsevier Ltd. **217:** 36-49.

Melvin Pomerantz, B. P., Hashem Akbari, and Sheng-Chieh Chang (2000). "The Effect of Pavements' Temperatures on Air Temperatures in Large Cities." Berkeley, California 94720**:** 1-16.

Mike, G. (2018). "Thermal emissivity and radiative heat transfer." Materio Performance Alloys Retrieved 06/04/2022, 2022, from https://materion.com/-/media/files/alloy/newsletters/technical-tidbits/issue-no-114-thermal-emissivity-and-radiative-heat-transfer.pdf.

Min, H. W., S. Kim and H. S. Kim (2017). "Investigation on thermal and mechanical characteristics of concrete mixed with shape stabilized phase change material for mix design." Construction and Building Materials, Elsevier Ltd. **149:** 749-762.

Mohseni, E., W. Tang and S. Wang (2019). "Development of thermal energy storage lightweight structural cementitious composites by means of macro-encapsulated PCM." Construction and Building Materials, Elsevier Ltd. **225:** 182-195.

Nizovtsev, M. I., V. Y. Borodulin, V. N. Letushko, V. I. Terekhov, V. A. Poluboyarov and L. K. Berdnikova (2019). "Heat transfer in a phase change material under constant heat flux." Thermophysics and Aeromechanics, Kutateladze Institute of Thermophysics SB RAS. **26:** 313-324.

Nowak, H. (1989). "The sky temperature in net radiant heat loss calculations from low-sloped roofs." Infrared Physics **29**(2-4): 231-232.

Qu, Y., J. Chen, L. Liu, T. Xu, H. Wu and X. Zhou (2020). "Study on properties of phase change foam concrete block mixed with paraffin / fumed silica composite phase change material." Renewable Energy, Elsevier Ltd. **150:** 1127-1135.

Šavija, B. (2018). "Smart crack control in concrete through use of phase change materials (PCMs): A review." Materials, MDPI AG. **11**.

Sharma, B., N. Neithalath, S. Rajan and B. Mobasher (2013). "Incorporation of Phase Change Materials into Cementitious Systems." Master's Thesis. Arizona State University, Phoenix, USA.

She, Z., Z. Wei, B. A. Young, G. Falzone, N. Neithalath, G. Sant and L. Pilon (2019). "Examining the effects of microencapsulated phase change materials on early-age temperature evolutions in realistic pavement geometries." Cement and Concrete Composites, Elsevier Ltd. **103:** 149-159.

Sivanathan, A., Q. Dou, Y. Wang, Y. Li, J. Corker, Y. Zhou and M. Fan (2020). "Phase change materials for building construction: An overview of nano-/micro-encapsulation." Nanotechnology Reviews, De Gruyter Open Ltd. **9:** 896-921.

Sukontasukkul, P., T. Sangpet, M. Newlands, D. Y. Yoo, W. Tangchirapat, S. Limkatanyu and P. Chindaprasirt (2020). "Thermal storage properties of lightweight concrete incorporating phase change materials with different fusion points in hybrid form for high temperature applications." Heliyon, Elsevier Ltd. **6**.

Vakhshouri, A. R. (2021). "Paraffin as Phase Change Material." IntechOpen.

WheatherUnderground. (2022). "Joe's Datacenter - Paseo West - KMOKANSA198." Joe's Datacenter - Paseo West - KMOKANSA198 Retrieved 05/21/2022, 2022, from https://www.wunderground.com/dashboard/pws/KMOKANSA198.

Zhou, D., C. Y. Zhao and Y. Tian (2012). "Review on thermal energy storage with phase change materials (PCMs) in building applications." Applied Energy, Elsevier Ltd. **92:** 593-605.

CHAPTER 6: LOW-COST PCM-MODIFIED CONCRETE FOR REDUCING DEICING NEEDS

6.1. Abstract

Application of deicing salts is a common technique to improve winter safety; however, the widespread salt application causes decreased infrastructure lifespan, and potential environmental pollution and is a high cost. In this study, low-cost thermal energy storage aggregates (TESA) were created with several different organic phase change materials (PCMs) possessing thermodynamic properties suitable for heat storage under freezing conditions. PCMs used in the study included individual blends of paraffin wax, soybean oil, and coconut oil. TESA was coated with latex to prevent leakage. The results showed the relative contribution of both sensible and latent heat storage behaviors. A methodology considering system energy input and discharge using a battery storage analogy is presented, allowing heat movement quantification under actual winter conditions. Results showed the most significant increase in heat storage and delay in freezing a combination PCM of paraffin wax and soybean oil. TESA concrete is one potential approach requiring little operational management to reduce the amount of deicing salts or other winter maintenance while minimizing environmental impacts and safety concerns. Hence, TESA could provide a sustainable and feasible option for cold regions.

Keywords: Snow, Ice, Deicing, phase change materials, concrete, heat storage

6.2. Introduction

Accumulation of snow and ice on the surface of concrete pavements can result in a loss of friction, creating unsafe driving conditions (Kenzhebayeva, Bakbolat et al. 2021). Often, frost action within the granular pavement layers can be aggravated by an ice enrichment process (Shi,

Zhang et al. 2018). However, numerous methods have been developed to combat deicing by making use of salts, mechanical deicing, a hydrophobic coating to the surfaces, ultrasonic treatment, or electric heating (Kenzhebayeva, Bakbolat et al. 2021). Each of these methods implies environmental and economic impacts on the maintenance of roads, where salts are mostly feasible (Sakulich and Bentz 2012). Calcium chloride ($CaCl_2$) and magnesium chloride ($MgCl_2$) are mainly utilized as deicing salts for road, asphalt, or sidewalk due to their better performance and commercial availability at a low cost. Regardless of the benefits of using salts, they still deteriorate concrete pavements. The detrimental effects of $CaCl_2$ and $MgCl_2$ on concrete pavements are categorized as (i) physical deterioration (e.g., salt scaling); (ii) chemical reactions between deicers and cement paste (e.g., a cation-oriented process, especially in the presence of $MgCl_2$ and $CaCl_2$ affecting alkali-carbonate reactivity); and (iii) deicers are aggravating aggregate and cement reactions (e.g., the anion-oriented process in the case of chlorides, acetates, and formates affecting alkali-silica reactivity) (Farnam, Esmaeeli et al. 2017, Xu, Xu et al. 2017, Shi, Zhang et al. 2018). Therefore, an innovative, multifunctional concrete pavement has been developed (Rocha Segundo and Carneiro. 2021).

Smart concrete pavement has different abilities, including photocatalytic, superhydrophobic, self-cleaning, deicing, self-healing, thermochromic, and latent heat thermal energy storage. These abilities allowed the pavement to react to external stimuli (Rocha Segundo and Carneiro. 2021). Thus, these abilities are developed using different materials such as dyes, nanoparticles, fibers, and phase change materials (PCMs) (Rocha Segundo and Carneiro. 2021). Since PCMs can store or release heat (Anupam, Sahoo et al. 2020), it can decrease the number of freeze and thaw cycles experienced by the pavement and increase the service life of concrete pavements (Sharifi 2016, Sumeru Nayak 2019). Therefore, selecting an appropriate PCM type and

incorporating technique plays a significant role in its performance. Also, it is essential to prevent the contact between PCMs and freshly mixed cement-based materials because it can negatively impact concretes' mechanical and durability properties, thus limiting field applications. A large latent heat storage capacity and a low melting point of PCM are also necessary for melting snow and ice (Sharifi 2016, Jung Heum Yeon 2018, Sharma, Jang et al. 2022). Faraj et al. (2020) indicated the necessity of considering the environmental and economic impact of incorporating PCMs in concrete (Faraj, Khaled et al. 2020).

The freeze and thaw cycles experienced by a bridge deck were reported by Bentz and Turpin 2007. To make different mortar samples, the authors impregnated coarse sand with three various polyethylene glycols, octodecane, and paraffin wax as PCMs (Bentz and Turpin 2007). The mortar specimens were placed in a control environmental chamber. Bentz and Turpin simulated the number of expected freeze-thaw cycles for bridge decks in twelve different climates available in the TMY2DATA files using an existing one-dimensional finite-difference computer code (CONCTEMP). The results showed that PCMs could reduce the freeze and thaw cycles experienced by concrete exposed to a winter environment (Bentz and Turpin 2007). Using a similar modeling program (CONCTEMP) and environmental chamber, Sakulich and Bentz (2012) reported that the incorporation of PCMs in bridge decks is one such technology that could increase the service lives of bridge decks (Sakulich and Bentz 2012). Farnam et al. (2017) reported two approaches of integrating paraffin oil as PCM (i) into a porous lightweight aggregate (LWA) and (ii) embedded into metal pipes. The concrete slabs were placed in a controlled environmental chamber, then artificial snow such as shave ice was made using cubic ice at 0°C and placed on the samples' surface with gentle compaction. As a result, it was reported that incorporating PCM in concrete pavement is feasible and practical (Farnam, Esmaeeli et al. 2017). Esmaeeli et al. (2018)

suggested that PCM-LWA cementitious materials are promising for enhancing the behavior of concrete pavements under freezing-thawing cycles (Esmaeeli, Farnam et al. 2017, Marani and Nehdi 2019). Yeon and Kim (2018) developed mortar containing N-tetradecane microencapsulated with tiny melamine-formaldehyde resin shells. The dry sample was insulated with 10 mm-thick polyoxymethylene plates. The mortar was placed in an environmental chamber equipped with a TH300 Hanyoung to control the temperature, set between -3 and -5 °C for the freeze-thaw test. The results show that PCM with a low melting point has the potential to prolong the service life of concrete pavements against freeze-thaw deteriorations even though its effect became minimal with prolonged exposure to an ambient temperature far below the transition temperature (Jung Heum Yeon 2018).

In the previous research works, the freezing and thaw cycles of concrete containing PCMs were carried out in the thermally controlled environmental chamber. The literature used artificial snow or ice and modeling programs to simulate conditions similar to road pavements during winter. Thus, the suggestions and predictions made in the literature could be diverse if the test were performed outside in actual winter weather conditions. This study investigates the field thermal performance of concrete containing low cost organic PCMs during winter season. The temperature profile, and energy stored or discharged by concrete are reported in this study.

6.3. Methodology

6.3.1. Materials and material production

Table 6.1 shows the mix design used in this research to make concrete samples. The materials were water, cement, sand, limestone aggregates, and expanded clay. Three types of TESA coated with latex were utilized namely TESA-PW, TESA-PWSO. ASTM C305-06 was used to mix five concretes samples (152x157.2x156 mm^3). The concrete differed from each other

by the types of aggregates as shown in Table 6.1. Concrete samples were cured, as reported by Kalombe, Sobhansarbandi, and Kevern (2022b).

Table 6.1: Mixture properties

Condition	Abs	SG	Cement	Sand	LST	EC	TESA	Water
	%		(kg/m^3)					
Control 1	0.8	2.72	3000	2379	3568	-	-	1529
Control 2	17.9	1.26	3000	2379	-	1677	-	1801
RMK 1	0.7	1.41	3000	2379	-	-	1882	1513
RMK 2	1.9	1.37	3000	2379	-	-	1826	1534
RMK 3	3.4	1.38	3000	2379	-	-	1840	1562

Note: RMK 1, RMK 2, RMK 3 stands for TESA made with paraffin wax, paraffin wax and soybean oil, coconut oil and soybean oil, Control 1: concrete made limestone aggregate (LST), control 2: concrete made expanded clay (EC) LWA. Abs: water absorption, and SG: specific gravity.

6.3.2. Temperature profiles

The temperature profile of control 1, control 2, RMK 1, RMK 2, and RMK 3 were recorded in the winter season from February 9th to 16th, 2022, in Kansas City, Missouri, United States. The minimum and maximum air temperature recorded by HOBO RX3000 Advance Remote Weather Station are reported in Table 6.2.

Table 6.2: Minimum and maximum air temperature in Kansas City from 7th to 16th February 2022

Date	Min	Max
Day and month	°C	
7-Feb	-2.54	14.73
8-Feb	2.93	18.95
9-Feb	4.56	15.07
10-Feb	0.83	12.71
11-Feb	-5.56	12.45
12-Feb	-10.43	0.98
13-Feb	-3.08	2.42
14-Feb	-1.10	13.50
15-Feb	-0.97	19.75
16-Feb	1.52	18.82

The specimens were placed on a flat surface on the roof. The sensor holder and thermal insulations were made of nylon rods and polystyrene, respectively. As depicted in Figure 6.1, t-wire thermocouples (error = ±1 °C) were placed in and out of the samples. The distance between t-wires was 68 mm from T1 to T2; 25 mm from T2 to T3; 25 mm from T3 to T4; 25 mm from T4 to T5; and 74 mm from T5 to T6. Nothing was separating the layers, but they were defined by the locations of thermocouples throughout a concrete cube. Then, the thermocouples from T1 to T6 were connected to a datalogger CR1000/multiplexer and software PC400 4.7–shortcut, to collect the temperature profiles of specimens every 5 min. The datalogger error is estimated at ± 0.1 °C over 0 to 40 °C, ± 0.3 °C from –25 to 50 °C, and ± 0.8 °C from –55 to 85 °C.± 0.3 °C (Campbell-Scientific 2018). The air temperature, wind speed, and dew point were obtained from the HOBO RX3000 Advance Remote Weather Station operating at the same location where the concrete field test was carried out.

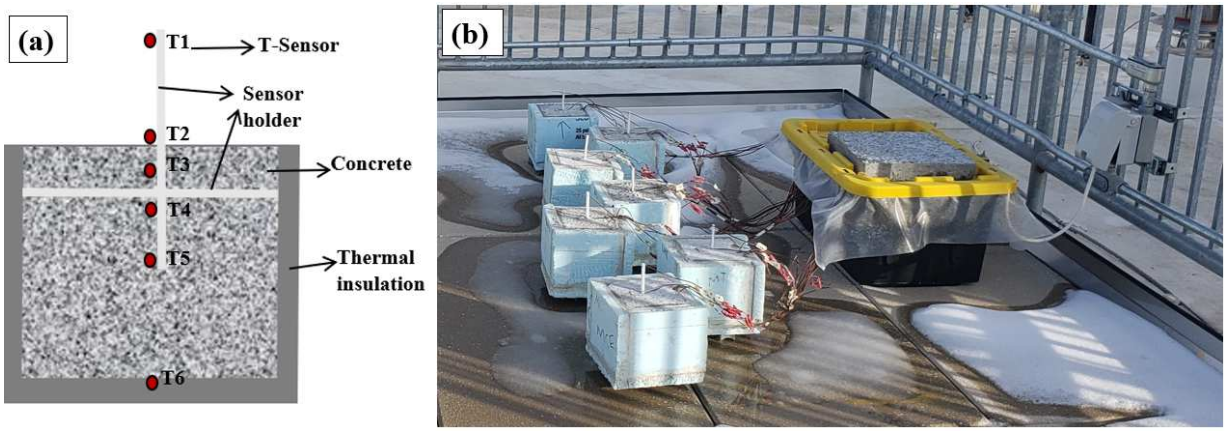

Figure 6.1: Concrete samples set-up: (a) t-wire sensors and thermal insulation, and (b) winter field tests

6.3.3. Heat storage

The heat stored or discharged by concrete samples from February 9th at 08:05 a.m. to February 16th at 07:20 a.m., 2022, was estimated using the conservation energy principles depicted in Figure 6.2. The heat storage was estimated from T2 to T5 at a thickness equivalent to 75 mm of the sample.

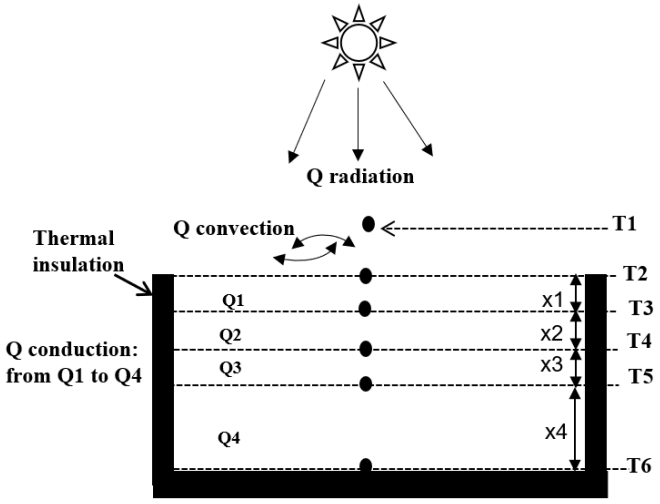

Figure 6.2: The Scenario for insulated sample containing t-wire sensors used to estimate the heat storage

As depicted in Figure 6.2**,** specimens were thermally insulated and only one cross-sectional dimension was exposed to air temperature, snow, and ice forming during winter. In order to

estimate the heat stored or discharged by each concrete, the following equations were developed using the scenario shown in Figure 6.2. The first concept used was the Stefan-Boltzmann's law, defined in equation (6.1):

$$Q_{Rad}(J) = \varepsilon\, \delta\, A\, t \left(T_2^4 - T_{sky}^4\right) \qquad (6.1)$$

where: Q_{Rad}: heat transfer by radiation [Joules (J)], Stephan-Boltzmann's constant (5.6703 x 10-8 W/m^2K^4), A: surface area of the specimen (m^2), t: time (s), T_2: the temperature on the surface of the sample (K^4), and: sky temperature (K^4) estimated using Nowak's equation (6.3) (Nowak 1989). The emissivity was determined as reported by Albatayneh et al. (2020), defined in equation (6.2):

$$\varepsilon = \left[0.787 + 0.767 \times \ln\left(\frac{\text{Dew point temperature}}{273}\right)\right] + 0.0224N - 0.0035N^2 + 0.00028N^3 \qquad (6.2)$$

where N: is the opaque sky cover, assumed to be 0.5 in this study (Albatayneh, Alterman et al. 2020). Dewpoint temperature obtained from HOBO RX3000 Advance Remote Weather Station. Then, the sky temperature was determined using equation (6.3) (Nowak 1989):

$$T_{sky}(kelvin) = 0.0553\ (T_{air})^{1.5} \qquad (6.3)$$

where T_{air}: air temperature obtained from HOBO RX3000 Advance Remote Weather Station. The heat transfer by convection took place in the air on top of the sample's surface. Newton's law represented the heat transfer by convection in equation (6.4):

$$Q_{Conv}\ (J) = A\, t\, h_{Conv}(T_2 - T_{air}) \qquad (6.4)$$

where Q_{Conv}: heat transfer by convection (J). The convective heat transfer coefficient was estimated using the equation (6.5) developed by Defraeye et al. using wind speed less than 5 m/s (Defraeye, Blocken et al. 2011).

$$h\left(\frac{W}{m^2K}\right) = (4 \times U) + 5.6 \qquad (6.5)$$

where U: wind speed (m/s). This study determined the heat transfer by conduction from the surface T2 to the center T5. The heat flux was estimated at two thicknesses x_1 and x_2 using equation (6.6):

$$Q_{HF}\left(W/m^2\right) = \frac{K\,(T_2 - T_3)}{x_1} \qquad (6.6)$$

where: Q_{HF}: heat flux (Wm^{-2}), k: thermal conductivity (W/mK) of the concrete sample measured at ambient temperature, T_3: temperature (K) at 25 mm below the surface of the specimen, and x_1: thickness (m) identified as the first layer in Figure 6.2 equivalent to 25 mm. The equation for the conservation of energy for a dry surface to determine the energy stored in the samples (Melvin Pomerantz 2000) is defined in equation (6.7):

$$Q_{storage}\,(J) = Q_{Rad} + Q_{Conv} - Q_{Cond} \qquad (6.7)$$

where, Q_{Rad} stands for a modified Fourier's law expression for heat transfer by conduction is represented in equation (6.8):

$$Q_{Rad}(J) = \frac{K\,A\,t\,(T_2 - T_3)}{x_1} \qquad (6.8)$$

This research assumed that all specimens were at the sample's steady-state, one-dimensional conduction, and constant thermal conductivity. Thus, the energy storage was determined per layer from x1 to x3, as depicted in Figure 6.2. Depending on the air temperature

and the temperature absorbed by concrete containing PCMs or TESA concrete. If the temperature reached in the TESA concrete samples was equivalent to the melting process of the PCMs in the TESA. The product of mass (m) and latent heat of fusion (H) of PCM in that concrete, expressed as "m x H," were added to the equation for energy stored calculation. Otherwise, "m x H," was not added. The heat stored at each layer was determined as follows:

Heat stored in layer one was determined using equation (6.9):

$$q_1\,(\mathrm{J}) = \mathrm{Q_{Rad}} + \mathrm{Q_{Conv}} - \frac{\mathrm{k\,A\,t\,(T_2 - T_3)}}{\mathrm{x_1}} + (m \times H)_{PCM} \qquad (6.9)$$

Considering $Q_{Rad} + Q_{Conv} = Q$

Heat stored in layer two was calculated using equation (6.10):

$$q_2\,(\mathrm{J}) = \mathrm{Q} - q_1 - \frac{\mathrm{k\,A\,t\,(T_3 - T_4)}}{\mathrm{x_2}} + (m \times H)_{PCM} \qquad (6.10)$$

Heat stored in layer three was estimated using equation (11):

$$q_3\,(\mathrm{J}) = \mathrm{Q} - q_1 - q_2 - \frac{\mathrm{k\,A\,t\,(T_4 - T_5)}}{\mathrm{x_3}} + (m \times H)_{PCM} \qquad (6.11)$$

After that, the total energy stored by the specimen from the surface (T2) to the center (T5) was calculated using equation (6.12):

$$\mathrm{Q_{storage}(J)} = q_1 + q_2 + q_3 \qquad (6.12)$$

6.4. Results and discussion

6.4.1. Temperature variations

Figure 6.3 shows the temperature profiles of the air temperature and control 1 for seven days in winter. Similar temperature profiles were obtained for control 2, RMK 1, RMK 2, and RMK 3. TESA concrete had a higher temperature than control 1 and control 2 at the surface, T2

in the daytime. However, the temperature difference was not significant between the embedded thermocouples within the sample because of the low temperature during the test period. The temperature varied from -10 °C to 23 °C. During this period, it was snowing, and ice was forming in the field test region. Due to the daily temperature fluctuation demonstrated in Figure 6.3, three sections, X (rapid drop), Y (freezing and thawing cycles), and Z (broad humped peaks), were limited/separated/created to determine the delays developed by concrete samples to reach the peak, freezing, and lowest temperatures. For concrete pavements, the freezing occurred mainly on the surface top layer of the concrete. Therefore, in this study, an average temperature of T2 and T3 was used to discuss the freezing behavior of all the concrete samples at X, Y, and Z.

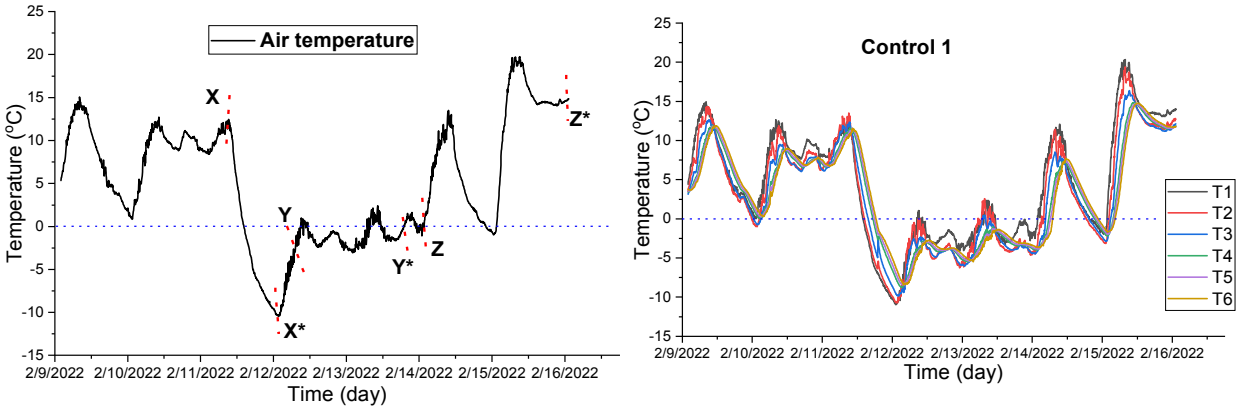

Figure 6.3: The temperature profile of air temperature and control 1

Table 6.3 shows the peak, freezing and the lowest temperature at the rapid drop from X to X* between the air temperature and the average temperature of T2 and T3 of control 1, control 2, RMK 1, RMK 2, and RMK 3. Thus, T2 and T3 represent a surface layer of 25 mm thickness.

Table 6.3: Section X-X* of the average temperature of T2 and T3 of concrete samples and air temperature, date and time

Sample	Date and time	Temperature (°C)
	Peak	
Air Temp	2/11/2022 15:20	12.453±0.39
Control 1	2/11/2022 15:10	12.775±0.31
Control 2	2/11/2022 15:25	11.945±0.30
RMK 1	2/11/2022 15:25	12.690±0.38
RMK 2	2/11/2022 15:20	13.425±0.82
RMK 3	2/11/2022 15:25	13.235±0.57
	Freezing	
Air Temp	2/11/2022 20:15	0.185±0.22
Control 1	2/11/2022 21:05	0.106±0.22
Control 2	2/11/2022 20:35	0.102±0.24
RMK 1	2/11/2022 21:20	0.097±0.20
RMK 2	2/11/2022 21:25	0.024±0.21
RMK 3	2/11/2022 21:25	0.001±0.20
	Lowest point	
Air Temp	2/12/2022 8:20	-10.217±0.21
Control 1	2/12/2022 8:25	-10.005±0.20
Control 2	2/12/2022 8:25	-10.135±0.26
RMK 1	2/12/2022 8:40	-10.445±0.24
RMK 2	2/12/2022 8:45	-10.205±0.23
RMK 3	2/12/2022 8:35	-10.160±0.18

As depicted in Table 6.3, the peak air temperature reached a rapid drop top with a 10 min delay compared to control 1 and 5 min before control 2. Thus, the surface of control 2 absorbed and accumulated heat faster than control 1. Also, control 2 reached a higher peak temperature than the air temperature surrounding the samples simultaneously. However, the air temperature reached

the freezing temperature (0 °C) first, followed 20 min later by control 2, then 30 min later by control 1. The lowest temperature was first reached by air temperature, followed simultaneously 5 min later by control 1 and control 1.

The RMK 1 and control 2 reached the peak temperature at a rapid drop simultaneously, but with a delay of 15 min compared to control 1. Meanwhile, the freezing temperature was first attained by control 2, followed 30 min later by control 1, then 20 min later by RMK 1. The delay in freezing of RMK 1 was attributed to the ability and capacity of PW to store heat and release it as the atmospheric temperature changed over time based on the principle of the second law of thermodynamics, heat moves from a hot body to a cold body. At the lowest temperature of the rapid drop, both controls simultaneously reached their lowest points. But RMK 1 got at the lowest end 15 min later because it accumulated a considerable amount of sensible heat, then discharged to the surface. Similar observations were made for RMK 2 and RMK 3 with the same delay of freezing of 45 min, respectively, compared to control 2. The rapid drop showed the necessity of using TESA in concrete production, which enhanced the thermal behavior of concrete exposed to snow and icing during winter.

Unlike the rapid drop, where the highest air temperature was about 12.453±0.39 °C, Figure 4 shows freezing and thawing cycles with the air peak temperature of approximately 0.979±0.53 °C and 2.416±0.40 °C from Y to Y*, respectively.

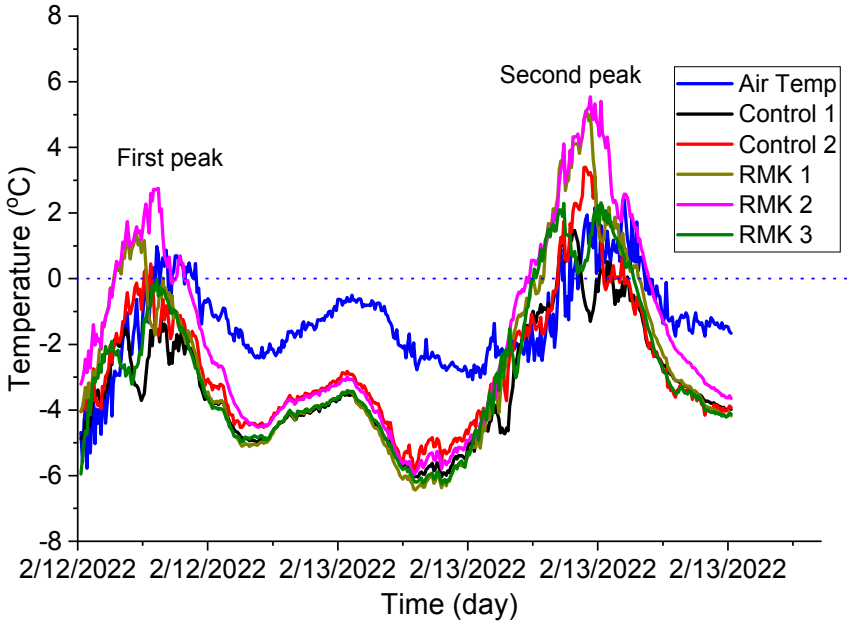

Figure 6.4: Section Y-Y*: air temperature and an average temperature of T2 and T3 of concrete specimens

As shown in Figure 6.4 and Table 6.4, the concrete sample of control 2 reached the peak temperature first, followed 20 min later by air temperature, then 15 min later by control 1. Since the peak air temperature was very low on this day, the maximum temperature of the air and control 1 were equal to their freezing temperatures, but control 2 reached the peak point 20 min earlier. Thus, the surface of control 2 froze first, then 20 min later, the air temperature reached the freezing point, then 15 min later was, the surface of control 1 froze. Meanwhile, the lowest point was attained first by the air temperature, followed 25 min later by control 2, then 10 min later by control 1, as shown in Table 6.4.

Table 6.4: Section Y-Y* (from first peak) of the average temperature of T2 and T3 of concrete samples and air temperature, date and time

Sample	Date and time	Temperature °C
	Peak	
Air Temp	2/12/2022 15:15	0.979±0.53
Control 1	2/12/2022 15:30	-1.252±0.19
Control 2	2/12/2022 14:55	0.456±0.45
RMK 1	2/12/2022 15:35	0.029±0.22
RMK 2	2/12/2022 15:20	2.753±0.55
RMK 3	2/12/2022 15:15	-0.015±0.20
	Freezing	
Air Temp	2/12/2022 15:15	0.979±0.16
Control 1	2/12/2022 15:30	-1.252±0.19
Control 2	2/12/2022 14:55	0.456±0.45
RMK 1	2/12/2022 15:35	0.029±0.22
RMK 2	2/12/2022 16:40	0.465±0.29
RMK 3	2/12/2022 15:15	-0.0145±0.16
	Lowest point	
Air Temp	2/12/2022 20:35	-2.410±0.05
Control 1	2/12/2022 21:10	-4.907±0.035
Control 2	2/12/2022 21:00	-4.533±0.05
RMK 1	2/12/2022 21:00	-5.016±0.02
RMK 2	2/12/2022 20:40	-4.520±0.03
RMK 3	2/12/2022 19:50	-4.971±0.08

As depicted in Figure 6.4 (first peak) and Table 6.4, RMK 1 reached the peak temperature last, which was 5 min and 30 min after control 1 and control 2, respectively. The Freezing point was attained first by RMK 1, followed 15 min later by control 2, then 35 min later by control 1. On this day, the air temperature was below 1 °C, and no sensible or latent heat mechanism could

occur in PW to heat the surface of RMK 1 to create a delay in the surface to freezing. As demonstrated in Figure 6.6-7, there was a deficit in heat storage in/on the sample. Meanwhile, the lowest point was attained by both RMK 1 and control 2 simultaneously, then 10 min later by control 1. However, RMK 2 reached the highest point 25 minutes after control 2 but 10 minutes before control 1. Also, RMK 2 attained the freezing point with a delay of 105 min and 70 min compared to control 2 and control 1, respectively. The retardation was attributed to the melting point and latent heat storage capacity of PWSO in RMK 2 (Kalombe, Sobhansarbandi, and Kevern 2022b). Thus, at the air temperature below 1 °C, RMK 2 could still have enough heat to heat the surface and create a significant delay in freezing the concrete's surface. Meanwhile, the lowest point was first reached by RMK 2, followed 20 min later by control 2, then 10 min later by control 1. RMK 2 had a long freeze delay and started charging before control 1 and control 2. Meanwhile, RMK 3 reached the peak temperature 20 minutes after control 2 but 15 minutes before control 1. The freezing and peak temperatures did not change for RMK 3 and control 1. Thus, the surface layer of control 2 froze first, followed 20 min later by RMK 3, then 15 min later by control 1. Among all TESA concrete, RMK 2 provided a better thermal performance by creating enormous retardation to freeze the surface.

On the other hand, Table 6.5 represents the results in Figure 6.4 (second peak). The concrete surface of control 1 attained the peak temperature first, followed 40 min later by control 2, then 125 min later by the air temperature surrounding the samples. Similarly, the freezing temperature was reached by control 1, then 70 min later by control 2, and the surrounding air reflected the cool temperature 135 min later. The lowest temperature was first attained by the air temperature, followed 90 min later by control 2, then 35 min later by control 1.

Table 6.5: Section Y-Y* (from second peak) of the average temperature of T2 and T3 of concrete samples and air temperature, date and time

Sample	Date and time	Temperature (°C)
	Peak	
Air Temp	2/13/2022 16:25	2.416±0.40
Control 1	2/13/2022 13:40	1.467±0.14
Control 2	2/13/2022 14:20	3.399±0.33
RMK 1	2/13/2022 14:20	5.103±0.29
RMK 2	2/13/2022 14:35	5.542±0.35
RMK 3	2/13/2022 15:10	2.316±0.24
	Freezing	
Air Temp	2/13/2022 17:30	0.142±0.46
Control 1	2/13/2022 14:05	0.127±0.56
Control 2	2/13/2022 15:15	0.541±0.30
RMK 1	2/13/2022 17:10	0.024±0.26
RMK 2	2/13/2022 17:40	0.181±0.27
RMK 3	2/13/2022 16:55	0.0105±0.28
	Low	
Air Temp	2/13/2022 20:45	-1.745±0.15
Control 1	2/13/2022 22:50	-4.085±0.03
Control 2	2/13/2022 22:15	-4.118±0.10
RMK 1	2/13/2022 22:50	-4.273±0.02
RMK 2	2/13/2022 23:25	-3.778±0.06
RMK 3	2/13/2022 22:15	-4.2675±0.05

However, Table 6.5 shows RMK 1 reached the peak temperature simultaneously with control 2, but control 1, 40 min earlier. RMK 1 attained the freezing temperature with a delay of 115 min and 185 min compared to control 2 and control 1, respectively. Meanwhile, RMK 1 and control 1 reached the lowest temperature simultaneously, but 35 min after control 2. On the other

hand, RMK 2 got the maximum temperature of 15 min and 55 min after control 2 and control 1, respectively. The delay for RMK 2 to freeze was 145 min and 215 min compared to the freezing temperature of control 2 and control 1, respectively. The lowest temperature was first reached by control 2, followed 35 minutes later by control 2, then 35 minutes later by RMK 2. Whereas RMK 3 attained the peak temperature of 90 min and 50 min after control 1 and control 2, respectively. Also, RMK 3 reached the freezing temperature with a delay of 170 min and 100 min compared to control 1 and control 2, respectively. RMK 3 and control 2 attained the lowest temperature simultaneously, then 45 min by control 1. For Figure 6.4, RMK 2 provided a long delay to freeze, followed by RMK 1, then RMK 3. Thus, the freezing and thawing cycles in Figure 6.4 demonstrate the effect of TESA concrete samples in delaying freezing time on the surface of concretes. Most delays were developed by RMK 2.

Figure 6.5 (main peak) shows the broad humped peak for air temperature and the average temperature of T2 and T3 for control 1, control 2, and RMK 2. The maximum, freezing, and lowest temperature, and time are depicted in Table 6.6.

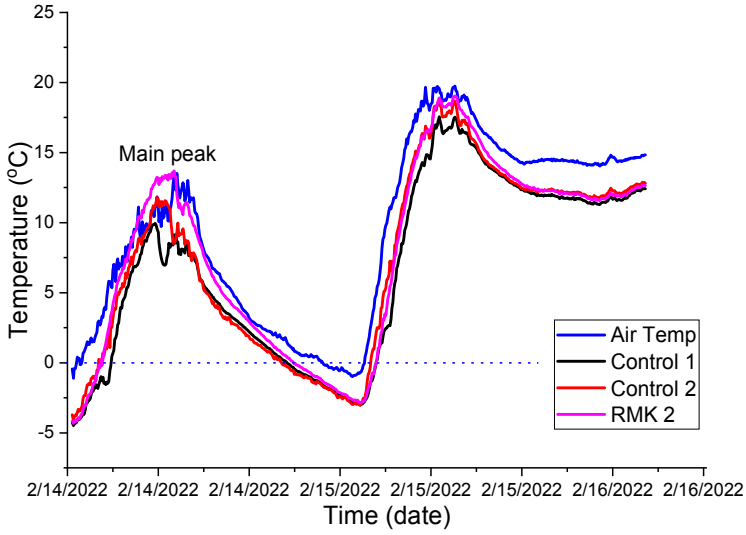

Figure 6.5: Section Z-Z*: Air temperature and an average temperature of T2-T3 of concrete specimens

Table 6.6: Section Z-Z* (from main peak) of the average temperature of T2 and T3 of concrete samples and air temperature, date and time

Sample	Date and time	Temperature (°C)
	Peak	
Air Temp	2/14/2022 15:45	13.504±0.53
Control 1	2/14/2022 13:55	9.955±0.49
Control 2	2/14/2022 14:05	11.800±0.22
RMK 1	2/14/2022 14:05	12.850±0.28
RMK 2	2/14/2022 15:30	13.700±0.38
RMK 3	2/14/2022 12:50	10.25±0.23
	Freezing	
Air Temp	2/15/2022 4:00	0.099±0.12
Control 1	2/15/2022 1:00	0.060±0.09
Control 2	2/15/2022 0:30	0.146±0.18
RMK 1	2/15/2022 1:10	0.023±0.10
RMK 2	2/15/2022 1:35	0.054±0.10
RMK 3	2/15/2022 1:15	0.0635±0.12
	Lowest point	
Air Temp	2/15/2022 6:35	-0.973±0.08
Control 1	2/15/2022 7:15	-3.002±0.05
Control 2	2/15/2022 7:15	-3.043±0.06
RMK 1	2/15/2022 7:15	-3.123±0.06
RMK 2	2/15/2022 7:15	-2.863±0.07
RMK 3	2/15/2022 7:15	-2.871±0.07

As shown in Table 6.5 and Figure 6.5, the sample surface of control 1 attained the maximum temperature first, followed 10 min later by control 2, then 100 min later by the air temperature surrounding the samples. The freezing temperature (0 °C) was reached firstly by control 2, followed 30 min later by control 2, then 180 min later by the air temperature. But the air temperature reached first the lowest temperature, then 40 min later both controls reached their

lowest points at the same time. On the other hand, the highest temperature attained by RMK 2 was 95 min and 85 min after control 1 and control 2, respectively. RMK 2 reached the freezing temperature with a delay of 35 min and 65 min compared to control 1 and control 2, respectively. RMK 2, control 1, and control 2 attained the lowest temperature simultaneously. RMK 1 and RMK 3's surface froze with a delay of 40 min and 45 min respective compared to control 2. Once again, TESA concretes created a delay to freezing compared to specimens made without PCMs. RMK 2 significantly created a long delay to freezing compared to RMK 1 and RMK 2.

Based on the results mentioned above, regardless of the peak temperature of the air surrounding the concrete samples, TESA concrete proved to be the ideal building material for winter due to the considerable delay time created to freeze the surface of concrete compared to control concretes. The rate of heating or cooling of the concrete surface was a function of the consistency of the air temperature (hot or cold) surrounding the sample. TESA concrete showed a short freezing delay at the rapid drop section (X-X*), considerable retardation in freezing at the freeze and thaw cycles section (Y-Y*), and a higher freezing delay at the broad humped peak section (Z-Z*) compared to control 2. The melting and solidification point and latent heat of the PCMs present in TESA played a significant role in the duration of the delay of freezing produced by concrete. With the most prolonged freezing delay, TESA concrete was RMK 2, followed by RMK 3, then RMK 1. Apart from delaying the surface from freezing, TESA concrete could increase the de-icing ice or snow rate if the air temperature surrounding the sample remained above the melting point of PCM in TESA for an extended period.

6.4.2. Energy storage

A significant amount of heat energy passed from the atmosphere into the specimens at 25 mm in Figure 6.6a than at 75 mm thickness in Figure 6.6b above-freezing air temperature. Similar

results were obtained at freezing or below freezing. A positive heat flux indicated the quantity of heat transfer from the atmosphere into the sample's surface and occurred during charging when the air temperature was above freezing. Negative heat flux was the synonym for the amount of heat released from the specimen to the surface and the surroundings, which occurred during discharging when the air temperature was below freezing, as depicted in Figure 6.6. In Figure 6.6a-b, RMK 1, control 1, and control 2 had more heat transferred from the surroundings into the samples than RMK 2 and RMK 3. However, RMK 1 had the lowest heat flux, thus meaning RMK 1 released/moved a higher amount of heat from the sample to the surface and surroundings. RMK 2 transferred the second most high amount of heat to the surface and surroundings, followed by RMK 3. The control specimens released a negligible quantity of heat to the surface and surroundings. TESA concrete provide better thermal insulation and heat energy necessary to delay freezing. Therefore, the sensible and latent heat mechanism of PW, PWSO, and COSO enhanced the heat flux of concrete.

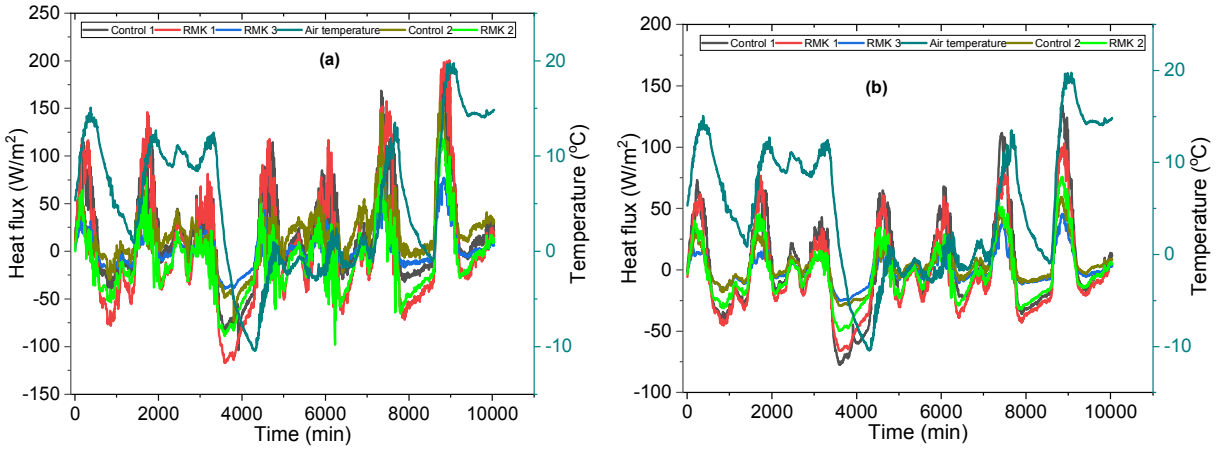

Figure 6.6: Heat flux of concrete samples and air temperature at: (a) 25 mm, and (b) 75 mm thickness.

As aforementioned, the charging or storing process of heat occurred when the air temperature was above freezing (> 0 °C). In contrast, the discharging or heat loss occurred at

freezing and below, as demonstrated in Figure 6.6-7. At a thickness of 25 mm in Figure 6.7, a considerable quantity of heat was absorbed by the concrete specimens, equivalent to double the amount of heat stored/absorbed at 75 mm thickness. Thus, a high amount of heat was absorbed by RMK 1, then RMK 2, followed by RMK 3 compared to control 1 and control 2. The thermal conductivity and latent heat storage capacity of PCMs embedded in TESA enhanced TESA concrete's thermal heat absorption. The PCMs experienced sensible and latent heat mechanisms necessary to keep the heat within the concrete for a specific period resulting in delaying freezing on the surface of the sample.

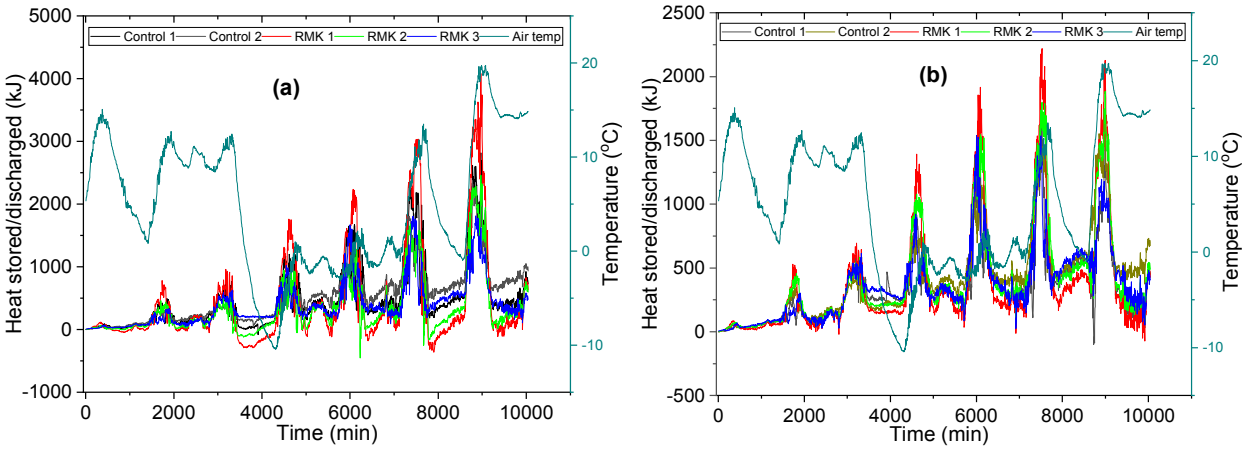

Figure 6.7: Heat stored/discharged of concrete samples and air temperature at of: (a) 25 mm, and (b) 75 mm thick

Figure 6.6-7 demonstrated how TESA concretes provided good thermal performance in the snow and ice forming season. The charging and discharging period of heat was a function of temperature variation with time. Suppose the sample maintained the temperature for a more extended period above freezing. In that case, TESA concrete could not only delay the freezing but also deice/melt the ice and snow forming on the surface of the concrete. Thus, reducing the use of deicing salts, heat, or other techniques would cause an environmental or economic impact on

maintaining concrete. Therefore, when used in concrete production as LWA, TESA provided sustainable and feasible types of concretes for the winter season and regions.

6.5. Conclusion and recommendation

The icing of pavements during cold temperatures represents significant pedestrian and vehicle safety concerns. De-icing salts and other routine winter maintenance activities are intended to improve safety but have considerable cost and environmental runoff concerns. This research demonstrated the ability of concrete produced with low-cost, organic PCM-impregnated expanded clay LWA TESA to delay surface freezing. The cold weather testing period included a rapid drop in air temperature from 11.6 °C to -8.8 °C in 18.5 hrs and a period of more regular thermal cycling through 0°C during night-time and daytime. The air temperature of the presented data passed through freezing (0°C) nine times. Concrete containing TESA stored heat when the air temperature exceeded the sample temperature and released heat when air temperature cooled, much like charging and discharging a battery.

The melting point and sensible and latent heat storage capacity of PCMs significantly influence TESA concrete performance. RMK 2 contained a combination of paraffin wax and soybean oil (PWSO) and produced the most significant delay of freezing at the concrete surface, followed closely by RMK 3, which was a blend of coconut and soybean oil (COSO). While many studies have shown paraffin wax (PW) to provide good high-temperature behaviour, the relatively high melting point means that only PW can realize sensible heat improvement alone. Thus, blending SO with PW or CO enhanced the thermal performance of concrete in the winter season by leveraging the lower melting points and latent heat capacity.

Charging and discharging of the TESA concrete depended on the daily fluctuation of winter temperature, with a longer charging time providing more delay to icing. This study demonstrated

the positive impacts low-cost PCMs could bring in the production of new building materials capable of resisting freezing and thawing, thus improving safety, environmental impacts and preventing deterioration of concrete experience globally by road pavements every winter.

6.6. Reference

Albatayneh, A., D. Alterman, A. Page and B. Moghtaderi (2020). "The Significance of sky temperature in the assessment of the thermal performance of buildings." Applied Sciences **10**(22).

Anupam, B. R., U. C. Sahoo and P. Rath (2020). "Phase change materials for pavement applications: A review." Construction and Building Materials, Elsevier Ltd. **247**.

Bentz, D. P. and R. Turpin (2007). "Potential applications of phase change materials in concrete technology." Cement and Concrete Composites. **29:** 527-532.

Defraeye, T., B. Blocken and J. Carmeliet (2011). "Convective heat transfer coefficients for exterior building surfaces: Existing correlations and CFD modelling." Energy Conversion and Management **52**(1): 512-522.

Esmaeeli, H. S., Y. Farnam, D. P. Bentz, P. D. Zavattieri and J. Weiss (2017). "Numerical simulation of the freeze-thaw behavior of mortar containing deicing salt solution." Materials and Structures, Springer **50**.

Faraj, K., M. Khaled, J. Faraj, F. Hachem and C. Castelain (2020). "Phase change material thermal energy storage systems for cooling applications in buildings: A review." Renewable and Sustainable Energy Reviews, Elsevier Ltd. **119**.

Farnam, Y., H. S. Esmaeeli, P. D. Zavattieri, J. Haddock and J. Weiss (2017). "Incorporating phase change materials in concrete pavement to melt snow and ice." Cement and Concrete Composites, Elsevier Ltd. **84:** 134-145.

Jung Heum Yeon, a. K.-K. K. b. (2018). "Potential applications of phase change materials to mitigate freeze-thaw deteriorations in concrete pavement." Construction and Building Materials **177**: 202-209

Kalombe, R. M., S. Sobhansarbandi, J. Kevern (2022)a. "Assessment of low-cost organic phase change materials for improving infrastructure thermal performance." Journal of Cleaner Production, Elsevier Ltd. (Pending)

Kalombe, R. M., S. Sobhansarbandi, J. Kevern (2022)b. "Hot weather performance of low-cost pcm-modified concrete for reducing heat storage." Construction and Building Materials, Elsevier Ltd. (Pending).

Kenzhebayeva, A., B. Bakbolat, F. Sultanov, C. Daulbayev and Z. Mansurov (2021). "A mini-review on recent developments in anti-icing methods." Polymers (Basel) **13**(23).

Marani, A. and M. L. Nehdi (2019). "Integrating phase change materials in construction materials: Critical review." Construction and Building Materials, Elsevier Ltd. **217:** 36-49.

Melvin Pomerantz, B. P., Hashem Akbari, and Sheng-Chieh Chang (2000). "The effect of pavements' temperatures on air temperatures in large cities." Berkeley, California 94720**:** 1-16.

Nowak, H. (1989). "The sky temperature in net radiant heat loss calculations from low-sloped roofs." Infrared Physics **29**(2-4): 231-232.

Rocha Segundo, E. F., V.T.F. Castelo Branco, S. Landi Jr., M.F. Costa, J. and O. Carneiro. (2021). "Review and analysis of advances in functionalized, smart, and multifunctional asphalt mixtures." Renewable and Sustainable Energy Reviews **51 (2021) 111552**.

Sakulich, A. R. and D. P. Bentz (2012). "Incorporation of phase change materials in cementitious systems via fine lightweight aggregate." Construction and Building Materials **35:** 483-490

Sharifi, N. P. (2016). "Application of phase change materials to improve the thermal performance of buildings and pavements. Doctoral of philosophy's dissertation. Worcester Polytechnic Institute.

Sharma, R., J. G. Jang and J. W. Hu (2022). "Phase-change materials in concrete: opportunities and challenges for sustainable construction and building materials." Materials (Basel) **15**(1).

Shi, L., H. Zhang, Z. Li, Z. Luo and J. Liu (2018). "Optimizing the thermal performance of building envelopes for energy saving in underground office buildings in various climates of China." Tunnelling and Underground Space Technology **77**: 26-35.

Sumeru Nayak, N. M. A. K., Sumanta Das (2019). "Microstructure-guided numerical simulation to evaluate the influence of phase change materials (PCMs) on the freeze-thaw response of concrete pavements." Construction and Building Materials **201** 246–256.

Xu, Y., Q. Xu, S. Chen and X. Li (2017). "Self-restraint thermal stress in early-age concrete samples and its evaluation." Construction and Building Materials, Elsevier Ltd. **134:** 104-115.

CHAPTER 7: CONCLUSION AND FURTHER STUDIES

7.1. Research summary

This study aimed to create a process of incorporating food-grade materials as PCMs into expanded clay LWA to form TESA to be used in the production of concrete capable of enhancing the thermal insulation of infrastructure in summer and resisting freezing and thawing cycles in winter weather.

Therefore, by achieving this aim, the present study provided the following highlights:

- Developed blends of coconut and soybean oil (COSO) and paraffin and soybean (PWSO), which possess melting points and great latent heat of fusion capacity appropriate for both high and low-temperature applications.
- Achieved high PCMs absorption impregnated expanded clay lightweight aggregates.
- Developed a low-cost and straightforward surface coating layer to minimize leakage.
- TESA-concrete improves thermal conductivities and provides better compressive strength.
- TESA-concrete provides excellent thermal insulation in summer and prolongs the delay in freezing in winter.

The findings mentioned above were achieved by answering the following questions:

Question 1. Can cooking oil be used as a phase change material? What are the most reliable low-cost PCMs?

Yes, cooking oil can be used as PCMs. The SO blends with CO or PW (COSO and PWSO) provided significant melting and solidification points, sensible and latent heat storage capacity. PCMs with a great melting process were in the order from PW, PWSO, to COSO. Even after eleven

manual thermal cycles at 80 °C for 6 hours, these PCMs still had better melting processes. This test was performed to show the worst scenario that could have happened to the PCMs when exposed to a constant high temperature for a prolonged duration. Thus, COSO and PWSO had a little shift in thermal properties after multiple thermal cycles and an insignificant thermal expansion.

Question 2. What process is used to incorporate PCMs into concrete? What are the thermal conductivities and compressive strength of TESA concrete?

The three PCMs were vacuum impregnated into LWA, and the absorption capacity was 30.20% for PW-TESA, 28.00% for PWSO-TESA, and 27.42% for COSO-TESA particles. Then, TESA was coated with latex using 10 wt% of the mass of TESA. Not many spots of leaks on the filter paper were observed during the leakage test, but after the test, the mass loss of the TESA particles was equivalent to 0.08% for COSO-TESA and 0.116% for PW-TESA, and 0.160% for PWSO-TESA. On the other hand, the thermal conductivity of concrete containing TESA was generally higher than the control mixture. The increased thermal conductivity was attributed to the increased mass (sensible) and melting (latent) process behaviors added to the concrete. Concrete containing TESA had a lower compressive strength than the control mixture containing normal-weight concrete but was not significantly different than the unimpregnated LWA control.

Question 3. What is the thermal performance of the produced TESA concrete under actual field summer and winter weather conditions?

In summer, TESA significantly improved the thermal properties of concrete by reducing heat penetration through sensible and latent mechanisms. TESA concrete stored a considerable quantity of heat in the surface layer (25 mm) compared to the control mixtures. TESA concrete

containing PW or RMK 1 provided higher thermal insulation, followed by COSO or RMK 3, then PWSO or RMK 2. Thus, the higher energy storage of concrete was a function of the higher amount of PCMs contained in TESA, the higher melting point, and the latent heat of fusion storage capacity of PCMs. The performance of RMK 1 and RMK 3 demonstrated that TESA concrete could be utilized to build cooler infrastructure in equatorial or tropical countries. TESA concrete can reduce conventional fossil energy currently used to cool hot regions. Thus, minimizing the emission of harmful gases responsible for climate changes and environmental pollution.

In winter, the melting point and sensible and latent heat storage capacity of PCMs significantly influence TESA concrete performance. RMK 2 produced the most significant delay of freezing at the concrete surface, followed closely by RMK 3. While many studies have shown paraffin wax (PW) to provide good high-temperature behavior, the relatively high melting point means that only PW can realize sensible heat improvement alone. Thus, blending SO with PW or CO enhanced the thermal performance of concrete in the winter season by leveraging the lower melting points and latent heat capacity. Charging and discharging of the TESA concrete depended on the daily fluctuation of winter temperature, with a longer charging time providing more delay to icing. This study demonstrated the positive impacts low-cost PCMs could bring in producing new building materials capable of resisting freezing and thawing cycles. Thus, TESA concrete improves safety and environmental impacts and prevents the deterioration of concrete experience globally by road pavements every winter.

7.2. Overall achievement and impact to the state of the practice

The findings of the present study added more value and changed the perception of food-grade materials such as soybean oil and coconut oil from low-cost cooking oil to the most feasible and

sustainable PCMs in the building and construction industry. The significance of this study could be summarized as follows:

- The materials utilized in this research, such as LWA, PCMs, or latex, can be found in developed/developing countries and are environmentally friendly and widely available at a low cost.
- The prepared and characterized COSO and PWSO had a little shift in thermal properties after multiple thermal cycles and an insignificant thermal expansion.
- Expanded clay LWA has a water absorption capacity of 17.9%. Thus, it could be helpful for internal water curing for concrete to store water and supply it to the cement paste during the cementitious reactions. However, TESA has a water absorption capacity between 0.67% and 3.01% because PCMs and anti-bleeding materials fill the pores. Therefore, TESA cannot be used as an internal water curing but as thermal energy storage materials in concrete.
- The thermal inertia of TESA concrete was investigated as a potential technique to reduce summer cooling needs for buildings and related infrastructure. TESA concrete demonstrated the ability to delay surface freezing in winter.
- Heat storage was calculated using a charging/discharging process with environmental conditions, which is analogous to evaluating battery charging and releasing under load. This technique allows the comparison of different materials and observation of heat flow into and out of various layers of the bulk sample.
- The thermal performance of the three types of TESA would depend on the melting and solidification processes of the PCMs used to make the TESA. Thus, the DSC analysis results would influence the selection of the types of PCMs and TESA before applying them

to different industries, including building, pavement, solar panels, or air conditioning systems, to enhance the thermal performance in those applications.

7.3. The novelty of the study

The novel findings of this study are listed below:

- The produced and characterized blends of COSO and PWSO
- The impregnation of COSO, PWSO, and PW to form TESA
- First actual field-collected data of the performance of TESA concrete in winter and summer weather.

7.4. Discussion of potential further research

Based on the observations made throughout the process of achieving the aim and objectives of this study, several recommendations can be made that would necessitate further investigation to improve the findings of the present study. Thus, the suggestions made for future studies are listed below:

- As the nature of TESA is to absorb heat, it may result in a reduced curing temperature for the concrete. With that, TESA may promote low heat of hydration, prevent thermal distress and cracking within thick sections, and low early strength. That may be a disadvantage in specific applications.
- The maturity method may be performed using TESA concretes to estimate strength. Concrete temperature multiplied by the time the concrete is maintained at that temperature is maturity.

- Standards, codes, and specifications may require TESA concrete to meet some requirements for building construction. These standards, codes, and specifications are essential for the performance and achievement of a contractor's concrete project.
- Investigating TESA concrete in winter and summer weather using a prototype building or pavements would promote the benefits of using TESA to produce concrete.
- The demand and necessity of TESA seem to be huge; thus, the increase in the production capacity of TESA at a larger scale.

REFERENCES

Akeiber, H. J., M. A. Wahid, H. M. Hussen and A. T. Mohammad (2014). "Review of development survey of phase change material models in building applications." Scientific World Journal, Hindawi Publishing Corporation. **2014**.

Al-Absi, Z. A., M. H. M. Isa and M. Ismail (2020). "Phase change materials (PCMs) and their optimum position in building walls." Sustainability (Switzerland), MDPI. **12**.

Albatayneh, A., D. Alterman, A. Page and B. Moghtaderi (2020). "The significance of sky temperature in the assessment of the thermal performance of buildings." Applied Sciences **10**(22).

Amaral, C., R. Vicente, P. A. A. P. Marques and A. Barros-Timmons (2017). "Phase change materials and carbon nanostructures for thermal energy storage: A literature review." Renewable and Sustainable Energy Reviews **79**: 1212-1228.

Anupam, B. R., U. C. Sahoo and P. Rath (2020). "Phase change materials for pavement applications: A review." Construction and Building Materials, Elsevier Ltd. **247**.

Badenhorst, H. and L. F. Cabeza (2017). "Critical analysis of the T -history method: A fundamental approach." Thermochimica Acta **650**: 95-105.

Baetens, R., B. P. Jelle and A. Gustavsen (2010). "Phase change materials for building applications: A state-of-the-art review." Energy and Buildings, Elsevier Ltd. **42:** 1361-1368.

Bamonte, P., A. Caverzan, N. Kalaba and M. Lamperti Tornaghi (2017). "Lightweight concrete containing phase change materials (PCMs): A numerical investigation on the thermal behaviour of cladding panels." Buildings, MDPI AG. **7**.

Bao, X., S. A. Memon, H. Yang, Z. Dong and H. Cui (2017). "Thermal properties of cement-based composites for geothermal energy applications." Materials, MDPI AG. **10**.

Barzin, R., J. J. J. Chen, B. R. Young and M. M. Farid (2015). "Application of PCM underfloor heating in combination with PCM wallboards for space heating using price based control system." Applied Energy **148**: 39-48.

Bayon, R. and E. Rojas (2019). "Development of a new methodology for validating thermal storage media: Application to phase change materials." International Journal of Energy Research **43**(12): 6521-6541.

Bentz, D. P. (2008). "A review of early-age properties of cement-based materials." Cement and Concrete Research **38**(2): 196-204.

Bentz, D. P. and R. Turpin (2007). "Potential applications of phase change materials in concrete technology." Cement and Concrete Composites. **29:** 527-532.

Campbell-Scientific (2018). OPERATOR'S MANUAL CR1000 Datalogger. Utah**:** 1-630.

Cellat, K., B. Beyhan, B. Kazanci, Y. Konuklu and H. Paksoy (2017). "Direct Incorporation of Butyl Stearate as Phase Change Material into Concrete for Energy Saving in Buildings." Journal of Clean Energy Technologies. **5:** 64-68.

Chandel, S. S. and T. Agarwal (2017). "Review of current state of research on energy storage, toxicity, health hazards and commercialization of phase changing materials." Renewable and Sustainable Energy Reviews **67**: 581-596.

Che, H., Q. Chen, Q. Zhong and S. He (2018). "The effects of nanoparticles on morphology and thermal properties of erythritol/polyvinyl alcohol phase change composite fibers." E-Polymers, European Polymer Federation. **18:** 321-329.

Choi, S., G. S. Ryu, K. T. Koh, G. H. An and H. Y. Kim (2019). "Experimental Study on the Shrinkage Behavior and Mechanical Properties of AAM Mortar Mixed with CSA Expansive Additive." Materials (Basel) **12**(20).

Cui, Y., J. Xie, J. Liu, J. Wang and S. Chen (2017). "A review on phase change material application in building." Advances in Mechanical Engineering, SAGE Publications Inc. **9**.

Dakhli, Z., K. Chaffar and Z. Lafhaj (2019). "The effect of phase change materials on the physical, thermal and mechanical properties of cement." Sci, MDPI AG. **1:** 27.

Dale P. Bentz, W. J. W. (2010). "Internal Curing: A 2010 State of the Art Review." National Institute of Standards and Technology.

Defraeye, T., B. Blocken and J. Carmeliet (2011). "Convective heat transfer coefficients for exterior building surfaces: Existing correlations and CFD modelling." Energy Conversion and Management **52**(1): 512-522.

Dhamodharan, P. and A. K. Bakthavatsalam (2020). "Experimental investigation on thermophysical properties of coconut oil and lauryl alcohol for energy recovery from cold condensate." Journal of Energy Storage, Elsevier Ltd. **31**.

Drissi, S., T. C. Ling, K. H. Mo and A. Eddhahak (2019). "A review of microencapsulated and composite phase change materials: Alteration of strength and thermal properties of cement-based materials." Renewable and Sustainable Energy Reviews, Elsevier Ltd. **110:** 467-484.

Elmozughi, A. F., L. Solomon, A. Oztekin and S. Neti (2014). "Encapsulated phase change material for high temperature thermal energy storage - Heat transfer analysis." International Journal of Heat and Mass Transfer, Elsevier Ltd. **78:** 1135-1144.

Esmaeeli, H. S., Y. Farnam, D. P. Bentz, P. D. Zavattieri and J. Weiss (2017). "Numerical simulation of the freeze-thaw behavior of mortar containing deicing salt solution." Materials and Structures **50**.

Faraj, K., M. Khaled, J. Faraj, F. Hachem and C. Castelain (2020). "Phase change material thermal energy storage systems for cooling applications in buildings: A review." Renewable and Sustainable Energy Reviews, Elsevier Ltd. **119**.

Faraj, K., M. Khaled, J. Faraj, F. Hachem and C. Castelain (2021). "Experimental Study on the Use of Enhanced Coconut Oil and Paraffin Wax Phase Change Material in Active Heating Using Advanced Modular Prototype." Journal of Energy Storage, Elsevier Ltd. **41**.

Farnam, Y., H. S. Esmaeeli, P. D. Zavattieri, J. Haddock and J. Weiss (2017). "Incorporating phase change materials in concrete pavement to melt snow and ice." Cement and Concrete Composites, Elsevier Ltd. **84:** 134-145.

Farnam, Y., M. Krafcik, L. Liston, T. Washington, K. Erk, B. Tao and J. Weiss (2016). "Evaluating the Use of Phase Change Materials in Concrete Pavement to Melt Ice and Snow." Journal of Materials in Civil Engineering, American Society of Civil Engineers (ASCE). **28:** 04015161.

Fenollera, M., J. L. Míguez, I. Goicoechea, J. Lorenzo and M. Á. Álvarez (2013). "The influence of phase change materials on the properties of self-compacting concrete." Materials. **6:** 3530-3546.

Fernandes, F., S. Manari, M. Aguayo, K. Santos, T. Oey, Z. Wei, G. Falzone, N. Neithalath and G. Sant (2014). "On the feasibility of using phase change materials (PCMs) to mitigate thermal cracking in cementitious materials." Cement and Concrete Composites, Elsevier Ltd. **51:** 14-26.

Ferrer, G., A. Solé, C. Barreneche, I. Martorell and L. F. Cabeza (2015). "Review on the methodology used in thermal stability characterization of phase change materials." Renewable and Sustainable Energy Reviews, Elsevier Ltd. **50:** 665-685.

Frigione, M., M. Lettieri and A. Sarcinella (2019). "Phase change materials for energy efficiency in buildings and their use in mortars." Materials, MDPI AG. **12**.

Gandhi, M., A. Kumar, R. Elangovan, C. S. Meena, K. S. Kulkarni, A. Kumar, G. Bhanot and N. R. Kapoor (2020). "A review on shape-stabilized phase change materials for latent energy storage in buildings." Sustainability (Switzerland), MDPI. **12:** 1-17.

Giro-Paloma, J., R. Al-Shannaq, A. I. Fernández and M. M. Farid (2016). "Preparation and characterization of microencapsulated phase change materials for use in building applications." Materials, MDPI AG. **9**.

Hasanabadi, S., S. M. Sadrameli and S. Sami (2021). "Preparation, characterization and thermal properties of surface-modified expanded perlite/paraffin as a form-stable phase change composite in concrete." Journal of Thermal Analysis and Calorimetry, Springer Science and Business Media B.V. **144:** 61-69.

Hawes, D. W., D. Banu and D. Feldman (1992). The stability of phase change materials in concrete. Solar Energy Materials and Solar Cells. **27:** 103-118

Hawes, D. W. and D. Feldman (1992). "Absorption of phase change materials in concrete." Solar Energy Materials and Solar Cells **27:** 91-101.

Henkensiefken, R., D. Bentz, T. Nantung and J. Weiss (2009). "Volume change and cracking in internally cured mixtures made with saturated lightweight aggregate under sealed and unsealed conditions." Cement and Concrete Composites **31**(7): 427-437.

Hu, Y., R. Guo, P. K. Heiselberg and H. Johra (2020). "Modeling PCM Phase Change Temperature and Hysteresis in Ventilation Cooling and Heating Applications." Energies **13**(23).

Hunger, M. and H. J. H. Brouwers (2008). "Natural Stone Waste Powders Applied to SCC Mix Design." Restoration of Buildings and Monuments. **14:** 131-140.

Hunger, M., A. G. Entrop, I. Mandilaras, H. J. H. Brouwers and M. Founti (2009). "The behavior of self-compacting concrete containing micro-encapsulated Phase Change Materials." Cement and Concrete Composites. **31:** 731-743.

Iten, M., S. Liu and A. Shukla (2016). "A review on the air-PCM-TES application for free cooling and heating in the buildings." Renewable and Sustainable Energy Reviews **61**: 175-186.

Jayalath, A., P. Mendis, R. Gammampila and L. Aye (2011). "Applications of phase change materials in concrete for sustainable built environment : a review." Proceedings of the International Conference on Structural Engineering. Construction and Management. **1:** 1-13.

Jayalath, A., R. San Nicolas, M. Sofi, R. Shanks, T. Ngo, L. Aye and P. Mendis (2016). "Properties of cementitious mortar and concrete containing micro-encapsulated phase change materials." Construction and Building Materials, Elsevier Ltd. **120:** 408-417.

Jung Heum Yeon, a. K.-K. K. b. (2018). "Potential applications of phase change materials to mitigate freeze-thaw deteriorations in concrete pavement." Construction and Building Materials **177**: 202-209.

Kahwaji, S. and M. A. White (2019). "Edible oils as practical phase change materials for thermal energy storage." Applied Sciences (Switzerland), MDPI AG. **9**.

Kakar, M. R., Z. Refaa, J. Worlitschek, A. Stamatiou, M. N. Partl and M. Bueno (2019). "Impregnation of lightweight aggregate particles with phase change material for its use in asphalt mixtures." International Symposium on Asphalt Pavement & Environment, Springer.

Kalombe, R. M., T. V. Ojumu, V. N. Katambwe, M. Nzadi, D. Bent, G. Nieuwouldt, G. Madzivire, J. Kevern and L. F. Petrik (2020). "Treatment of acid mine drainage with coal fly ash in a jet loop reactor pilot plant." Minerals Engineering, Elsevier Ltd. **159**.

Kalombe, R. M., V. T. Ojumu, C. P. Eze, S. M. Nyale, J. Kevern and L. F. Petrik (2020). "Fly ash-based geopolymer building materials for green and sustainable development." Materials **13**: 1-17.

Kalombe, R. M., S. Sobhansarbandi, J. Kevern (2022)a. "Assessment of low-cost organic phase change materials for improving infrastructure thermal performance." Journal of Cleaner Production, Elsevier Ltd. (Pending).

Kalombe, R. M., S. Sobhansarbandi, J. Kevern (2022)b. "Hot weather performance of low-cost pcm-modified concrete for reducing heat storage." Construction and Building Materials, Elsevier Ltd. (Pending).

Kasaeian, A., L. bahrami, F. Pourfayaz, E. Khodabandeh and W. M. Yan (2017). "Experimental studies on the applications of PCMs and nano-PCMs in buildings: A critical review." Energy and Buildings, Elsevier Ltd. **154:** 96-112.

Kastiukas, G., X. Zhou and J. Castro-Gomes (2016). "Development and optimisation of phase change material-impregnated lightweight aggregates for geopolymer composites made from aluminosilicate rich mud and milled glass powder." Construction and Building Materials, Elsevier Ltd. **110:** 201-210.

Kenisarin, M. M., K. Mahkamov, S. C. Costa and I. Makhkamova (2020). "Melting and solidification of PCMs inside a spherical capsule: A critical review." Journal of Energy Storage **27**.

Kenzhebayeva, A., B. Bakbolat, F. Sultanov, C. Daulbayev and Z. Mansurov (2021). "A mini-review on recent developments in anti-icing methods." Polymers (Basel) **13**(23).

Khudhair, A. M. and M. M. Farid (2004). "A review on energy conservation in building applications with thermal storage by latent heat using phase change materials." Energy Conversion and Management, Elsevier Ltd. **45:** 263-275.

Kurdi, A., N. Almoatham, M. Mirza, T. Ballweg and B. Alkahlan (2021). "Potential phase change materials in building wall construction—a review." Materials, MDPI. **14**.

Li, M., Z. Wu and J. Tan (2013). "Heat storage properties of the cement mortar incorporated with composite phase change material." Applied Energy, Elsevier Ltd. **103:** 393-399.

Liao, W., A. Kumar, K. Khayat and H. Ma (2019). "Multifunctional lightweight aggregate containing phase change material and water for damage mitigation of concrete." ES Materials & Manufacturing.

Liao, W., C. Zeng, Y. Zhuang, H. Ma, W. Deng and J. Huang (2021). "Mitigation of thermal curling of concrete slab using phase change material: A feasibility study." Cement and Concrete Composites, Elsevier Ltd. **120**.

Ling, T. C. and C. S. Poon (2013). "Use of phase change materials for thermal energy storage in concrete: An overview." Construction and Building Materials. **46:** 55-62.

Liu, F., J. Wang and X. Qian (2017). "Integrating phase change materials into concrete through microencapsulation using cenospheres." Cement and Concrete Composites, Elsevier Ltd. **80:** 317-325.

Majo, M., R. Sanchez, P. Barcelona, J. Garcia, A. I. Fernandez and C. Barreneche (2021). "Degradation of fatty acid phase-change materials (PCM): New Approach for Its Characterization." Molecules **26**(4).

Marani, A. and M. L. Nehdi (2019). "Integrating phase change materials in construction materials: Critical review. Construction and Building Materials, Elsevier Ltd. **217:** 36-49.

Martínez, A., M. Carmona, C. Cortés and I. Arauzo (2020). "Characterization of thermophysical properties of phase change materials using unconventional experimental technologies." Energies **13**(18).

Melvin Pomerantz, B. P., Hashem Akbari, and Sheng-Chieh Chang (2000). "The effect of pavements' temperatures on air temperatures in large cities." Berkeley, California 94720**:** 1-16.

Memon, S. A., H. Z. Cui, H. Zhang and F. Xing (2015). "Utilization of macro encapsulated phase change materials for the development of thermal energy storage and structural lightweight aggregate concrete." Applied Energy, Elsevier Ltd. **139:** 43-55.

Mike, G. (2018). "Thermal emissivity and radiative heat transfer." Materio Performance Alloys Retrieved 06/04/2022, 2022, from https://materion.com/-/media/files/alloy/newsletters/technical-tidbits/issue-no-114-thermal-emissivity-and-radiative-heat-transfer.pdf.

Min, H. W., S. Kim and H. S. Kim (2017). "Investigation on thermal and mechanical characteristics of concrete mixed with shape stabilized phase change material for mix design." Construction and Building Materials, Elsevier Ltd. **149:** 749-762.

Mohseni, E., W. Tang and S. Wang (2019). "Development of thermal energy storage lightweight structural cementitious composites by means of macro-encapsulated PCM." Construction and Building Materials, Elsevier Ltd. **225:** 182-195.

Muller, L., G. Rubio-Perez, A. Bach, N. Munoz-Rujas, F. Aguilar and J. Worlitschek (2020). "Consistent DSC and TGA methodology as basis for the measurement and comparison of thermo-physical properties of phase change materials." Materials (Basel) **13**(20).

Nazir, H., M. Batool, F. J. Bolivar Osorio, M. Isaza-Ruiz, X. Xu, K. Vignarooban, P. Phelan, Inamuddin and A. M. Kannan (2019). "Recent developments in phase change materials for energy storage applications: A review." International Journal of Heat and Mass Transfer **129**: 491-523.

Niall, D., R. P. West and S. McCormack (2016). "Assessment of two methods of enhancing thermal mass performance of concrete through the incorporation of phase-change materials."

SDAR* Journal of Sustainable Design & Applied SDAR* Journal of Sustainable Design & Applied Research Research. **4:** 2016-2027.

Nizovtsev, M. I., V. Y. Borodulin, V. N. Letushko, V. I. Terekhov, V. A. Poluboyarov and L. K. Berdnikova (2019). "Heat transfer in a phase change material under constant heat flux." Thermophysics and Aeromechanics, Kutateladze Institute of Thermophysics SB RAS. **26:** 313-324.

Nowak, H. (1989). "The sky temperature in net radiant heat loss calculations from low-sloped roofs." Infrared Physics **29**(2-4): 231-232.

Okogeri, O. and V. N. Stathopoulos (2021). "What about greener phase change materials? A review on biobased phase change materials for thermal energy storage applications." International Journal of Thermofluids, Elsevier B.V. **10**.

Omaraa, E., W. Saman, F. Bruno and M. Liu (2017). "Modified T-history method for measuring thermophysical properties of phase change materials at high temperature." AIP Conference Proceedings. **1850**(1)

Pielichowska, K. and K. Pielichowski (2014). "Phase change materials for thermal energy storage." Progress in Materials Science, Elsevier Ltd. **65:** 67-123.

Pilehvar, S., A. M. Szczotok, J. F. Rodríguez, L. Valentini, M. Lanzón, R. Pamies and A. L. Kjøniksen (2019). "Effect of freeze-thaw cycles on the mechanical behavior of geopolymer concrete and Portland cement concrete containing micro-encapsulated phase change materials." Construction and Building Materials, Elsevier Ltd. **200:** 94-103.

Pons, O., A. Aguado, A. I. Fernández, L. F. Cabeza and J. M. Chimenos (2014). "Review of the use of phase change materials (PCMs) in buildings with reinforced concrete structures." Materiales de Construccion, Inst. de Ciencias de la Construccion Eduardo Torroja. **64**.

Qu, Y., J. Chen, L. Liu, T. Xu, H. Wu and X. Zhou (2020). "Study on properties of phase change foam concrete block mixed with paraffin / fumed silica composite phase change material." Renewable Energy, Elsevier Ltd. **150:** 1127-1135.

Rathod, M. K. (2018). "Phase change materials and their applications." Phase Change Materials and Their Applications, InTech.

Rathod, M. K. and J. Banerjee (2013). "Thermal stability of phase change materials used in latent heat energy storage systems: A review." Renewable and Sustainable Energy Reviews. **18:** 246-258.

Rocha Segundo, E. F., V.T.F. Castelo Branco, S. Landi Jr., M.F. Costa, J. and O. Carneiro. (2021). "Review and analysis of advances in functionalized, smart, and multifunctional asphalt mixtures." Renewable and Sustainable Energy Reviews **51 (2021) 111552**.

Safira, L., N. Putra, T. Trisnadewi, E. Kusrini and T. M. I. Mahlia (2020). "Thermal properties of sonicated graphene in coconut oil as a phase change material for energy storage in building applications." International Journal of Low-Carbon Technologies, Oxford University Press. **15:** 629-636.

Sakulich, A. R. and D. P. Bentz (2012). "Incorporation of phase change materials in cementitious systems via fine lightweight aggregate." Construction and Building Materials. **34:** 483-490

Santiago Acosta, R. D., J. A. Otero, E. M. Hernández Cooper and R. Pérez-Álvarez (2019). "Thermal expansion effects on the one-dimensional liquid-solid phase transition in high temperature phase change materials." AIP Advances **9**(2).

Šavija, B. (2018). "Smart crack control in concrete through use of phase change materials (PCMs): A review." Materials, MDPI AG. **11**.

Sharifi, N. P. (2016). "Application of phase change materials to improve the thermal performance of buildings and pavements." Doctoral of philosophy's dissertation. Worcester Polytechnic Institute. Massachusetts.

Sharma, A., V. V. Tyagi, C. R. Chen and D. Buddhi (2009). "Review on thermal energy storage with phase change materials and applications." Renewable and Sustainable Energy Reviews. **13:** 318-345.

Sharma, B., N. Neithalath, S. Rajan and B. Mobasher (2013). "Incorporation of phase change materials into cementitious systems." Master's thesis. Arizona State University. Arizona.

Sharma, R., J. G. Jang and J. W. Hu (2022). "Phase-Change Materials in Concrete: Opportunities and Challenges for Sustainable Construction and Building Materials." Materials (Basel) **15**(1).

She, Z., Z. Wei, B. A. Young, G. Falzone, N. Neithalath, G. Sant and L. Pilon (2019). "Examining the effects of microencapsulated phase change materials on early-age temperature evolutions in realistic pavement geometries." Cement and Concrete Composites, Elsevier Ltd. **103:** 149-159.

Shi, L., H. Zhang, Z. Li, Z. Luo and J. Liu (2018). "Optimizing the thermal performance of building envelopes for energy saving in underground office buildings in various climates of China." Tunnelling and Underground Space Technology **77**: 26-35.

Sivanathan, A., Q. Dou, Y. Wang, Y. Li, J. Corker, Y. Zhou and M. Fan (2020). "Phase change materials for building construction: An overview of nano-/micro-encapsulation." Nanotechnology Reviews, De Gruyter Open Ltd. **9:** 896-921.

Srivastava, Y., A. D. Semwal, V. A. Sajeevkumar and G. K. Sharma (2017). "Melting, crystallization and storage stability of virgin coconut oil and its blends by differential scanning calorimetry (DSC) and Fourier transform infrared spectroscopy (FTIR)." J Food Sci Technol **54**(1): 45-54.

Sukontasukkul, P., E. Intawong, P. Preemanoch and P. Chindaprasirt (2016). "Use of paraffin impregnated lightweight aggregates to improve thermal properties of concrete panels." Materials and Structures/Materiaux et Constructions, Kluwer Academic Publishers. **49:** 1793-1803.

Sukontasukkul, P., T. Sangpet, M. Newlands, D. Y. Yoo, W. Tangchirapat, S. Limkatanyu and P. Chindaprasirt (2020). "Thermal storage properties of lightweight concrete incorporating phase change materials with different fusion points in hybrid form for high temperature applications." Heliyon, Elsevier Ltd. **6**.

Sumeru Nayak, N. M. A. K., Sumanta Das (2019). "Microstructure-guided numerical simulation to evaluate the influence of phase change materials (PCMs) on the freeze-thaw response of concrete pavements." Construction and Building Materials **201** 246–256.

Sun, Z., L. Li, X. Cheng, J. Zhu, Y. Li and W. Zhou (2021). "Thermal properties and the prospects of thermal energy storage of mg-25%cu-15%zn eutectic alloy as phase change material." Materials (Basel) **14**(12).

Thienel, K. C., T. Haller and N. Beuntner (2020). "Lightweight concrete-from basics to innovations." Materials (Basel) **13**(5).

Tyagi, V. V., S. C. Kaushik, S. K. Tyagi and T. Akiyama (2011). "Development of phase change materials based microencapsulated technology for buildings: A review." Renewable and Sustainable Energy Reviews. **15:** 1373-1391.

Urgessa, G., K. K. Yun, J. Yeon and J. H. Yeon (2019). "Thermal responses of concrete slabs containing microencapsulated low-transition temperature phase change materials exposed to realistic climate conditions." Cement and Concrete Composites, Elsevier Ltd. **104**.

Vakhshouri, A. R. (2021). "Paraffin as Phase Change Material." IntechOpen.

Wang, R., M. Ren, X. Gao and L. Qin (2018). "Preparation and properties of fatty acids based thermal energy storage aggregate concrete." Construction and Building Materials, Elsevier Ltd. **165:** 1-10.

Weiss, J., K. Snyder, J. Bullard and D. Bentz (2013). "Using a saturation function to interpret the electrical properties of partially saturated concrete." Journal of Materials in Civil Engineering, American Society of Civil Engineers (ASCE). **25:** 1097-1106.

Weiss, W. J. and O. Burkan Isgor (2018). "Examining how saturation and pore solution chemistry impact durability test methods, specifications and service life models (keynote)." Reactive-Transport Modeling in Porous MediaResistivity. Formation Factor and Transport.

WheatherUnderground. (2022). "Joe's Datacenter - Paseo West - KMOKANSA198." Joe's Datacenter - Paseo West - KMOKANSA198 Retrieved 05/21/2022, 2022, from https://www.wunderground.com/dashboard/pws/KMOKANSA198.

Xie, J., Y. Li, W. Wang, S. Pan, N. Cui and J. Liu (2013). "Comments on Thermal Physical Properties Testing Methods of Phase Change Materials." Advances in Mechanical Engineering **5**.

Xu, Y., Q. Xu, S. Chen and X. Li (2017). "Self-restraint thermal stress in early-age concrete samples and its evaluation." Construction and Building Materials, Elsevier Ltd. **134:** 104-115.

Yang, G., Y. J. Yim, J. W. Lee, Y. J. Heo and S. J. Park (2019). "Carbon-filled organic phase-change materials for thermal energy storage: A review." Molecules, MDPI AG. **24**.

Yang, L., X. Jin, Y. Zhang and K. Du (2021). "Recent development on heat transfer and various applications of phase-change materials." Journal of Cleaner Production, Elsevier Ltd. **287**.

Zeinelabdein, R., S. Omer, E. Mohamed and G. Gan (2018). "Free cooling using phase change material for buildings in hot-arid climate." International Journal of Low-Carbon Technologies, Oxford University Press. **13:** 327-337.

Zhang, D., Z. Li, J. Zhou and K. Wu (2004). "Development of thermal energy storage concrete. Cement and Concrete Research." **34:** 927-934.

Zhou, D., C. Y. Zhao and Y. Tian (2012). "Review on thermal energy storage with phase change materials (PCMs) in building applications." Applied Energy, Elsevier Ltd. **92:** 593-605.

Zhou, D., Y. Zhou, Y. Liu, X. Luo and J. Yuan (2019). "Preparation and Performance of Capric-Myristic Acid Binary Eutectic Mixtures for Latent Heat Thermal Energy Storages." Journal of Nanomaterials, Hindawi Limited. **2019**.

VITA

Rosicky Methode Kalombe was born on January 13th, 1992, in Lubumbashi, Democratic Republic of the Congo. He attended high school at Institute Kashobwe and graduated in 2010. Then, in 2011, he moved to Cape Town, South Africa, for university studies. In 2016, he graduated with a bachelor's in Chemical Engineering. Simultaneously, from 2015 -2018, Rosicky worked as a research assistant at the environmental and nano sciences research group in Cape Town, South Africa. In 2018, Rosicky graduated with a master's in Chemical Engineering. Then, in 2019, Rosicky started the Ph.D. program in Civil Engineering and Geosciences in Kansas City, Missouri, United States of America.